DOWNLINK SCHEDULING OPTIMIZATION AND PERFORMANCE ANALYSIS OVER FADING CHANNELS IN A CDMA NETWORK

by

RAYMOND KWAN

B.A.Sc., University of British Columbia, 1996
M.A.Sc., University of British Columbia, 1998

A THESIS SUBMITTED IN PARTIAL FULFILMENT OF
THE REQUIREMENTS FOR THE DEGREE OF

DOCTOR OF PHILOSOPHY

in

THE FACULTY OF GRADUATE STUDIES
(Electrical and Computer Engineering)

THE UNIVERSITY OF BRITISH COLUMBIA

February 2006

Abstract

Due to technological advances in mobile communications, together with the explosive growth of internet access, transmitting multimedia applications over wireless channels is no longer a remote concept. In third generation (3G) multimedia CDMA networks, a variety of techniques will be used to meet the quality of service (QoS) requirements for various types of traffic. These include adaptive modulation and coding (AMC) which improves performance by adapting the employed modulation and coding scheme (MCS) to changing channel conditions and multicode transmission which provides higher bit rates to mobile stations (MS's).

The problem of allocating radio resources in the downlink of a CDMA network is first studied. In particular, the modulation and coding schemes, numbers of multicodes, and transmit powers used for all MS's are jointly chosen so as to maximize the total transmission bit rate, subject to certain constraints. In addition, a scheduler which uses knowledge of MS traffic loads is also proposed and shown to yield a significant improvement in throughput. The proposed multiuser schedulers are optimal in terms of system throughput. However, the implementation complexity can be high. Consequently, a suboptimal scheme is proposed, in which resources are allocated sequentially on a per-MS basis. Essentially, the sequential scheme reduces the problem of multiuser resource optimization to a single user problem, thereby greatly reducing complexity. Numerical results show that the performance of the sequential scheme is generally close to optimal if the MS's are ordered optimally.

The thesis also addresses the problem of downlink single user scheduling in the context of AMC and multicodes with imperfect channel estimation. Since the selection of MCS and number of multicodes requires an estimation of the downlink channel quality, it is important

to assess the performance degradation due to estimation errors. It is shown that the system throughput is quite sensitive to channel estimation errors, and methods are proposed to reduce the resulting degradations.

In multiuser scheduling, the aim is to select users with good channel conditions so as to improve the system performance. The selection process is a classical problem in the theory of order statistics. Since users are generally located in different parts of a cell, their respective channels can often be assumed independent, but their fading statistics are not necessarily identical. In this thesis, some useful general results assuming independent and non-identically distributed (i.n.d.) order statistics over the Nakagami and Weibull fading channels are derived. The thesis also proposes a new statistical distribution for the CDMA downlink signal-to-interference ratio given that the simultaneously transmitted interfering and desired signals from the same base station undergo the same fading process. Finally, a simple method for approximating complex statistical distributions which arise in the study of wireless communications is investigated. The resulting relatively simple approximations are shown to be quite accurate.

Table of Contents

List of Tables

List of Figures

List of Abbreviations

3GPP	Third Generation Partnership Project.
AF	Amount of Fading.
AM	Adaptive Modulation.
AMC	Adaptive Modulation and Coding.
AQAM	Adaptive Quadrature Amplitude Modulation.
BER	Bit Error Rate.
BLER	Block Error Rate.
BPSK	Binary Phase Shift Keying.
BS	Base Station.
CDF	Cumulative Distribution Function.
CDMA	Code-Division Multiple Access.
CSI	Channel State Information.
EGC	Equal-Gain Combining.
EM	Expectation Maximization.
FSMC	Finite-State Markov Chain.
GSC	Generalized Selection Combining.
GOSC	General Order Selection Combining.
HMM	Hidden Markov Model.
HSDPA	High Speed Downlink Packet Access.
IID	Independent and Identically Distributed.

IND	Independent and Non-identically Distributed.
JO	Joint Optimization.
OVSF	Orthogonal Variable Spreading Factor.
MCS	Modulation and Coding Scheme.
MGF	Moment Generating Function.
MINLP	Mixed Integer Nonlinear Programming.
MRC	Maximal Ratio Combining.
MS	Mobile Station.
OVSF	Orthogonal Variable Spreading Factor.
PDF	Probability Density Function.
PF	Proportional Fair.
MPF	Modified Proportional Fair.
QAM	Quadrature Amplitude Modulation.
QoS	Quality of Service.
QPSK	Quadrature Phase Shift Keying.
RRM	Radio Resource Management.
RV	Random Variable.
SC	Selection Combining.
SER	Symbol Error Rate.
SINR	Signal-to-Interference-and-Noise Ratio.
SIR	Signal-to-Interference Ratio.
SNR	Signal-to-Noise Ratio.
SO	Sequential Optimization.
TTI	Transmission Time Interval.
WCDMA	Wide-band Code Division Multiple Access.

List of Symbols

α	Orthogonality factor
α_i, β_i	Distribution parameters of the fading channel models for the i^{th} branch diversity combining
$\alpha_k(j)$	Forward probability of state j at time k
β_1	Skewness of a distribution (in the context of Pearson's systems of distribution)
β_2	Kurtosis of a distribution (in the context of Pearson's systems of distribution)
$\beta_k(j)$	Backward probability of state j at time k
Δ_i	Conservative factor
ϵ_0	QoS related frame error rate target
ϵ_{γ_i}	Estimation error for the received SIR
γ_i	Received SIR for MS i
$\tilde{\gamma}_{i,j}^{(min)}$,$\tilde{\gamma}_{i,j}$	AMC selection thresholds for MS i and MCS j
γ_i'	Maximum possible downlink SIR for MS i if a power $\hat{P}_i$ is allocated to MS i
$\hat{\gamma}_i$	Estimated received SIR for MS i
ζ	Scheduling deviation factor
η	Scheduling efficiency
η_f	Improvement factor
η_p	Power efficiency
η_R	Effective bit rate ratio
$\overline{\eta}_R$	Average effective bit rate ratio
κ	Selection parameter for Pearson's systems of distributions

$\lambda_{i,j}$	SIR requirement for MCS j and MS i at a given QoS
$\pi_k(i)$	The probability that the channel is in state k at time k
ρ	Correlation coefficient
$a_{i,j}$	Transition probability that the channel SIR is in state j given that the it was in state i at the pervious scheduling instant
$\hat{a}_{i,j}$	Estimated state transitional probability from state i to state j
$b_i(y_k)$	The condition pdf of the observation Y_k given that the channel is in state i at time k
B_i	The number of bits in the buffer for MS i at the beginning of a scheduling period
D_i	Normalized buffer size for MS i
g	Spreading factor
h_i	Path gain between the desired BS and MS i
$h_{k,i}$	Path gain between BS k and MS i
$I_i^{(r)}$	Received interference power at MS i
I_N	Thermal noise
J	Maximum number of MCS's
L	Number of MS's to be scheduled; number of branches for selection diversity
M_j	Number of points in the signal constellation for MCS j
n_i	Number of multicodes for MS i
N_{max}	Maximum number of multicodes (channelization codes) for the BS
$N_{i,max}$	Maximum number of multicodes (channelization codes) that MS i can support
P_i	Downlink transmit power for MS i
P_{max}	Maximum power allocated for scheduling at the BS
$\overline{P}_s$	Average symbol probability
P_T	Total available downlink transmit power for the BS
$\hat{P}_i$	Maximum downlink power available to MS i
$r_{i,j}$	Basic bit rate for MCS j and MS i

$R_c^{(j)}$	Code rate for MCS j
R_i	Bit rate (assigned) for MS i
$\tilde{R}_i(\gamma_i\|\hat{\gamma}_i)$	Effective bit rate for MS i at γ_i for a given value of $\hat{\gamma}_i$
$\tilde{R}_i(\gamma_i)$	Effective bit rate for MS i at γ_i
$\overline{R_i(\gamma_i\|\Delta_i)}$	Average effective bit rate given a specific value of Δ_i
$\overline{R}$	Average effective bit rate
R_{tot}	Total bit rate for all scheduled MS's
T_a	Scheduling period
$v_{k,i}$	The ratio of the path gain between BS k and MS i to the path gain between the desired BS and MS i, i.e. $h_{k,i}/h_i$
W	Chip rate

Note: In this thesis, in order to distinguish a random variable from its outcome, the former is denoted by a capital letter, whereas the latter is denoted by a small letter.

Acknowledgments

This work would not have been possible without the support of many people. I am most of all indebted to my advisor, Dr. Cyril Leung, who has shown immense patience and support throughout many years - making himself available even outside regular working hours. His comments are always useful and constructive. Thanks to the Natural Sciences and Engineering Research Council (NSERC) of Canada for awarding me a Post Graduate Scholarship (PGS) as well as support from NSERC Grant OGP0001731 and the UBC PMC-Sierra Professorship in Networking and Communications. They have provided me with the financial means to engage in and complete this work. I would like to thank my thesis examination committee members and the external examiner for their time and efforts. And finally, thanks to my wife Jenny and my parents, who have helped and supported me in all possible ways.

To my family.

Chapter 1

Introduction

1.1 Background

Due to the ubiquity of Internet access, together with the technological advances in mobile communications, wireless multimedia applications have become a reality. However, such applications can potentially be very resource demanding. Due to the nature of multimedia applications, many types of traffic can be encountered with different characteristics and Quality of Service (QoS) requirements [1]. The ability to allocate limited radio resources efficiently to these different traffic types while meeting their QoS requirements is a difficult task. Thus, radio resource management (RRM) is considered to be an important topic in the wireless industry.

As pointed out in [1], the RRM functionalities and requirements for the downlink and the uplink of a Code Division Multiple Access (CDMA) system are different. For example, the total transmit power at the base station is limited, and is shared among users. Thus, as the number of users increases, the average power allocated to each user decreases. In other words, the number of supported downlink users is limited by the available power at the base station. On the uplink, on the other hand, the power resource is not centrally shared by the users as in the downlink, since each user has its own power amplifier. However, each additional user increases the interference level at base station receiver. Thus, the number of supported uplink users is related to the amount of interference that the base station receiver experiences. In general, the goal of downlink resource management is to efficiently allocate the limited downlink power to maximize the throughput, while the goal of uplink resource

management is typically to minimize the mobile transmit power so that less interference is seen at the base station and to extend battery life.

A number of papers have addressed the issues of uplink scheduling [2]-[16]. In [2, 3], an uplink dynamic resource scheduling mechanism is suggested for QoS provisioning in Wide-Band Code Division Multiple Access (WCDMA) by means of optimal power assignment and code hopping. The transmit power level is minimized while meeting the QoS requirements for the admitted users. In addition, the spreading gain for variable bit rate (VBR) services is dynamically adjusted so that a higher spreading gain can be used when the required bit rate is low. With a higher spreading gain, a lower uplink transmit power is required, and the interference can be reduced. Such reduction in interference can lead to an overall increase in capacity.

In [4], a combined rate and power control scheme for the uplink is proposed in which the transmission rate is kept constant while the power is adjusted via power control when the channel condition is above a certain threshold. On the other hand, when the channel condition falls below the threshold, the power is kept constant while the transmission rate is reduced. This simple hybrid power/rate control effectively reduces the interference in the uplink, and leads to a capacity increase.

In [5], resource allocation is formulated as a constrained optimization problem. The objectives are to minimize power or to maximize bit rates on the uplink of a CDMA system. The former reduces the interference seen in other cells, and the latter tries to achieve the best possible throughput for the users. Bounds were developed on the total number of users of each class that can be supported simultaneously while meeting the QoS and resource constraints. In [6], two transmission modes are considered for maximizing the throughput for delay tolerant users. In the first mode, all users are allowed to transmit when they wish, whereas in the second mode, users are time-scheduled so that only a limited number of them can transmit at any given time. It has been shown that the second mode effectively reduces the interference seen by the transmitting users so that higher bit rates can be achieved, even

though only a fraction of the time is allowed for each user. In [7], a non-linear optimization problem is considered in which the total power of different mobiles is minimized while achieving their minimum guaranteed throughput.

In [8], a jointly optimal power and spreading gain allocation strategy is provided to maximize the instantaneous non-real-time throughput for the uplink CDMA network, subject to constraints on peak mobile transmission power and the total received power at the base station. In the model, the spreading gain is assumed to be continuous, and there is no constraint on the bit rate.

In [9]-[11], the problem of optimal rate and power adaptation for multirate CDMA on the uplink is considered, in which each user has a bit error rate (BER) constraint while having a fixed set of transmission rates to select from. An optimal uplink rate adaptation scheme is proposed and analyzed, in which the optimal number of multicodes are allocated to each scheduled user, and the minimum needed power for each user is determined.

In [12], the throughput maximization problem for a CDMA uplink is expressed in terms of the spreading gains and transmit powers of the users, and the problem is solved using nonlinear programming. The results suggest that all resources should be allocated to the user with the highest path gain. This approach maximizes the total throughput at the expense of fairness. The authors then extend the proposed strategy by allowing all users to be served on a time-sharing basis. The results suggest a modest loss in the total throughput, but a significant increase in fairness.

In [13]-[16], a scheme for optimal resource management for uplink transmission in WCDMA is proposed. The idea is to guarantee the quality-of-service (QoS) by efficiently allocating radio resources such as power and bit rate. The model takes the form of a mathematical programming optimization problem, in which the main objective is to maximize a utility function subject to certain QoS requirements. In [13], both the single and multiple-cell scenarios are considered. In particular, the multiple-cell scenario is formulated as a mixed integer non-linear programming problem. In this work, the bit rate is assumed to be con-

tinuous.

Since the downlink transmit power of the base station is shared among users, intelligent scheduling is typically desirable to efficiently utilize such a limited resource. A number of studies are devoted to downlink scheduling [17]-[34]. In [17, 18], the optimization problem for the downlink WCDMA system is examined using dynamic programming. The objective is to maximize the total offered bit rate by allocating user specific power and bit rate given a total power constraint at the base station. In all cases, no limits on the user bit rate or the number of channelization codes are considered. In [19, 20, 21], the issues of the optimum rate and power allocation for the downlink CDMA system in a multiple cell environment are addressed based on the channel condition of each user at the beginning of each scheduling period. The idea is to maximize the sum of the assigned bit rates for all users under certain SIR and downlink transmit power constraints.

In [22, 23], it is shown that in a CDMA network, the optimal strategy for scheduling downlink transmission to data users is to transmit to one user at a time at full power rather than transmit to several users simultaneously. In [24], it is also found that such one-by-one scheduling for downlink can yield superior throughput performance compared to that of the simultaneous transmission case. The authors also point out that the one-by-one scheme is more energy efficient compared to other scheduling schemes in requiring less energy for delivering the same amount of data. Also discussed is a distributed power assignment scheme for such one-by-one scheduler in a non-fading environment. In [25], the one-by-one scheduling scheme is discussed for a fading environment, and different scheduling algorithms are compared in terms of their fairness. In [26], the problem of optimum power allocation for sharing the capacity in a fair way over the whole network is investigated. A distributed power control algorithm is proposed which allocates the powers so that a uniform throughput is obtained among users.

Although throughput is an important measure of network performance, fairness is also needed to ensure user satisfaction [27]-[34]. In [27], a user with the highest measure T is

given the downlink power $P(t)$, where

$$T = \frac{(C/I)_k(t)}{R_k(t)} \tag{1.1}$$

and $(C/I)_k(t)$ is the signal-to-interference ratio of the k^{th} user at time t, and $R_k(t)$ is the throughput of user k averaged over a certain time window up to time t. Thus, instead of giving resources to the user with the highest C/I, the incorporation of the throughput $R_k(t)$ in the selection criterion introduces fairness by "punishing" a user who has enjoyed a high throughput. A proportional fair (PF) algorithm for the downlink is proposed in [28], in which the power P is allocated to the m best users based on their channel conditions. Each user k receives his share of power P_k, which is proportional to the channel gain of that user. An asymptotic analysis of such an algorithm is provided in [29]. In [30], delay sensitivity is incorporated into the proportional fair algorithm. The new modified proportional fair (MPF) scheduling algorithm is shown to be able to provide effective and fair service to both real and non real time data.

In [31, 32], an optimization model is proposed for maximizing a certain utility function given a probabilistic fairness constraint. In this model, only a single user out of N users is allowed to be scheduled at each given time slot. However, on average, each user is to be scheduled for a pre-defined fraction of the total time. The goal of the scheduling scheme is to maximize the average system performance by exploiting the time-varying channel conditions. Following [31, 32], the authors in [33, 34] extend previous works by incorporating multiple users.

1.1.1 WCDMA Transport Channels for Packet Access

One of the most popular technologies being proposed for the air interface of third generation mobile networks is code division multiple access (CDMA). The specification of WCDMA has been developed in the 3GPP (3rd Generation Partnership project) standardization forum

[1, 35]. A WCDMA network consists of a number of logical network elements, which are grouped into the Radio Access Network (RAN), which handles all radio-related functionalities, and the Core Network (CN), which is responsible for switching and routing calls and data connections to the external networks. In the 3GPP specification, the Radio Access Network is termed UMTS Terrestrial Radio Access Network (UTRAN). A reference diagram of the network elements is given in Figure 1.1. More detailed descriptions of the elements can be found in [1, 35].

In WCDMA, there are three types of transport channels that can be used to transmit packet

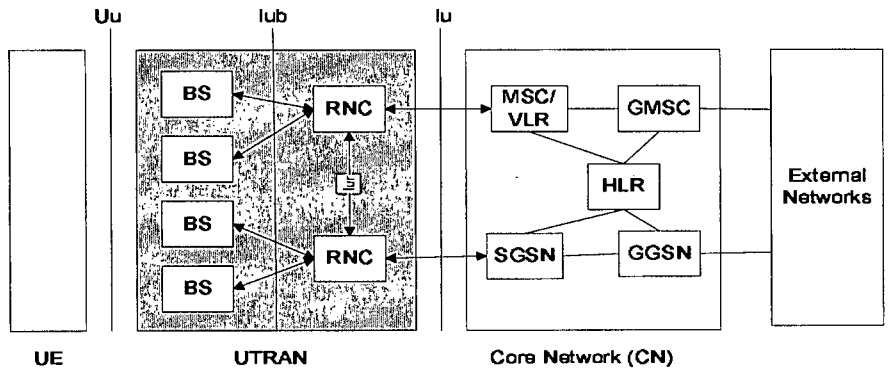

Figure 1.1: UMTS Network elements.

data [1, 36]. They are the common, the dedicated, and the shared transport channels. Common channels do not have a feedback channel, and, therefore, cannot have fast closed loop power control, but only open loop power control or fixed power. In addition, these channels do not support soft handover. Due to the lack of fast closed loop power control, more interference is generated, and, therefore, they are only designed to carry a small amount of data. The dedicated channel, on the other hand, requires dedicated resources. The advantage of the dedicated channel is that it supports fast closed loop power control and soft handover. As a result, less interference is generated than for the common channels. The disadvantage is that more time is required to set up a dedicated channel through signalling than a common channel. In addition, a dedicated channel ties up radio resources for the entire call duration,

and, thus, is not resource-efficient for bursty traffic. The shared channels are designed to carry bursty packet data by sharing a single physical channel, i.e. orthogonal code, between a number of users in a time division multiplex manner. The advantage of the shared channels is that they do not tie up resources as the dedicated channel does, and, thus, are more resource efficient. In addition, transmitting data in a time division fashion improves the overall throughput by reducing the own-cell interference [22]. The conceptual difference between the dedicated and the shared channels is illustrated in Figure 1.2. Throughout this document, the terms time-shared channel and shared channel will be used interchangeably.

The transport channel for packet data is selected based on the resource requirements of the

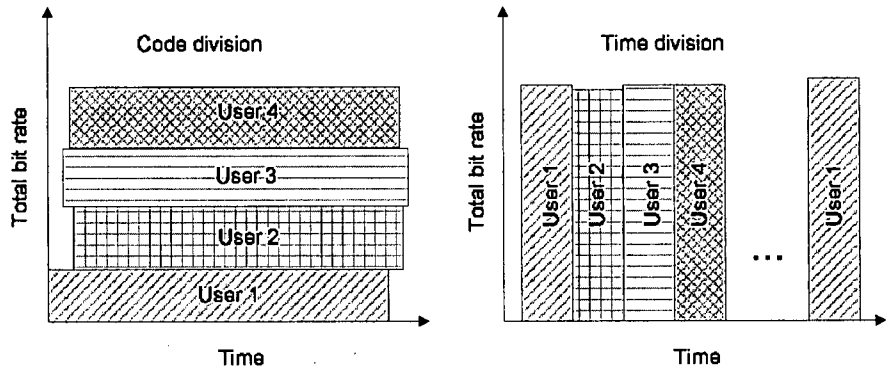

Figure 1.2: (Left) Code division for the dedicated channel, and (right) time division for the shared channel.

services, the amount of data, and the interference levels in the air interface. In WCDMA, the Downlink Shared Channel (DSCH) is a shared transport channel, which is intended to carry packet traffic in the user plane from the UTRAN network to the User Equipment (UE). The DSCH is a time-shared channel with fast power control and fast scheduling but without soft handover. Some examples of simulation studies on the system performance with DSCH can be found in [37]-[39]. Recently, in 3GPP, a scheme called the High Speed Downlink Packet Access (HSDPA) has been proposed, in which a number of new features are incorporated into the DSCH, resulting a new transport channel called the High Speed Downlink Shared Channel (HS-DSCH).

1.1.2 High Speed Downlink Packet Access

The development of the third generation (3G) wireless network infrastructure allows a rich variety of traffic types, each with its own QoS rquirements, to be transmitted over the wireless channel. Efficient radio resource allocation algorithms are therefore important. In addition, it is anticipated that the downlink traffic will be especially important because much of the high-speed internet access and broadcast services are transmitted in the downlink. In order to offer such broadband packet data transmission services, HSDPA [1, 40] is currently under investigation in 3GPP.

HSDPA is the Release 5 extension of the WCDMA specification with a new transport channel called High-Speed Downlink Shared Channel (HS-DSCH). The special feature of this channel is that a certain amount of channelization codes and power in a cell are considered as a common resource that is dynamically shared among users in the time domain. Instead of using power control as in the case of the dedicated channel (DCH), HS-DSCH keeps the transmit power constant while adjusting the bit rate according to the channel condition via Adaptive Modulation and Coding (AMC). Additional features include multicode transmission, Multiple-Input-Multiple-Output (MIMO), and *fast* Hybrid Automatic Repeat reQuest (HARQ) [41].

A number of HSDPA simulation studies on the network performance have been reported [42]-[46], which focus mainly on the most popular scheduling algorithms such as the round robin (RR) algorithm, the Maximum C/I (signal-to-interference ratio) algorithm, and the proportionally fair (PF) algorithm. The idea of the first scheme is to schedule the queued user in a first-come-first-served basis, and is generally known to be fair from the user's point of view. The second scheme requires knowledge of the user's channel quality, and selects the user with the best channel quality so that the network resource usage can be optimized. This scheme generally yields the highest throughput, but handicaps users with poor channels. The third scheme is a compromise in which users are assigned radio resources

that are proportional to the ratio of their instantaneous to long term channel qualities. In these papers, the number of multicodes is assumed to be statically allocated. In [47]-[49], the AMC and the number of multicodes are jointly selected for a single user based on the channel quality. In all cases, the power and multicode resources are not optimized for serving multiple users simultaneously.

1.1.3 Adaptive Modulation and Coding

It is well known that adapting the transmission parameters in a wireless system to changing channel conditions can be advantageous. In the case of fast power control [1, 35], the transmission power is adjusted based on the channel fading. Thus, a good channel condition requires lower transmission power to maintain the target signal quality at the receiver. The process of changing transmission parameters to compensate for variations in channel conditions is known as *link adaptation.* Besides power control, adaptive modulation and coding (AMC) is also used for link adaptation [41],[50]-[54]. The goal of AMC is to change the modulation and channel coding scheme according to the varying channel conditions. In this scheme, a terminal with favorable channel conditions can be assigned a higher order modulation with a higher channel coding rate, and a lower order modulation with a lower channel coding rate when channel conditions are unfavourable.

Higher order modulations provide better spectral efficiency at the expense of worse error rate performance. A lower channel coding rate provides better error correction capability than the same type of coding with a higher coding rate. Thus, with a proper combination of the modulation order and channel coding rate, it is possible to design a set of modulation and coding schemes (MCS), from which an adaptive selection is made per transmission-time-interval (TTI) such that an improved spectral efficiency can be achieved under good channel conditions. At each selection of the MCS, the criterion should be such that the probability of erroneous decoding of a Transmission Block is below a threshold value.

In [55, 56], the signal-to-interference (SIR) ratio as well as the ACK/NACK feedback

information of the Hybrid ARQ (HARQ) are used to control the threshold values for choosing the MCS. It is proposed in [55] that when the current received SIR falls within a limited range ($\pm\alpha$) on either side of one of the current thresholds, then the threshold value is increased by Δ_{up} if an ACK is recevied, and decreased by Δ_{down} if a NACK is received. Subsequently, the next appropriate MCS is chosen based on the updated set of thresholds. In [57], it is proposed to perform the MCS selection based solely upon the ACK/NACK feedback information of the HARQ. The idea is to decrease the MCS order by one if a number of consecutive or accumulative NACK's are received, and increase the MCS order by one if a number of consecutive ACK's are received. A higher MCS order provides a higher bit rate at the expanse of a power/error rate performance. A number of variations have also been proposed. With these schemes, no feedback information regarding the received signal quality is needed, thereby reducing the system complexity. In [58], the average channel signal-to-noise ratio (SNR) over a frame duration is quantized and modelled as a first-order finite-state Markov process. The MCS is selected in each state of this Markov model in order to maximize the average throughput in that state.

1.1.4 Adaptive Modulation and Coding with Multicodes

Multicode transmission is employed [1, 10] to increase the bit rate by splitting the bits of a Transmission Block to more than one channelization code at each transmission interval (TI). Thus, during each transmission interval, more data can be transmitted. In this scheme, a high rate data stream is divided into a number of lower rate data sub-streams, which are transmitted in parallel synchronous orthogonal multicode channels. It has been shown that multicode yields better performance compared to the single code scheme in a multipath environment [59, 60]. With the single code scheme, a lower spreading factor is required to provide the same bit rate as that of the multicode scheme. From the perspective of power and bandwidth, both schemes provide the same throughput. However, in the presence of multipath fading, the single code scheme suffers a slightly greater performance degradation.

In [61], it is proposed to select the number of multicodes based on the amount of data in the downlink data buffer so as to avoid assigning more multicodes than needed. However, the MCS and the corresponding number of multicodes are selected separately, resulting in sub-optimal resource allocation. Simulation studies of the HSDPA performance with multicodes have been performed in [42, 47, 48]. In [47, 48], the multicodes and MCS are selected dynamically in the HSDPA transmission environment with an extensive dynamic WCDMA network simulator [62]. A single user algorithm for joint optimization of MCS and multicodes given the power and code constraint has been proposed in [49]. The idea is to use as many multicodes as possible for the lowest order MCS. Note that every time an extra code is used, more power is required to maintain a given QoS requirement. Once the code resource is exhausted, and if more power resource is still available, the next higher order MCS is invoked with the highest possible number of multicodes that the power limit allows. The whole procedure is repeated until all the code and power resources are exhausted. Finally, the combination of the number of multicodes and the MCS is selected which gives the highest bit rate.

1.2 Motivation

1.2.1 Issues in Multiuser Scheduling

In a typical communication channel, the transmission rate is closely related to the SIR, which, in turn, is tightly influenced by the transmission power. Such coupling between the transmission rate and power gives rise to a rich variety of schemes which can enhance the performance of a CDMA network in both uplink and downlink. The downlink is particularly relevant to consider because it is commonly expected that data traffic will be asymmetric with the bulk of the traffic directed from the base station to the user. In [22], using a simplified model which assumes a linear relationship between bit rate and transmit power, it was found that it is optimal for a base station to transmit to only one data user at a time.

Moreover, it was shown that a base station, when on, should transmit at maximum power for optimality. The above-mentioned assumptions may often not be valid. For example, the introduction of adaptive modulation results in a non-linear relationship between the bit rate and transmit power. In such a case, an optimal power allocation (to maximize the total allocated bit rate) may result in transmissions to more than one mobile at a time.

In [49], an algorithm is provided for jointly selecting an optimal combination of MCS and the number of multicodes for a single user in the context of HSDPA, given code and power constraints, as well as the user's channel condition. The first objective of this thesis is to examine the resource allocation problem for many users.

At first glance, it may appear that to optimize the total throughput in a multi-user system, the single-user algorithm given in [49] can by applied with minor modifications. Unfortunately, this is not the case. Unlike the single user case, in which the MCS, the power, and the number of multicodes are the main concerns, the multiuser case also has to deal with how the optimal sharing of code and power resources is done among the users. Some important issues that need to be addressed are (1) if transmitting to a single mobile is not necessarily optimal from the total throughput point of view, what is the optimal number of mobiles be given a fixed set of orthogonal codes and a maximum power of the base station that are to be shared among these mobiles? (2) How would the code and power resources be optimally allocated to each mobile given that the total reserved power and codes are limited? (3) Which modulation scheme should each allocated mobile use? A similar allocation problem was studied using exhaustive search in [63]. However, the complexity using exhaustive search is very high [64].

In most existing throughput optimization problems, it is assumed that users always have data to be sent. However, in reality, the user data are not always back-logged, and the throughput may be different from the total assigned bit rate. By taking into account not only the channel conditions of the users, but also the amount of data in the user buffers, the actual throughput can be improved. In [65], the authors studied the issue of dynamic

fair scheduling in the uplink WCDMA system by taking into account the traffic information. In [66, 67], single user scheduling schemes are proposed in the downlink, which use both the traffic information and channel variations in order to reduce the waiting and processing delays. The scheduling in [65] addresses only the uplink WCDMA, in which the power and code resources are not shared among different users centrally as in the downlink. The proposed scheduling schemes in [66, 67] are designed to take into account the user traffic load as a mean to reduce the overall delay and the throughput is not necessarily optimal. The problem of load-sensitive, joint optimization for multiple users will be investigated, and the model will include AMC and multicodes.

To schedule resources efficiently, the channel quality for each user is needed. However, the quantity may not be very accurate since some kind of estimation from the mobile is typically involved. As a result, the system performance degrades. The impact of imperfect channel estimation upon the system performance is a topic which is studied.

1.2.2 Issues in Channel Statistical Characterization

Since the use of AMC relies on the channel quality indicator fed-back from the mobile, statistical characterizations of the received channel quality is important for studying average throughput performance. In addition, if the distribution of the channel gain is known, more intelligent scheduling schemes can be designed. For example, most link adaptation systems rely mainly on the mean of the downlink SIR over a scheduling period as a way to quantify the channel quality. More complete knowledge of the distribution can be helpful in further optimize resource allocation. For example, it opens up the possibility for the base station to optimize resources statistically, taking into account the possible extent of each mobile's channel variations at a given time. More specifically, such additional knowledge enables the construction of stochastic optimization models, whereby uncertainties can be incorporated

[68, 69, 70][1]. A stochastic approach for optimizing scheduling is not considered in this thesis. Rather, the probability distributions of the downlink received SIR are derived.

Traditionally, a Gaussian approximation (GA) is often used to model the statistics of the interference for a CDMA system. However, as pointed out in [71], GA is not necessarily accurate in the context of the downlink performance analysis. The reason is that GA is based on the central limit theorem (CLT), which is not really applicable for the downlink since the interference due to the simultaneously transmitted signals by the same base station to different users are not statistically independent. In addition, CLT assumes a large number of interfering signals, which is not necessarily the case for downlink multiuser scheduling, due to the limited available downlink orthogonal channelization codes as in HSDPA.

In downlink scheduling, selecting the user with the best channel condition has been suggested to maximize the network throughput [22]. However, as mentioned earlier, this scheme is not necessarily optimal due to the non-linear nature of the rate and transmit power relationship. A sub-optimal method for multiuser scheduling is to allocate resources to users sequentially based on their channel conditions. In fact, from the system throughput point of view, it is more efficient to allocate resources to the user with the best channel condition, and the remaining resources to the next best user and so on. For performance analysis, such a scheme motivates the need to obtain the ranked statistics of the channel conditions among users. In this thesis, the term *general selection diversity* is used as compared to *selection diversity* where the statistics of only the highest channel condition is examined as in the context of antenna selection combining [72]. In addition, since the users are situated at different locations of the cell, it is reasonable to assume that their channels are independent but non-identically distributed (i.n.d.). One aim of this thesis is to examine the statistics of such ranked channel conditions for different fading models.

[1]Note that if the knowledge of higher order statistics of the channel are known, more sophisticated optimization models can be developed.

1.3 Thesis Overview

This thesis is written in the manuscript-based format according to the guideline specified by the University of British Columbia, in which each individual chapter is a published, in-press, accepted, submitted or draft manuscript written in a common format. The entire thesis is divided into two parts. The first part, which consists of chapters 2 - 5, focuses mainly on the issues of adaptive modulation and coding with dynamic multicodes and power allocations. The second part, which consists of chapters 6 - 8, examines the statistical distributions of the received channel quality over fading channels.

In chapter 2, the problem of joint multiuser optimization is addressed in the context of AMC and multicodes for a downlink CDMA system with and without user traffic load information. Instead of allocating resources for multiple users jointly at the base-station, a sub-optimal approach is taken in which the resources are allocated sequentially among users. The proposed sequential method eliminates the need for mathematical programming, making it an attractive alternative for performance analysis. In chapter 3, the effect of imperfect channel estimation on system performance is addressed. The imperfect channel model is further extended to the Nakagami fading channel in chapter 4. By casting the fading channel model into a discrete-state Hidden Markov Model (HMM), it is shown in chapter 5 that the effect of the imperfect channel estimate from the mobile can be reduced with an appropriate channel state estimation at the base station. In chapter 6, a new statistical model for the downlink received SIR over the Nakagami fading channel is proposed, in which the interfering signals from the same base station are dependent on the desired signal. In chapter 7, some statistical results are presented for general selection diversity, in which the fading channels are assumed to be i.n.d. Finally, in chapter 8, a statistical method known as the *Pearson system of distributions* is proposed to approximate complex statistical distributions which arise in wireless communications. Such an approximation is very useful especially for performance analysis when the distribution of certain channel parameter cannot

be expressed in closed-form.

References

[1] H. Holma and A. Toskala, Eds., *WCDMA for UMTS Radio Access for Third Generation Mobile Communications.* John Wiley & Sons, 2002.

[2] H. O. O. Gurbuz, "Dynamic Resource Scheduling for Variable QoS Traffic in W-CDMA," in *Proc. of IEEE International Conference on Communications, ICC'99*, vol. 2, June 1999, pp. 703 – 707.

[3] ——, "Dynamic Resource Scheduling Schemes for W-CDMA Systems," *IEEE Communication Magazine*, vol. 38, no. 10, pp. 80 – 84, October 2000.

[4] W. L. J. Liu, S. Zhu, "A Combined Rate and Power Control Scheme and Its Impact on the Capacity of Multimedia DS-CDMA Systems," in *Proc. of International Conference on Info-tech and Info-net, ICII'01*, vol. 2, October - November 2001, pp. 156 – 161.

[5] A. Sampath, P. Kumar, and J. Holtzman, "Power Control and Resource Management for a Multimedia CDMA Wireless System," in *Proc. of 6th IEEE International Symposium on Personal, Indoor and Mobile Radio Communications PIMRC'95*, vol. 1, September 1995, pp. 21–25.

[6] S. Ramakrishna and J. Holtzman, "A Scheme for Throughput Maximization in a Dual-Class CDMA System," *IEEE Journal on Selected Areas in Communication*, vol. 16, no. 6, pp. 830 –844, August 1998.

[7] S. B. S. Kandukuri, "Simultaneous Rate and Power Control in Multirate Multimedia CDMA Systems," in *Proc. of 6th IEEE International Symposium on Sread Sprectrum Technology and Application*, vol. 2, September 2000, pp. 570 – 574.

[8] S. J. Oh and K. M. Wasserman, "Adaptive Resource Allocation in Power Constrained CDMA Mobile Networks," in *Proc. of IEEE Wireless Communications and Networking Conference, WCNC'99*, vol. 1, September 1999, pp. 510 – 514.

[9] S. A. Jafar and A. Goldsmith, "Optimal Rate and Power Adaptation for Multirate CDMA," in *Proc. of 52th IEEE Vehicular Technology Conference, Fall*, vol. 3, Sept. 2000, pp. 994 –1000.

[10] ——, "Adaptive Multicode CDMA for Uplink Throughput Maximization," in *Proc. of IEEE Vehicular Technology Conference, Spring*, vol. 1, May 2001, pp. 6–9.

[11] ——, "Adaptive Multirate CDMA for Uplink Throughput Maximization," *IEEE Transactions on Wireless Communications*, vol. 2, no. 2, pp. 218–228, March 2003.

[12] S. Ulukus and L. J. Greenstein, "Throughput Maximization in CDMA Uplinks Using Adaptive Spreading and Power Control," in *Proc. of 6th IEEE International Symposium on Sread Sprectrum Technology and Application*, vol. 2, September 2000, pp. 565 – 569.

[13] M. Soleimanipour, W. Zhuang, and G. H. Freeman, "Optimal Resource Management in Wireless Multimedia Wideband CDMA Systems," *IEEE Transactions on Mobile Computing*, vol. 2, no. 3, pp. 143–160, April-June 2002.

[14] ——, "An Algorithm for Maximal Resource Utilization in Wireless Multimedia CDMA Communication," in *Proc. of 48th IEEE Vehicular Technology conference VTC'98*, vol. 3, May 1998, pp. 2594 – 2598.

[15] ——, "Modeling and Resource Allocation in Wireless Multimedia CDMA Systems," in *Proc. of 48th IEEE Vehicular Technology conference VTC'98*, vol. 2, May 1998, pp. 1279 – 1283.

[16] ——, "Optimal Resource Management in Multimedia WCDMA Systems," in *Proc. of IEEE Global Telecommunication Conference GLOBECOM 2000*, vol. 3, Nov.-Dec. 2000, pp. 1544–1547.

[17] S. Kahn, M. K. Gurcan, and O. O. Oyefuga, "Downlink Throughput Optimization for Wideband CDMA Systems," *IEEE Communication Letters*, vol. 7, no. 5, pp. 251 – 253, May 2003.

[18] S. Kahn and M. K. Gurcan, "A Reduced Dimensionality Algorithm for Downlink Throughput Optimization in Wideband CDMA Systems," in *Proc. of IEEE Global Telecommunication Conference GLOBECOM'02*, vol. 1, November 2002, pp. 794 – 798.

[19] R. Vannithamby and E. S. Sousa, "An Optimum Rate/Power Allocation Scheme for Downlink in Hybrid CDMA/TDMA Cellular System," in *Proc. of IEEE Vehicular Technology Conference, Fall VTC'00*, vol. 4, September 2000, pp. 1734 – 1738.

[20] ——, "Resource Allocation and Scheduling Schemes for WCDMA Downlinks," in *Proc. of IEEE International Conference on Communications ICC'01*, vol. 5, June 2001, pp. 1406 – 1410.

[21] D. I. Kim, E. Hossain, and V. K. Bhargava, "Downlink Joint Rate and Power Allocation in Cellular Multirate WCDMA Systems ," *IEEE Transactions on Wireless Communications*, vol. 2, no. 1, pp. 69 – 80, January 2003.

[22] A. Bedekar, S. C. Borst, K. Ramanan, P. A. Whiting, and E. M. Yeh, "Downlink Scheduling in CDMA Data Network," Centrum Voor Wiskunde en Informatica, Probability, Networks, and Algorithms (PNA) PNA-R9910, Oct. 1999.

[23] ——, "Downlink Scheduling in CDMA Data Network," in *Proc. of IEEE Global Telecommunications Conference, GLOBECOM '99*, vol. 5, Dec. 1999, pp. 2653–2657.

[24] F. Berggren, S. L. Kim, R. Jantti, and J. Zander, "Joint Power Control and Intracell Scheduling of DS-CDMA Nonreal Time Data," *IEEE Journal on Selected Areas in Communications*, vol. 19, no. 10, pp. 1860–1870, Oct. 2001.

[25] F. Berggren and R. Jantti, "Asymptotically Fair Scheduling on Fading Channels," in *Proc. of 56th IEEE Vehnicular Technology Conference VTC'02*, vol. 4, September 2002, pp. 1934 –1938.

[26] F. Berggren, "Distributed Power Control for Throughput Balancing in CDMA Systems," in *Proc. of 12th IEEE International Personal, Indoor and Mobile Radio Communications*, vol. 1, Sept.- Oct. 2001, pp. C–24 – C–28.

[27] D. Tse, "Forward-Link Multiuser Diversity Through Rate Adaptation and Scheduling," *Bell Laboratories Presentation*, 1999.

[28] J. M. Holtzman, "CDMA Forward Link Waterfilling Power Control," in *Proc. of 51st IEEE Vehicular Technology Conference*, vol. 3, May 2000, pp. 1663 –1667.

[29] ——, "Asymptotic Analysis of Proportional Fair Algorithm," in *Proc. of 12th IEEE International Symosium on Personal, Indoor and Mobile Radio Communications*, vol. 2, September-October 2001.

[30] G. Barriac and J. M. Holtzman, "Introducting Delay Sensitivity into the Proportional Fair Algorithm for CDMA Donwlink Scheduling," in *IEEE 7th Symp. on Spread-Spectrum Tech. & Appl.*, Sept 2002, pp. 2–5.

[31] X. Liu, E. K. P. Chong, and N. B. Shroff, "Transmission Scheduling for Efficient Wireless Utilization," in *Proc. of IEEE INFOCOM*, 2001, pp. 776 – 785.

[32] ——, "Opportunistic Transmission Scheduling With Resource-Sharing Constraints in Wireless Networks," *IEEE Journ. on Selected Areas in Communications*, vol. 19, no. 10, pp. 2053 – 2063, October 2001.

[33] Y. Liu and E. Knightly, "Opportunistic Fair Scheduling over Multiple Wireless Channels," in *Proc. of IEEE INFOCOM Conference*, vol. 2, March 30 - April 3 2003, pp. 1106 – 1115.

[34] J. W. Lee, R. R. Mazumdar, and N. B. Shroff, "Opportunistic Power Scheduling for Multi-Server Wireless Systems with Minimum Performance Constraints," in *Proc. of IEEE INFOCOM Conference*, 2004.

[35] Http://www.3gpp.org.

[36] "Technical Specification Group Radio Access Network; Physical channels and mapping of transport channels onto physical channels (FDD)," 3rd Generation Partnership Project, Tech. Rep.

[37] A. Ghosh, M. Cudak, and K. Felix, "Shared Channels for Packet Data Transmission in W-CDMA," in *Proc. of 50th IEEE Vehicular Technology Conference (VTC)*, vol. 2, September 1999, pp. 943 – 947.

[38] R. Kwan and M. Rinne, "Performance analysis of the Downlink shared channel," in *International Conference of Telecommunication (ICT)*, 2001.

[39] A. Mate, C. Caldera, and M. Rinne, "Performance of the Packet Traffic on the Downlink Shared Channel in a WCDMA Cell," in *International Conference of Telecommunication (ICT)*, 2001.

[40] S. Parkvall, E. Englund, P. Malm, T. Hedberg, M. Persson, and J. Peisa, "WCDMA evolved – High-speed packet-data services ," *Ericsson Review*, no. 2, pp. 56 – 65, 2003.

[41] "Physical Layer Aspects of UTRA High Speed Downlink Packet Access," 3rd Generation Partnership Project, Technical Report 3G TR25.858, 2002.

[42] T. J. Moulsley, "Throughput of High Speed Downlink Packet Access for UMTS," in *Proc. of 2nd IEE International Conference on 3G Mobile Communication Technologies*, no. 477, March 2001, pp. 363 – 367.

[43] ——, "Performance of MTS High Speed Downlink Packet Access for Data Streaming Applications," in *Proc. of 3rd IEE International Conference on 3G Mobile Communication Technologies*, no. 489, May 2002, pp. 302 – 307.

[44] R. Love, A. Ghosh, and L. J. R. Nikides, "High Speed Downlink Packet Access Performance," in *Proc. of 53th IEEE Vehicular Technology Conference VTC'01*, vol. 3, May 2001, pp. 2234 – 2238.

[45] Y. Ofuji, A. Morimoto, S. Abeta, and M. Sawahashi, "Comparison of Packet Scheduling Algorithms Focusing on User Throughput in High Speed Downlink Packet Access," in *Proc. of 13th IEEE International Conference on Persoanl, Indoor and Mobile Radio Communications*, vol. 3, September 2002, pp. 1462 – 1466.

[46] A. Furuskar, S. Parkvall, M. Persson, and M. Samuelsson, "Performance of WCDMA high speed packet data," in *The 55th IEEE Proc. of Vehicular Technology Conference (VTC)*, vol. 3, May 2002, pp. 1116 – 1120.

[47] E. Poutiainen, R. Kwan, S. Hämäläinen, and P. Chong, "Performance Study of the High Speed Downlink Packet Access (HSDPA) in a WCDMA Network," in *CDMA International Conference CIC'01*, Nov. 2001.

[48] R. Kwan, P. Chong, and M. Rinne, "The Effect of Code-Multiplexing on the High Speed Downlink Packet Access (HSDPA) in a WCDMA Network," in *Wireless Communication and Networking Conference WCNC*, vol. 3, March 2003, pp. 1728 – 1732.

[49] ——, "Analysis of the adaptive modulation and coding algorithm with the multicode transmission," in *Proc. of 56th IEEE Vehicular Technology Conference VTC'02*, vol. 4, September 2002, pp. 2007 – 2011.

[50] Y. Zhao, "Theoretical Study of Link Adaptation Algorithms for Adaptive Modulation in Wireless Mobile Communication Systems," in *IEEE Proc. of Universal Personal Communications, ICUPC'98*, vol. 1, October 1998, pp. 587 – 591.

[51] K. Chawla and X. Qiu, "Throughput Performance of Adaptive Modulation in Cellular Systems," in *Proc. of IEEE Universal Personal Communications, ICUPC'98*, vol. 2, October 1998, pp. 945–950.

[52] N. C. Ericsson, "Adaptive Modulation and Scheduling for Fading Channels," in *Proc. of IEEE Global Telecommunications Conference, Globecom'99*, vol. 5, December 1999, pp. 2668–2672.

[53] ——, "Adaptive Modulation and Scheduling of IP traffic over Fading Channels," in *Proc. of IEEE Vehicular Technology Conference, VTC'99-fall*, vol. 2, September 1999, pp. 849–853.

[54] S. Falahati. and A. Svensson, "Hybrid Type-II ARQ Schemes with Adaptive Modulation Systems for Wireless Channels," in *Proc. of IEEE Vehicular Technology Conference, VTC'99-fall*, vol. 5, September 1999, pp. 2691–2695.

[55] M. Nakamura, Y. Awad, and S. Vadgama, "Adaptive Control of Link Adaptation for High Speed Downlink Packet Access (HSDPA) in W-CDMA," in *Proc. of 5th International Symposium on Wireless Personal Multimedia Communications*, vol. 2, October 2002, pp. 382 – 386.

[56] "Selection of MCS levels in HSDPA," NEC and Telecom Modus, Technical Document R1-01-0589, May 2001.

[57] J. Lee, R. Arnott, K. Hamabe, and N. Takano, "Adaptive Modulation Switching Level Control in High Speed Downlink Packet Access Transmission," in *Proc. of 3rd IEE 3G Mobile Communication Technologies*, May 2002, pp. 156 – 159.

[58] A. K. K. J. Yang, N. Tin, "Adaptive Modulation and Coding in 3G Wireless Systems," in *Proc. of IEEE Vehicular Technology Conference VTC'02*, vol. 1, September 2002, pp. 544 – 548.

[59] S. J. Lee, H. W. Lee, and D. K. Sung, "Capacities of Single-Code and Multicode DS-CDMA Systems Accommodating Multiclass Service," *IEEE Trans. on Vehicular Technology*, vol. 48, no. 2, pp. 376 –384, March 1999.

[60] M. Fan, T. Minn, and K. Y. Siu, "Performance of Multirate Techniques in WCDMA," in *Proc. of 54th IEEE Vehicular Technology Conference*, vol. 4, Oct. 2001, pp. 2262–2266.

[61] W. S. Jeon, D. G. Jeong, and B. Kim, "Design of Packet Transmission Scheduler for High Speed Downlink Packet Access Systems," in *Proc. of 55th IEEE Vehicular Technology Conference VTC'02*, vol. 3, May 2002, pp. 1125 – 1129.

[62] S. Hamalainen, H. Holma, and K. Sipil, "Advanced WCDMA Radio Network Simulator," in *Proc. of IEEE Personal, Indoor and Mobile Radio Communications, PIMRC'99*, vol. 2, September 1999, pp. 951–955.

[63] D. I. Kim, E. Hossain, and V. K. Bhargava, "Dynamic rate and Power Adaptation for Forward Link Transmission Using High-Order Modulation and Multicode Formats in Cellular WCDMA Networks," in *Proc. of 53th IEEE GLOBECOM*, vol. 1, December 2003, pp. 393 – 397.

[64] E. A. Eiselt and C.-L. Sandblom, *Integer Programing and Network Models.* Springer, 2000.

[65] L. Xu, X. Shen, and J. W. Mark, "Dynamic Fair Scheduling With QoS Constraints in Multimedia Wideband CDMA Cellular Networks," *IEEE Trans. on Wireless Communications*, vol. 3, no. 2, pp. 60 – 73, January 2004.

[66] M. Hu, J. Zhang, and J. Sadowsky, "Size-Aided Opportunistic Scheduling in Wireless Networks," in *Proc. of IEEE Global Telecommunications Conference GLOBECOM*, vol. 1, 1 - 5 December 2003, pp. 538 – 542.

[67] Z. Gao and S. Q. Li, "A Packet Scheduling Scheme in Wireless CDMA Data Network," in *Proc. of IEEE International Conference on Communications, Cicuits, and Systems, and West Sino Expositions*, vol. 1, June 29 - July 1 2002, pp. 211 – 215.

[68] F. S. Hillier and G. J. Kieberman, *Introduction to Mathematical Programming*, 2nd ed. McGraw-Hill, Inc, 1995.

[69] J. K. Sengupta, *Stochastic Programming.* New York: North-Holland, 1972.

[70] S. Sen and J. L. Higle, "An Introductory Tutorial on Stochastic Linear Programming Models," *Interfaces*, vol. 29, no. 2, pp. 33 – 61, March-April 1999.

[71] J. O. Sebeni and C. Leung, "Performance of Concatenated Walsh/PN Spreading Sequences for CDMA Systems," in *Proc. of 49th IEEE Vehicular Technology Conference (VTC)*, Houston, Texas, May 1999.

[72] M. K. Simon and M.-S. Alouini, *Digital Communication over Fading Channels*, 2nd ed. John Wiley & Sons, 2005.

Chapter 2

Optimal Downlink Scheduling Schemes for CDMA Networks

2.1 Introduction

The development of the third generation (3G) wireless network infrastructure allows a rich variety of traffic to be transmitted over the wireless channel. Each type of traffic has its own quality of service (QoS) requirements. Radio resource allocation algorithms are needed which will yield efficient use of resources. It is anticipated that downlink traffic will be especially important since most of the high-speed internet access and broadcast services traffic is in the downlink direction. In order to offer such broadband packet data transmission services, a high speed downlink packet access (HSDPA) channel has been incorporated in the 3GPP standard [1].

It is well known that adapting the transmission parameters in a wireless system to changing channel conditions can be advantageous. In the case of fast power control [2], the transmission power is adjusted based on channel fading. Under good channel conditions a relatively low transmission power is required to maintain the target signal quality at the receiver. The process of changing transmission parameters to compensate for variations in channel conditions is known as link adaptation. Besides power control, adaptive modulation

[1]The material in this chapter is largely based on the following:
(1) R. Kwan and C. Leung, "Optimal Downlink Scheduling Schemes for CDMA Networks." *Proc. of IEEE Wireless Communications and Networking Conference (WCNC'04)*, vol. 4, Atlanta, Georgia, March 2004.
(2) R. Kwan and C. Leung, "Downlink Scheduling Optimization in CDMA Networks." IEEE Communications Letters, vol. 8, No. 10, 2004.
(3) R. Kwan and C. Leung, "Channel-Based Downlink Scheduling Schemes for CDMA Networks." *Proc. of IEEE Vehicular Technology Conference (VTC'04)*, vol. 1, Los Angeles, California, Sept. 2004.
(4) R. Kwan and C. Leung, "Load-Based Downlink Scheduling Schemes for CDMA Networks." *Proc. of IEEE Vehicular Technology Conference (VTC'04)*, vol. 1, Los Angeles, California, Sept. 2004.

and coding (AMC) is another means for performing link adaptation [1, 3], and is used in the 3GPP HSDPA channel. The goal of AMC is to change the modulation and channel coding according to the varying channel conditions. In order to increase the bit rate, orthogonal multicode transmission is also used in the 3GPP standard [1, 2].

A scheme is proposed in [4] for maximizing the uplink throughput in a CDMA network by selecting the appropriate transmit powers and multicodes used by the mobile stations (MS's). In [5], the authors proposed a single user algorithm for selecting the MCS and the number of multicodes for HSDPA. In [6], the single user algorithm is applied sequentially for multiple users. In [7], it is found that the optimal strategy for scheduling downlink transmission in a CDMA network is to transmit to one MS at a time at full power rather than to transmit to several MS's simultaneously. This finding is based on a model which assumes that a linear relationship exists between the transmission bit rate and the transmit power for a fixed modulation scheme and error rate. This assumption is not valid when AMC is employed. The model also does not include any MS constraints such as maximum bit rate. In addition, in HSDPA [2], even though the orthogonal codes are used, orthogonality between two codes are not necessarily maintained due to multipath. In this chapter, a more realistic model is used to examine the problem of joint optimization using mathematical programming for multiple users in terms of MCS's schemes, number of multicodes, and transmit powers in the downlink of a CDMA system. This model is termed the *channel-based model*, which takes into account only the MS channel conditions. An optimization model which takes into account the amount of data in the MS buffers is also proposed. In this approach, the optimization takes into account both the MS channel conditions as well as the MS buffer sizes, and is termed the *load-based model* for simplicity.

Simple analytical models for the single MS optimization are also developed, which take into account AMC and multicodes, as well as the power and multicode constraints, without the use of mathematical programming. Based on the single MS analysis, a sequential optimization algorithm is described for the multiple MS scenario. The idea is to allocate

resources to MS's one at a time. Finally, the performance attainable with the proposed sequential optimization algorithm is compared to that obtainable with joint optimization.

2.2 System Model

We consider the model of a target base station, BS **A**, with a downlink high-speed traffic channel which employs AMC and multicodes. The downlink per-code signal-to-interference ratio (SIR), γ_i, at MS i, $i = 1, \ldots, L$, is given by

$$\gamma_i = \frac{h_i P_i / n_i}{I_i^{(r)}} = \frac{P_i / n_i}{\xi_i} \tag{2.1}$$

where P_i is the power that BS **A** has allocated for the traffic channel to MS i, and n_i is the number of multicodes allocated by BS **A** to MS i. The term ξ_i represents the ratio of the total received interference and noise power $I_i^{(r)}$ to the path gain h_i between BS **A** and MS i. It is assumed in (2.1) that each multicode of MS i is allocated the same power. We assume that the BS **A** performs a resource allocation once every scheduling period of duration T_a seconds, and the value of ξ_i is assumed to be constant during T_a.

In order to satisfy the block error rate (BLER) QoS requirement when MS i uses modulation and coding scheme (MCS) $j, j = 1, \ldots, J$, we require that $\gamma_i \geq \lambda_{i,j}$, where $\lambda_{i,j}$ is the SIR requirement for MCS j to achieve MS i's target BLER of ϵ_i. Using (2.1) and setting $\gamma_i = \lambda_{i,j}$, the minimum required power allocation $P_{i,j}(n_i)$ for MS i which employs MCS j with n_i multicodes is given by

$$P_{i,j}(n_i) = n_i \lambda_{i,j} \xi_i. \tag{2.2}$$

For a given target BLER value ϵ_0, $\lambda_{i,j}$ can be obtained from $f_j(\lambda_{i,j}) = \epsilon_0$, where $f_j(.)$ represents the BLER vs. SIR relationship for MCS j. The transmission bit rate to MS i

assuming MCS j and n_i multicodes is given by

$$R_{i,j} = n_i r_{i,j}, \tag{2.3}$$

where the basic bit rate $r_{i,j}$ is given by

$$r_{i,j} = \frac{W}{g} R_c^{(j)} \log_2 M_j. \tag{2.4}$$

In (2.4) W is the chip rate, $R_c^{(j)}$ is the code rate for MCS j, M_j is the number of points in the modulation constellation for MCS j and g is the spreading factor. For simplicity, it is assumed that all MS's use the same spreading factor. In this model, it is also assumed that the multipath interference due to the desired and interfering signals coming from BS **A** have the same effect on the detection of the desired signal, and that the allocation does not affect the interference.

2.3 Joint Optimization Model

2.3.1 Channel-Based Model

The objective is to maximize the sum of the bit rates assigned to all MS's for each scheduling period T_a, given a maximum allowable BS high-speed traffic channel power, P_{max}, a maximum number, N_{max}, of multicodes that the BS can allocate collectively to all MS's and certain per-MS constraints. Specifically, the optimization problem is formulated as a mixed integer, non-linear programming (MINLP) problem as follows:

$$\max_{\mathbf{a},\mathbf{n}} \left\{ \sum_{i=1}^{L} \sum_{j=1}^{J} a_{i,j} r_{i,j} n_i - \upsilon \right\}, \tag{2.5}$$

subject to

$$
\begin{aligned}
a_{i,j} &\in \{0,1\}, && (2.6)\\
\sum_{j=1}^{J} a_{i,j} &= 1, && (2.7)\\
n_i &\leq N_{i,max}, && (2.8)\\
\sum_{i=1}^{L} n_i &\leq N_{max}, && (2.9)\\
P_i &= \sum_{j=1}^{J} a_{i,j} P_{i,j}(n_i) = \sum_{j=1}^{J} a_{i,j} n_i \lambda_{i,j} \xi_i, && (2.10)\\
\sum_{i=1}^{L} P_i &\leq P_{max}. && (2.11)
\end{aligned}
$$

In (2.5) $\mathbf{a} = [a_{i,j}]$ is a L-by-J matrix, and $\mathbf{n} = [n_1, n_2, ..., n_L]$. The integer programming variable $a_{i,j}$ takes on value 1 if and only if MS i is to use MCS j. The parameter $N_{i,max}$ represents the maximum number of multicodes that MS i can be allocated and is typically less than N_{max} [1]. The term ρ is a factor which is introduced to minimize the required power and the number of multicodes needed in maximizing the total bit rate. It is convenient to use

$$
\upsilon = \tau\left(\frac{\sum_{i=1}^{L} P_i}{P_{max}} + \frac{\sum_{i=1}^{L} n_i}{N_{max}}\right) \qquad (2.12)
$$

where τ is a small constant, e.g. 10^{-3}, used to ensure that the factor υ has a negligible effect on the value of the objective function (2.5).

2.3.2 Load-Based Model

In section 2.3.1, the optimization model implicitly assumes that the buffer for each MS at the BS is never empty, i.e. there are always data to be sent to all MS's. In such a case, the transmit bit rate is identical to the assigned bit rate. However, this is not so if MS's are not always back-logged. It would be wasteful to assign more resources to an MS in a scheduling

period than what is needed to empty the MS's buffer. The problem of allocating resources should then take into account the amount of data waiting in the MS buffers.

In this section, we consider such an optimization problem and study the resulting efficiency gains. Similar to the channel-based model, we assume that the BS **A** performs a resource allocation once every scheduling period of duration T_a seconds and that new data arrive at the MS buffers only just before the start of a new scheduling period. The channel is assumed to be more or less constant during any T_a seconds. Let

$$R_i = \sum_{j=1}^{J} a_{ij} r_{ij} n_i, \quad \forall i = 1, \ldots, L \tag{2.13}$$

be the bit rate allocated to MS i. Let B_i be the number of bits in the buffer for MS i at the beginning of a scheduling period. For convenience, we define the normalized buffer size for MS i as

$$D_i = B_i / W T_a, \quad \forall i = 1, \ldots, L. \tag{2.14}$$

The optimization problem is then formulated as

$$\max_{\mathbf{a},\mathbf{P},\mathbf{n}} \left\{ \sum_{i=1}^{L} \min \left(\sum_{j=1}^{J} \frac{a_{ij} r_{ij} n_i}{W}, D_i \right) - \upsilon \right\}, \tag{2.15}$$

subject to (2.6)-(2.11).

Let $A_i = R_i T_a$ and Q_i denote the number of bits allocated and the number of bits actually sent to MS i during the scheduling period. We can write

$$Q_i = \min \{ A_i^*, B_i \}. \tag{2.16}$$

where $A_i^* = T_a R_i^*$ and R_i^* is the allocated bit rate for MS i with the optimal values a_{ij}^*, n_i^* and P_i^*. Denote the total number of bits sent and the total number of bits allocated

during the scheduling period by $Q = \sum_{i=1}^{L} Q_i$ and $A = \sum_{i=1}^{L} A_i$ respectively.

The total bit rate during the scheduling period is given by

$$R_{tot} = Q/T_a \tag{2.17}$$

$$= \sum_{i=1}^{L} \min(\sum_{j=1}^{J} a_{i,j}^* n_i^* r_{i,j}, D_i W) \tag{2.18}$$

Three other measures of the effectiveness of a scheduling scheme are useful. The scheduler efficiency, η, is defined as

$$\eta = Q/A. \tag{2.19}$$

and the scheduler deviation factor, ζ, is defined as

$$\zeta = \frac{1}{WT_a} \sum_{i=1}^{L} |A_i - B_i|. \tag{2.20}$$

The power efficiency η_p is defined as

$$\eta_p = \frac{R_{tot}}{\sum_{i=1}^{L} P_i}. \tag{2.21}$$

The term η is used to quantify the efficiency of the scheduling. Ideally, η should be as close to 1 as possible, so that the allocated resources are utilized efficiently. The term ζ is used to quantify the discrepancy between the normalized buffer size and the actual allocation. It is desirable to have as small a value of ζ as possible. The power efficiency η_p describes the total bit rate achieved per unit of power, and should be as high as possible.

2.3.3 Numerical Results

A model for the joint optimization of variable parameter values in a CDMA downlink high-speed traffic channel was formulated in Section 2.3.1. We now provide some numerical

results obtained by solving (2.5) using the linearized models described on the Appendix A. For illustration purposes, let the received total interference and noise power, $I_i^{(r)}$, for MS i be

$$I_i^{(r)} = \alpha h_i P_T + \sum_{k \in \mathcal{B}} I_k h_{k,i} + I_N, \tag{2.22}$$

where P_T is the total transmit power of the target BS $\mathbf{A}$, I_k is the transmit interference power due to the k^{th} BS in the interfering BS set $\mathcal{B}$ and I_N is the background noise power. The term $h_{k,i}$ is the path gain from interfering BS k to MS i. The orthogonality factor, α, is used to model possible intra-cell interference. Correspondingly, ξ_i is given by

$$\xi_i = \alpha P_T + \sum_{k \in \mathcal{B}} I_k h_{k,i}/h_i + I_N/h_i, \tag{2.23}$$

$$= \alpha P_T + \sum_{k \in \mathcal{B}} I_k v_{k,i} + I_N/h_i, \tag{2.24}$$

where $v_{k,i} = h_{k,i}/h_i$. To simplify the presentation of results, we assume that there is only one BS in the interfering BS set $\mathcal{B}$, and that the effect of background noise is negligible.

The default parameter values used are listed in Table 2.1. For the results obtained in this section, the value $v_{1i} = 0.0016$ is used. Fig. 2.1 shows the total bit rate, $R_{tot} = \sum_{i=1}^{L} R_i^*$, for the optimal values of $\mathbf{a}, \mathbf{P}, \mathbf{n}$ as a function of the maximum allowable power P_{max}, with $\alpha = 0.1$ and 0.4 for both a continuous and an integer number of multicodes, assuming that the MS buffers are backlogged. It can be seen that the commonly used, but unrealistic assumption of a continuous number of multicodes results in a slight overestimation of the total bit rate.

Fig. 2.2 shows the allocated MS powers as a function of P_{max}. Depending on the values of α and P_{max}, the BS may transmit to only one MS or to several MS's simultaneously. We note that this finding differs from that in [7] which states that the BS should only transmit to one MS at a time in order to reduce the intra-cell interference. The difference is due to

three main factors: (1) the non-linear relationship between the allowed user bit rate R_i and power P_i when AMC is used, (2) the absence in [7] of any constraints on the bit rates or powers which can be allocated to MS's, and (3) the difference between SIR expressions in (2.1) and [7]. In our model, an increase in P_i does not necessarily yield an increase in R_i. An incremental increase in P_{max} causes a power reallocation among the MS's in such a way as to realize the greatest incremental increase in bit rate. It can be seen that for $\alpha = 0.1$ the power allocated for transmission to MS 1 saturates at 7.2 W. This can be explained as follows: when P_{max} reaches 12.9 W, MS 1 is using the maximum number of multicodes. The total bit rate, R_{tot}, is plotted as a function of P_{max} for $\alpha = 0.1$ and 0.4 in Fig. 2.3. Curves for two cases are shown: in Case 1, the BS is constrained to only transmit to one MS at a time whereas in Case 2 it can transmit to any number of MS's at a time. It can be seen that R_{tot} can be significantly higher in Case 2 compared to Case 1. For example, for $\alpha = 0.1$ and $P_{max} = 14.0$ watts, $R_{tot} = 8.4$ Mbps for Case 2; this value drops to 3.6 Mbps if transmission is restricted to one MS at a time as in Case 1.

The results shown in Fig. 2.4 are for $\alpha = 0.1$, and $\mathbf{v_1} = (0.007 \;\; 0.0065 \;\; 0.006)$ where the ith component of $\mathbf{v_1}$ is the ratio of the path gains for the interfering BS and own BS of MS i. Assume a maximum of 3 MS's are allocated resources at the beginning of every scheduling period. The buffer content size ratio vector for the three MS's with respect to the first MS is $\mathbf{D}/D_1 = (D_1 \;\; D_2 \;\; D_3)/D_1 = (1 \;\; 2.2 \;\; 3.5)$. The top part of Fig. 2.4 shows the total bit rate R_{tot} as given in (2.18) as a function of total normalized buffer content size $D = \sum_{i=1}^{L} D_i$ for both the basic (channel-based) and load-based models[2]. It can be seen that a modest bit rate increase can be obtained with load based optimization. It might be noted that due to the limit on the available power and the number of multicodes, the total bit rate approaches a limiting value as D is increased. The bottom part of Fig. 2.4 shows the scheduler efficiency as a function of D. The load based optimization may result in a much

[2]For the basic model, the values for $a^*_{i,j}$ and n^*_i are obtained based on (2.5), so that the assignments are independent on the MS buffer sizes.

higher efficiency even though the difference in bit rates of the basic and load-based models is relatively small. This is because some of the allocated rates in the basic model may be much higher than the corresponding rates in the load-based model.

Fig. 2.5 is similar to Fig. 2.4, except that $\mathbf{v_1} = (0.005 \;\; 0.006 \;\; 0.008)$. In this case, the MS with the best channel condition among the three MS's, i.e. MS 1, has the smallest buffer content size. Since the basic scheduler only takes the channel condition into account, the highest bit rate would naturally be assigned to MS 1. However, MS 1 has the least amount of data to send and may not fully utilize its allocated amount. As a result, Fig. 2.5 shows that the load-based scheduler yields a significantly higher bit rate than the basic scheduler.

Fig. 2.6 shows the power efficiency η_p as a function of total normalized buffer content size D for $\alpha = 0.1$, $\mathbf{D}/D_1 = (1 \;\; 2.2 \;\; 3.5)$ and $\mathbf{v_1} = (0.007 \;\; 0.0065 \;\; 0.006)$ for both the basic and load-based models. Fig. 2.7 is similar to Fig. 2.6, except that $\mathbf{v_1} = (0.005 \;\; 0.006 \;\; 0.008)$. In both cases, the value of η_p is higher for the load-based scheduler as compared to the basic scheduler. The reason is that the former attempts to allocate resources taking into account the load information. Thus, less resources will generally be allocated to an MS with a smaller amount of data to transmit. Without knowing the load information, the basic scheduler allocates the same resources regardless of the amount of data in the MS buffers. As a result, extra resources may be unnecessarily allocated. Since the allocated rates for the load-based scheduler depend on D, the discrete nature of the AMC and multicodes gives rise to the fluctuations in the curve for the load-based scheduler.

Fig. 2.8 shows the deviation factor ζ as a function of total normalized buffer content size D for $\alpha = 0.1$, $\mathbf{D}/D_1 = (1 \;\; 2.2 \;\; 3.5)$ for both the basic and load-based models. The top part of Fig. 2.8 corresponds to $\mathbf{v_1} = (0.007 \;\; 0.0065 \;\; 0.006)$, while the bottom part corresponds to $\mathbf{v_1} = (0.005 \;\; 0.006 \;\; 0.008)$. From the definition, when ζ is small, there is little difference between the number of allocated bits and the actual number of bits in the buffer at the beginning of a scheduling period. Ideally, ζ should be as close to zero as possible. However, this may not always be possible due to the following reason: when the traffic load is high,

the amount of data in the buffers exceed what can be allocated given the available resources. As shown in Fig. 2.8, the load-based scheduler has a significantly smaller deviation factor compared to the basic scheduler at low to moderate traffic loads. At high traffic load, both schedulers can only deliver a small portion of data in the buffer during T_a due to the limited available resources, and the deviation factors increase. The deviation factors for the two schedulers approach one another at high load. This is because when the buffers are always back-logged the basic and load-based schedulers produce the same resource allocation.

Parameter	Value
MCS	QPSK(1/2, 3/4), 16-QAM(1/2, 3/4)
Channel Coding	Turbo Code
Chip rate (W)	3.84 Mcps
Spreading Factor (g)	16
N_{max}	15
P_T	18 watts
I_1	18 watts
α	0.1
τ	0.001
I_N	negligible
ϵ_0	$\sim 10^{-3}$

Table 2.1: List of parameter values.

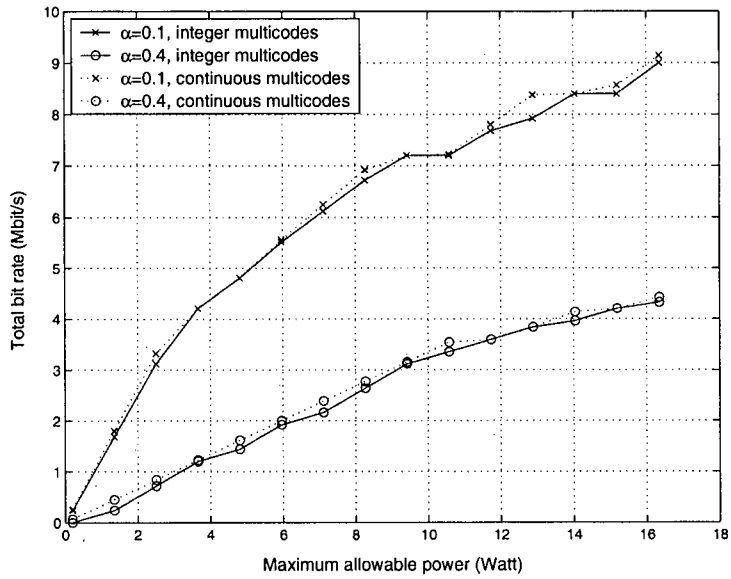

Figure 2.1: Total bit rate as a function of the maximum allowable power, P_{max}, for $\alpha = 0.1$ and 0.4, assuming an integer and a continuous number of multicodes.

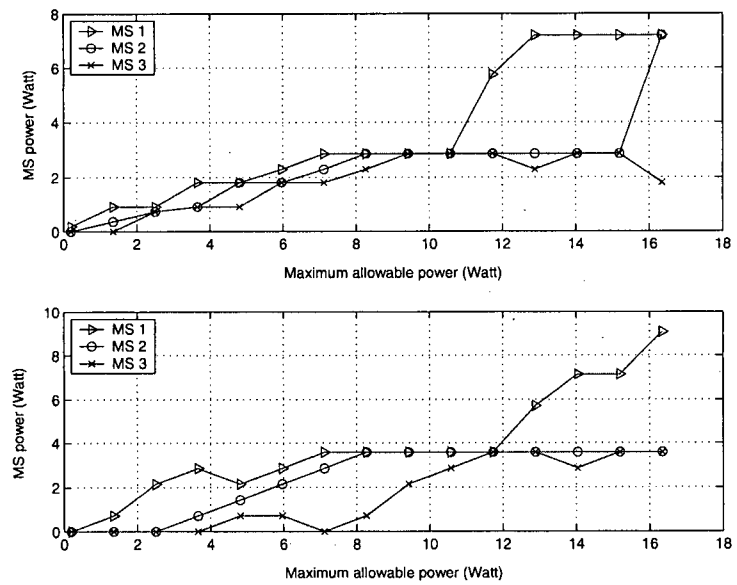

Figure 2.2: Allocated MS power as a function of the maximum allowable power, P_{max}. Top: $\alpha = 0.1$, Bottom: $\alpha = 0.4$, assuming an integer number of multicodes.

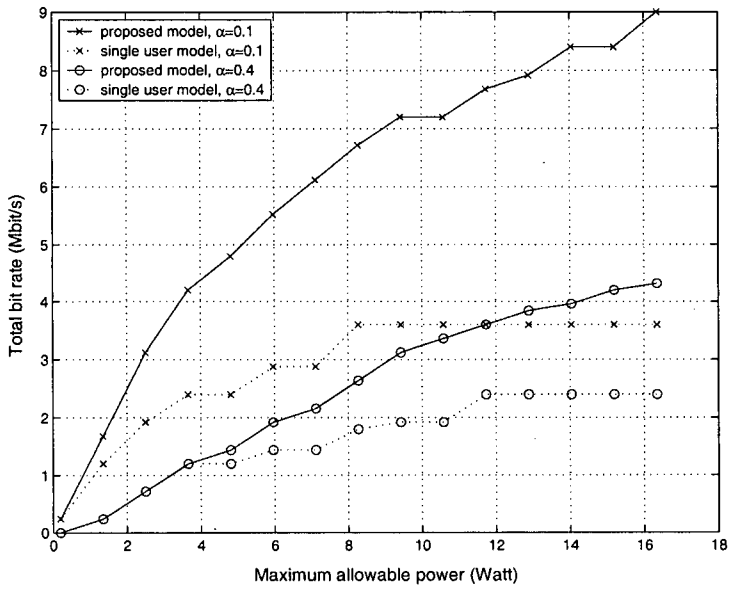

Figure 2.3: Total bit rate as a function of the maximum allowable power, P_{max} at $\alpha = 0.1$ and 0.4 for the proposed model and the single user model, assuming an integer number of multicodes.

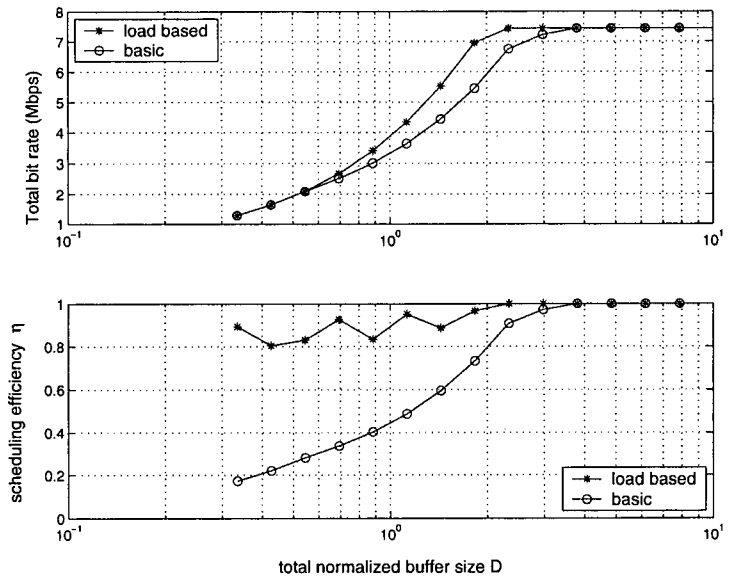

Figure 2.4: (Top) Total bit rate R_{tot} (Bottom) Scheduler efficiency η as a function of total normalized buffer size D for $\alpha = 0.1$, $P_{max} = 10W$, $N_{i,max} = 10$, $\mathbf{D}/D_1 = (1 \ \ 2.2 \ \ 3.5)$ and $\mathbf{v_1} = (0.007 \ \ 0.0065 \ \ 0.006)$ for both basic and load-based models.

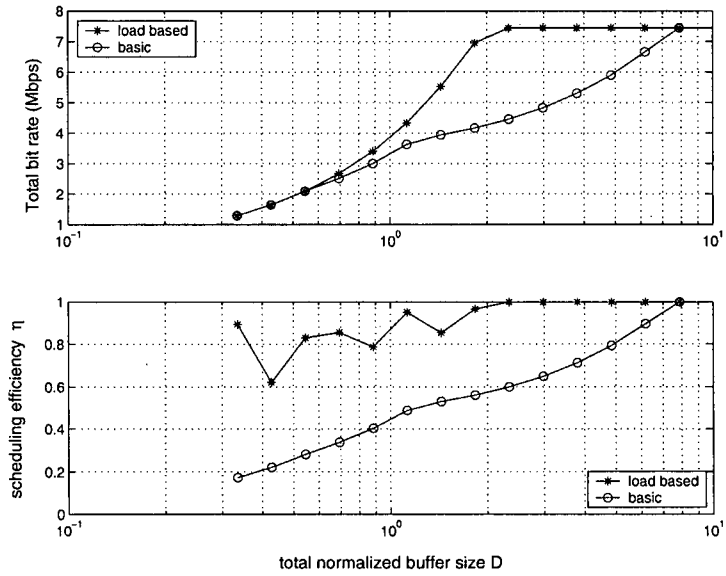

Figure 2.5: (Top) Total bit rate R_{tot} (Bottom) Scheduler efficiency η as a function of total normalized buffer size D for $\alpha = 0.1$, $P_{max} = 10W$, $N_{i,max} = 10$, $\mathbf{D}/D_1 = (1 \ \ 2.2 \ \ 3.5)$ and $\mathbf{v_1} = (0.005 \ \ 0.006 \ \ 0.008)$ for both basic and load-based models.

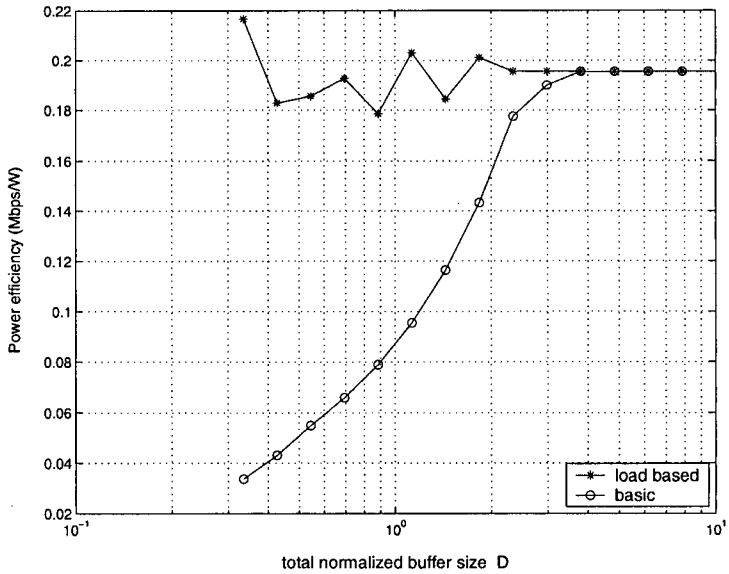

Figure 2.6: Power efficiency η_p as a function of total normalized buffer size D for $\alpha = 0.1$, $P_{max} = 10W$, $N_{i,max} = 10$, $\mathbf{D}/D_1 = (1 \ \ 2.2 \ \ 3.5)$ and $\mathbf{v_1} = (0.007 \ \ 0.0065 \ \ 0.006)$ for both basic and load-based models.

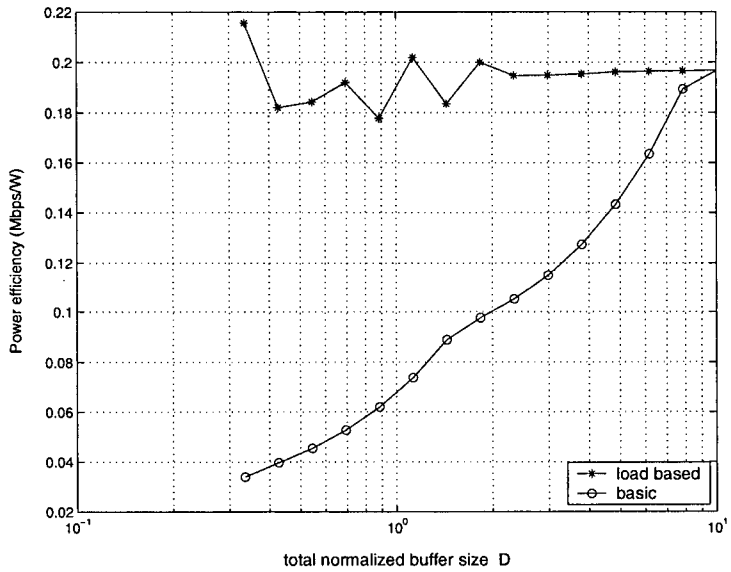

Figure 2.7: Power efficiency η_p as a function of total normalized buffer size D for $\alpha = 0.1$, $P_{max} = 10W$, $N_{i,max} = 10$, $\mathbf{D}/D_1 = (1 \quad 2.2 \quad 3.5)$ and $\mathbf{v_1} = (0.005 \quad 0.006 \quad 0.008)$ for both basic and load-based models.

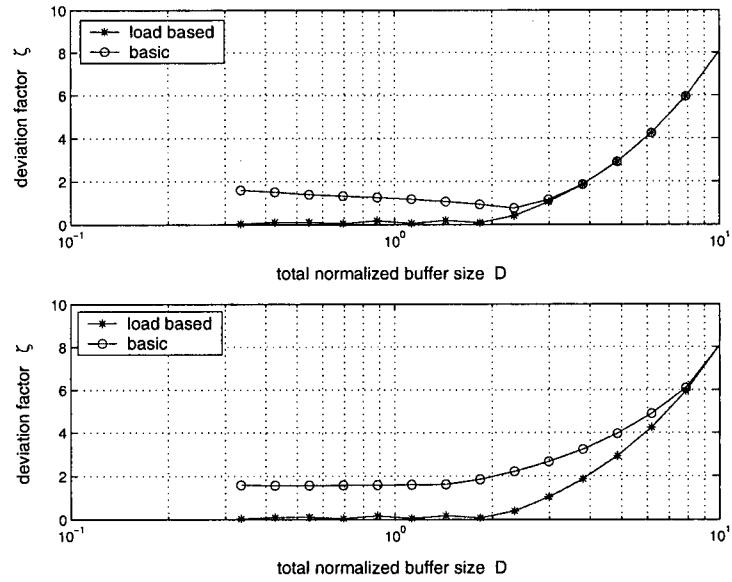

Figure 2.8: Deviation factor ζ as a function of total normalized buffer size D for $\alpha = 0.1$, $P_{max} = 10W$, $N_{i,max} = 10$, $\mathbf{D}/D_1 = (1 \quad 2.2 \quad 3.5)$ and (Top) $\mathbf{v_1} = (0.007 \quad 0.0065 \quad 0.006)$ (Bottom) $\mathbf{v_1} = (0.005 \quad 0.006 \quad 0.008)$ for both basic and load-based models.

2.4 Sequential Optimization Model

In section 2.3, an optimization approach was used which jointly optimizes the power, number of multicodes and MCS for each MS and implicitly, the number of MS's which are allocated resources in order to maximize the allocated bit rate for the system. While this may be a desirable goal, the computational complexity associated with mixed-integer, nonlinear programming (MINLP) can be high [8]. One way to reduce the computational burden is to independently optimize the bit rate for each MS instead of optimizing the sum of the bit rates for all MS's. After allocating resources for the first MS, the optimization for the next MS is based on the remaining resources. Such a sequential optimization (SO) technique can lower the computational complexity by allowing the optimization to be done independently for each MS. However, the optimized sum of the MS bit rates is generally higher than the sum of the optimized MS bit rates. This optimization is used in the multiple MS sequential optimization algorithm described in sections 2.4.1 and 2.4.2 for the channel-based and load-based optimization models respectively.

2.4.1 Channel-based Model

Single MS Optimization - Continuous Number of Multicodes

Let the downlink maximum possible received signal-to-interference ratio (SIR) of MS i be given by

$$\gamma_i' = \hat{P}_i/\xi_i, \tag{2.25}$$

where $\hat{P}_i$ is the power available to MS i. Assuming that multicode transmission is used, that the number of multicodes is continuous, and that all codes share the power equally, the maximum number, $\tilde{N}_{i,j}$, of codes that can be transmitted while achieving the target BLER

of ϵ_0 for each code is given by

$$\tilde{N}_{i,j} = \min\left(\frac{\gamma_i'}{\lambda_{i,j}}, N_{i,max}\right). \tag{2.26}$$

The bit rate for MS i with MCS j given $\tilde{N}_{i,j}$ multicodes would be

$$R_{i,j} = r_{i,j}\tilde{N}_{i,j}, \tag{2.27}$$

$$= \begin{cases} r_{i,j}\left(\frac{\gamma_i'}{\lambda_{i,j}}\right), & \text{if } \gamma_i' < \lambda_{i,j}N_{i,max}, \\ r_{i,j}N_{i,max}, & \text{if } \gamma_i' \geq \lambda_{i,j}N_{i,max}. \end{cases} \tag{2.28}$$

where the basic bit rate $r_{i,j}$ is given in (2.4).

In the model, it is assumed that $\{\lambda_{i,j} < \lambda_{i,j+1},\ j = 1, ..., J-1\}$, and $\{r_{i,j} < r_{i,j+1},\ j = 1, ..., J-1\}$, which are realistic in practical applications of AMC. It is also assumed that the ratio $r_{i,j}/\lambda_{i,j}$ decreases with j [2]. With the combination of AMC and multicodes, at a given γ_i', the optimal MS bit rate R_i is the maximum bit rate that can be provided among all MCS's, i.e.

$$R_i = \max_{j\in\{1,...,J\}} R_{i,j}. \tag{2.29}$$

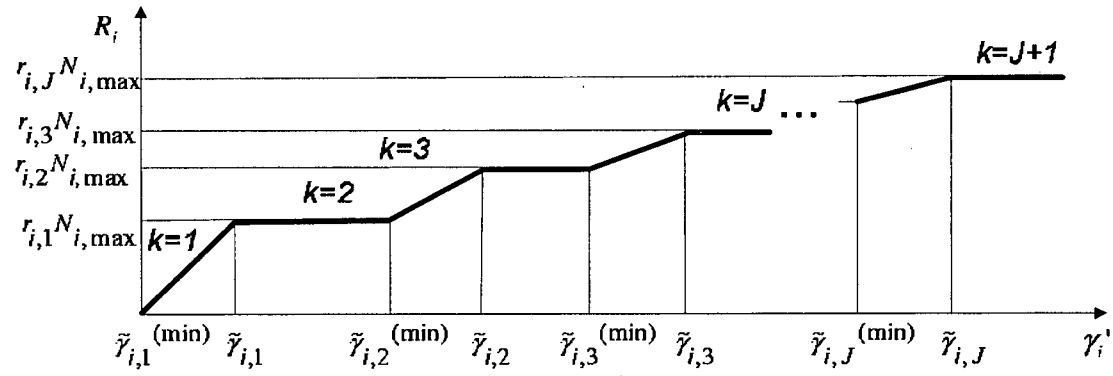

Figure 2.9: Allocated MS bit rate as a function of γ_i'.

A typical plot of R_i as a function of γ_i' is shown in Fig. 2.9. As γ_i' increases from 0, an

increasing number of multicodes can be utilized, resulting in an increase in R_i. For γ_i' close to 0, MCS 1 would be used due to the poorer error performance of higher order MCS's. As γ_i' reaches $\tilde{\gamma}_{i,1}$, the maximum number, $N_{i,max}$, of multicodes allowed for MS i is used. Further increase in γ_i' does not allow a higher number of multicodes to be allocated. At this stage, the next higher order MCS still gives a lower bit rate due to the poorer error performance. When γ_i' reaches $\tilde{\gamma}_{i,2}^{(min)}$, $j = 2$ (i.e. MCS 2) is selected, and $R_i = R_{i,2}$. In a similar way, R_i increases with increasing γ_i' until $j = J$ and $N_{i,max}$ is reached. Therefore, given γ_i', the problem of evaluating R_i reduces to determining the set of thresholds $\{\tilde{\gamma}_{i,j}, \forall j = 1, ..., J\}$ and $\{\tilde{\gamma}_{i,j}^{(min)}, \forall j = 1, ..., J\}$.

The threshold $\tilde{\gamma}_{i,j}$ is given by

$$\tilde{\gamma}_{i,j} = \lambda_{i,j} N_{i,max}, j = 1, ..., J. \tag{2.30}$$

The threshold $\tilde{\gamma}_{i,j}^{(min)}$ can be obtained by solving the equation relating the highest effective bit rate of the MCS $j-1$ with the lowest effective bit rate of the MCS j. Thus,

$$N_{i,max} r_{i,j-1} = r_{i,j} \frac{\tilde{\gamma}_{i,j}^{(min)}}{\lambda_{i,j}}, j = 2, ...J, \tag{2.31}$$

which yields

$$\tilde{\gamma}_{i,j}^{(min)} = \lambda_{i,j} \frac{r_{i,j-1}}{r_{i,j}} N_{i,max}, j = 2, ..., J. \tag{2.32}$$

It might be noted that $\tilde{\gamma}_{i,1}^{(min)} = 0$ and $\tilde{\gamma}_{i,J+1}^{(min)} = \infty$. The optimal number, N_i, of multicodes for MS i is given by

$$n_i = \begin{cases} \gamma_i'/\lambda_{i,j}\ ,\ \tilde{\gamma}_{i,j}^{(min)} \leq \gamma_i' < \tilde{\gamma}_{i,j},\ 1 \leq j \leq J \\ N_{i,max}\ ,\ \tilde{\gamma}_{i,j} \leq \gamma_i' < \tilde{\gamma}_{i,j+1}^{(min)},\ 1 \leq j \leq J. \end{cases} \tag{2.33}$$

Subsequently, the optimal single MS bit rate R_i and transmit power P_i are given by

$$R_i = r_{i,j} n_i, \tag{2.34}$$

$$P_i = \lambda_{i,j} n_i \xi_i. \tag{2.35}$$

Note that the index j in (2.34) and (2.35) is selected based on a suitable value obtained in (2.33).

Integer Number of Multicodes

With an integer number of multicodes, the optimization becomes difficult due to the fact that the range of γ_i' over which MCS j is optimal may consist of several disjoint intervals. We consider here a procedure which gives near optimal results. The term $\tilde{\gamma}_{i,j}^{(min)}$ can be obtained as follows. Let $\beta_{i,j} \in (0, \infty)$ be the smallest value such that

$$r_{i,j} \left\lfloor \frac{\beta_{i,j}}{\lambda_{i,j}} \right\rfloor \geq r_{i,j-1} N_{i,max}, \quad 2 \leq j \leq J. \tag{2.36}$$

Then

$$\tilde{\gamma}_{i,j}^{(min)} = \begin{cases} 0 & , \ j = 1 \\ \beta_{i,j} & , \ 1 < j \leq J \\ \infty & , \ j = J+1. \end{cases} \tag{2.37}$$

The number, n_i, of multicodes for MS i is now given by

$$n_i = \begin{cases} \lfloor \gamma_i'/\lambda_{i,j} \rfloor & , \ \tilde{\gamma}_{i,j}^{(min)} \leq \gamma_i' < \tilde{\gamma}_{i,j}, \ 1 \leq j \leq J \\ N_{i,max} & , \ \tilde{\gamma}_{i,j} \leq \gamma_i' < \tilde{\gamma}_{i,j+1}^{(min)}, \ 1 \leq j \leq J. \end{cases} \tag{2.38}$$

Using (2.38), the power P_i and bit rate R_i allocated to MS i are given by (2.35) and (2.34) respectively.

Multi-MS Sequential Optimization

In section 2.4.1, we considered the channel-based optimization of MCS and number of multicodes for a single MS. The joint optimization for many MS's can be computationally complex. Based on the results for a single MS, we now consider a (sub-optimal) successive optimization procedure which takes into account multiple MS's at each scheduling instant. The main idea is to schedule each MS independently based on the available remaining resources. Generally, to maximize the assigned total bit rate, the MS's should be ordered accordingly to channel conditions with the first MS having the best channel condition. The procedure is outlined in the following:

1. Set $i = 1$
2. Set $\hat{P}_i = P_{max}$, and $N_{i,max} = \min\{N_{i,max}, N_{max}\}$
3. Compute $\tilde{\gamma}_{i,j}$ as given in (2.30), and $\tilde{\gamma}_{i,j}^{(min)}$ as given in (2.32) for the continuous case or (2.37) for the integer case
4. Using (2.33) or (2.38), (2.34) and (2.35), compute the number of multicodes n_i, the bit rate R_i, and the power P_i allocated to MS i
5. Calculate the remaining resources

$$N_{max} \longleftarrow N_{max} - n_i, \tag{2.39}$$

$$P_{max} \longleftarrow P_{max} - P_i. \tag{2.40}$$

6. If $N_{max} > 0$ and $P_{max} > 0$, increment i by 1 and go to step 2; otherwise go to step 7
7. Prepare for the next scheduling period.

2.4.2 Load-Based Model

Single MS Optimization - Continuous Number of Multicodes

If packets arrive at the buffers for the different MS's in a random fashion, the buffer content sizes can be taken into account to improve resource allocation. Given that the normalized buffer content size for MS i is D_i, the bit rate required to empty the buffer in T_a second is D_iW. Furthermore, let $C_{i,k}^{(r)}, k = 1, 2, \ldots, J+1$ be the event that D_iW falls in the k th bit rate region shown in Fig. 2.9, i.e.

$$r_{i,k-1}N_{i,max} < D_iW \leq r_{i,k}N_{i,max}, k = 1, 2, \ldots, J+1, \tag{2.41}$$

where $r_{i,0} = 0$ and $r_{i,J+1} = \infty$.

The basic idea behind load-based scheduling is to tailor the number of multicodes and power depending upon the bit rate region which D_iW falls into. We choose to maximize the allocated bit rate R_i while using the minimum amount of power. An alternative is to maximize R_i using the minimum number of multicodes. The required number, $n_i^{(r)}$, of multicodes, the MS bit rate $r_i^{(r)}$, and the MS power $P_i^{(r)}$ are given by

$$n_i^{(r)} = \begin{cases} (D_iW)/r_{i,k}, & \text{if } C_{i,k}^{(r)}, k = 1, 2, \ldots, J, \\ N_{i,max}, & \text{if } C_{i,k}^{(r)}, k = J+1, \end{cases} \tag{2.42}$$

$$r_i^{(r)} = r_{i,j}\, n_i^{(r)}, \tag{2.43}$$

$$P_i^{(r)} = \lambda_{i,j}\, n_i^{(r)} \xi_i, \tag{2.44}$$

and the selected MCS j is given by

$$j = \min(k, J) \text{ if } C_{i,k}^{(r)}, k = 1, 2, \ldots, J+1. \tag{2.45}$$

The corresponding required SIR is given by

$$\gamma_i^{(r)} = P_i^{(r)}/\xi_i. \tag{2.46}$$

When power resources are unlimited, (2.42), (2.43), and (2.44) are optimal given the buffer content size B_i. However, due to the varying channel conditions, the available γ_i' might not be able to support what is required from (2.46). Under such a circumstance, the allocation of resources should not only reflect the buffer content size B_i, but also the available SIR γ_i'. Let $\mathcal{C}_{i,j}$ and $\overline{\mathcal{C}_{i,j}}$ be the conditions such that

$$\mathcal{C}_{i,j} \equiv \tilde{\gamma}_{i,j}^{(min)} \leq \gamma_i' \leq \tilde{\gamma}_{i,j},\ 1 \leq j \leq J \tag{2.47}$$

$$\overline{\mathcal{C}_{i,j}} \equiv \tilde{\gamma}_{i,j} \leq \gamma_i' \leq \tilde{\gamma}_{i,j+1}^{(min)},\ 1 \leq j \leq J \tag{2.48}$$

are true. The resulting optimal number, n_i, of multicodes, the bit rate R_i, and the power P_i for MS i are given by

$$n_i = \begin{cases} n_i^{(r)}, & \text{if } \gamma_i{}^{(r)} \leq \gamma_i', \\ \frac{\hat{P}_i}{\lambda_{i,j}\xi_i}, & \text{if } (\gamma_i{}^{(r)} > \gamma_i') \wedge \mathcal{C}_{i,j}, \\ N_{i,max}, & \text{if } (\gamma_i{}^{(r)} > \gamma_i') \wedge \overline{\mathcal{C}_{i,j}}. \end{cases} \tag{2.49}$$

$$R_i = r_{i,j} n_i, \tag{2.50}$$

$$P_i = \lambda_{i,j} n_i \xi_i. \tag{2.51}$$

Integer Number of Multicodes

With an integer number of multicodes, the optimization becomes difficult due to the fact that the range of γ_i' over which MCS j is optimal may consist of several disjoint intervals. We consider here a procedure which gives near optimal results.

The term $\tilde{\gamma}_{i,j}^{(min)}$ can be obtained as follows. Let $\beta_{i,j} \in (0, \infty)$ be the smallest value such

that

$$r_{i,j}\left\lfloor\frac{\beta_{i,j}}{\lambda_{i,j}}\right\rfloor \geq r_{i,j-1}N_{i,max}, \quad 2 \leq j \leq J, \tag{2.52}$$

and is given by

$$\tilde{\gamma}_{i,j}^{(min)} = \begin{cases} 0 \quad , j = 1 \\ \beta_{i,j} \ , \ 1 < j \leq J \\ \infty \quad , j = J+1. \end{cases} \tag{2.53}$$

Due to the discrete nature of the multicodes, (2.42) must be modified. The desired number of multicodes for MS i is given by

$$n_i^{(r)} = \begin{cases} \lceil (D_i W)/r_{i,k} \rceil, & \text{if } \mathcal{C}_{i,k}^{(r)}, 1 \leq k \leq J, \\ N_{i,max}, & \text{if } \mathcal{C}_{i,k}^{(r)}, k = J+1. \end{cases} \tag{2.54}$$

Again, due to the available γ_i' for MS i, the desired power P_i and number of multicodes $n_i^{(r)}$ may not always be allocated. Taking γ_i' into account, the resulting number of multicodes n_i', bit rate R_i', and power P_i' are given by

$$n_i' = \begin{cases} n_i^{(r)}, & \text{if } \gamma_i^{(r)} \leq \gamma_i', \\ \lfloor \frac{\hat{P}_i}{\lambda_{i,j}\xi_i} \rfloor, & \text{if } (\gamma_i^{(r)} > \gamma_i') \wedge \mathcal{C}_{i,j}, \\ N_{i,max}, & \text{if } (\gamma_i^{(r)} > \gamma_i') \wedge \overline{\mathcal{C}_{i,j}}. \end{cases} \tag{2.55}$$

$$R_i' = r_{i,j} n_i', \tag{2.56}$$

$$P_i' = \lambda_{i,j} n_i' \xi_i. \tag{2.57}$$

Let j be the selected MCS. Due to the function $\lfloor . \rfloor$ in (2.55), the performance can still be

improved when the condition

$$C_{i,j}^{(q)} \equiv (r_{i,j-1}N_{i,max} > R_i') \wedge (\lambda_{i,j-1}N_{i,max} \leq \gamma_i'), \quad j = 2, ..., J \tag{2.58}$$

is taken into account. The number of multicodes n_i, bit rate R_i, and power P_i are given by

$$n_i = \begin{cases} n_i', & \text{if } \overline{C_{i,j}^{(q)}}, \\ N_{i,max}, & \text{if } C_{i,j}^{(q)}. \end{cases} \tag{2.59}$$

$$R_i = \begin{cases} R_i', & \text{if } \overline{C_{i,j}^{(q)}}, \\ r_{i,j-1}N_{i,max}, & \text{if } C_{i,j}^{(q)}. \end{cases} \tag{2.60}$$

$$P_i = \begin{cases} P_i', & \text{if } \overline{C_{i,j}^{(q)}}, \\ \lambda_{i,j-1}N_{i,max}\ \xi_i, & \text{if } C_{i,j}^{(q)}. \end{cases} \tag{2.61}$$

Subsequently, the required SIR for MS i would then be $\gamma_i = P_i/\xi_i$.

Multi-MS Sequential Optimization

The multi-MS sequential optimization for the load-based system is similar to that described in section 2.4.1, except that (2.49)-(2.51) or (2.59)-(2.61) are used instead in step 4. The total bit rate R_{tot} is given by

$$R_{tot} = \sum_{i=1}^{L} \min\left(R_i, D_i W\right), \tag{2.62}$$

where R_i is given in (2.50) or (2.60) for continuous or discrete multicodes respectively.

Due to differences in the channel conditions and buffer content sizes among the MS's, the order of resource allocation to the MS's will generally affect the total allocated bit rate. The optimal ordering can be determined exactly by exhaustive search when the number of

MS's is small[3], or heuristically using a combinatorial technique [9] such as *Tabu search* when the number of MS's is large.

2.4.3 Numerical Results

Channel-Based Model

Using the default parameter values listed in Table 2.1, we now provide some numerical results obtained by solving (2.5) for the joint optimization, and the procedure outlined in section 2.4.1 for the sequential optimization. Fig. 2.10 shows the total bit rate $R_{tot} = \sum_{i=1}^{L} R_i$ as a function of P_{max} when $\mathbf{v_1} = [v_{1,1}\ v_{1,2}\ v_{1,3}] = [0.005\ 0.006\ 0.007]$ and $N_{i,max} = 5$ for both joint and sequential optimization, assuming a continuous and an integer number of multicodes. As P_{max} increases, higher order MCS's can be supported. As a result, higher bit rates can be obtained. As expected, the R_{tot} obtained from joint optimization is always superior to that obtained from sequential optimization. With joint optimization, R_{tot} increases monotonically with P_{max}. The joint optimization model ensures that just enough power is allocated to maximize the total bit rate. Thus, increasing P_{max} will not result in a decrease in R_{tot}. On the other hand, the sequential optimization procedure does not guarantee that R_{tot} increases monotonically with P_{max}. A scenario is possible in which increasing P_{max} results in the first MS taking most if not all of the power available to achieve a certain bit rate. However, if P_{max} is slightly reduced, the first MS might require much less power, leaving enough power for the second MS so that the combined bit rate for both MS's might exceed that of the MS in the first scenario. It can also be observed that for joint optimization, a continuous number of multicodes typically provides a slightly higher bit rate than the integer number of multicodes case. In contrast, for sequential optimization, the bit rate with an integer number of multicodes can be higher and the difference in R_{tot} can be much bigger.

[3]This case may generally be valid in the context of HSDPA since with a fixed spreading factor of 16, the number of multicodes, and hence the number of simultaneously supported MS's, is limited [1].

Fig. 2.11 shows the power efficiency η_p as a function of P_{max} when $\mathbf{v_1}$ = [0.005 0.006 0.007] for both joint and sequential optimizations. As expected, a higher bit rate can be achieved using a higher order MCS at the expense of a higher transmit power. It can be seen that η_p decreases monotonically with P_{max} for joint optimization. This is not always true for sequential optimization.

Fig. 2.12 shows the total bit rate R_{tot} as a function of P_{max} for joint and sequential optimization for two different channel conditions (case 1) $\mathbf{v_1}$ = [0.8 0.8 0.8] and (case 2) $\mathbf{v_1}$ = [0.005 0.005 0.005]. It can be seen that even though joint optimization can provide a significantly higher bit rate R_{tot} compared to sequential optimization when the channel conditions are good (i.e. case 2), the improvement is relatively small when the channel conditions are poor (i.e. case 1). The reason is that when the interference level is high, the limited resources can be allocated to fewer MS's.

Fig. 2.13 shows R_{tot} as a function of P_{max} when $\mathbf{v_1}$ = [0.2 0.6 0.9] for joint optimization, and (case 1) $\mathbf{v_1}$ = [0.2 0.6 0.9] and (case 2) $\mathbf{v_1}$ = [0.9 0.6 0.2] for sequential optimization. The result shows that the order of allocation of resources to MS's based on their channel conditions is important for sequential optimization. It also suggests that a higher assigned total bit rate can generally be achieved when the MS's are ordered according to their channel conditions with the first MS having the best channel condition.

It is interesting to compare the system performance obtained by our channel-based optimization model with a more restrictive sequential optimization model presented in [6], in which the maximum allowable power is shared equally among the MS's. This model can be viewed as a special case of our proposed sequential model. The performance of this model is evaluated using simulations in [6]. In order to distinguish the model [6] from our model, the former will be referred to as sequential optimization with equal power allocation (SO-EPA), while latter is simply referred to as sequential optimization (SO).

Figs. 2.14 and 2.15 show the total bit rate R_{tot} as a function of the maximum allowable power P_{max} with $\mathbf{v_1}$ = [0.005 0.006 0.007] for JO, SO, and SO-SPA, for $N_{i,max}$ = 5 and

$N_{i,max} = 10$ respectively. As shown in Fig. 2.14, SO does not necessarily perform better than SO-SPA. In this example, the first MS has the best channel quality, followed by the second MS and then the third MS. Since the maximum number, $N_{1,max}$, of multicodes is 5, SO attempts to achieve a higher bit rate for the first MS using a higher order MCS, which, in turn, requires a higher power allocation. As a result, less power is available to MS 2 and MS 3, and their available multicodes may not be fully utilized. Since the available power is shared equally under SO-EPA, a higher multicode utilization can be achieved. Since it is more power efficient to increase bit rate using more multicodes than higher order modulations [5], SO is not necessarily better than SO-SPA when $N_{i,max}$ or P_{max} is small. However, for larger values of $N_{i,max}$ or P_{max}, the performance of SO is generally better than that of SO-SPA as shown in Fig. 2.15. In all cases, JO outperforms both SO and SO-SPA as expected.

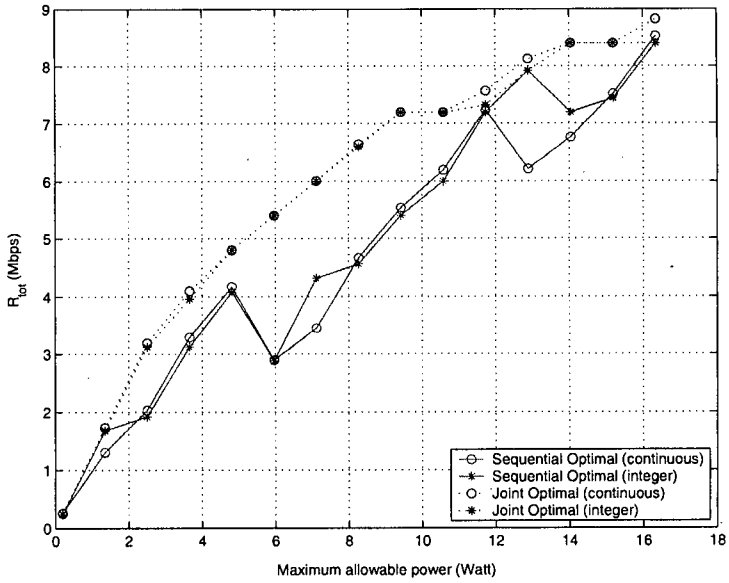

Figure 2.10: Total bit rate R_{tot} as a function of the maximum allowable power P_{max} with $\mathbf{v_1} =$ [0.005 0.006 0.007] for both joint and sequential optimization, assuming a continuous and an integer number of multicodes.

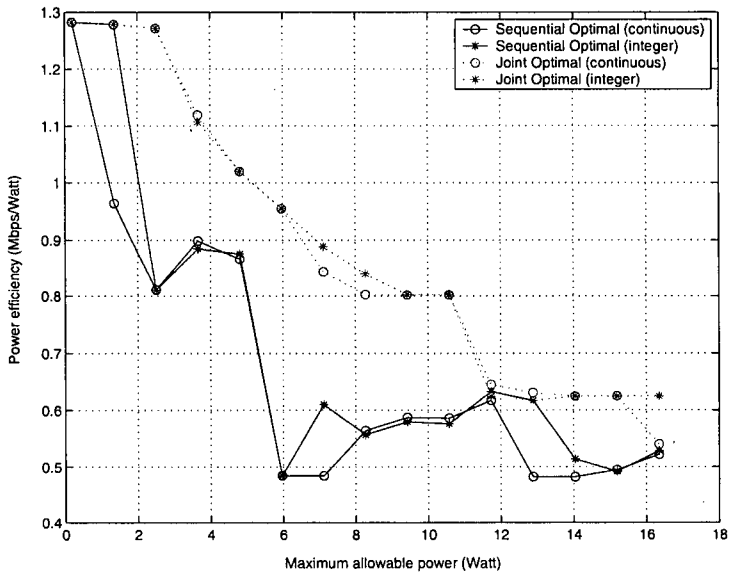

Figure 2.11: Power efficiency η_p as a function of the maximum allowable power P_{max} with $\mathbf{v_1}$ = [0.005 0.006 0.007] for both joint and sequential optimization, assuming a continuous and an integer number of multicodes.

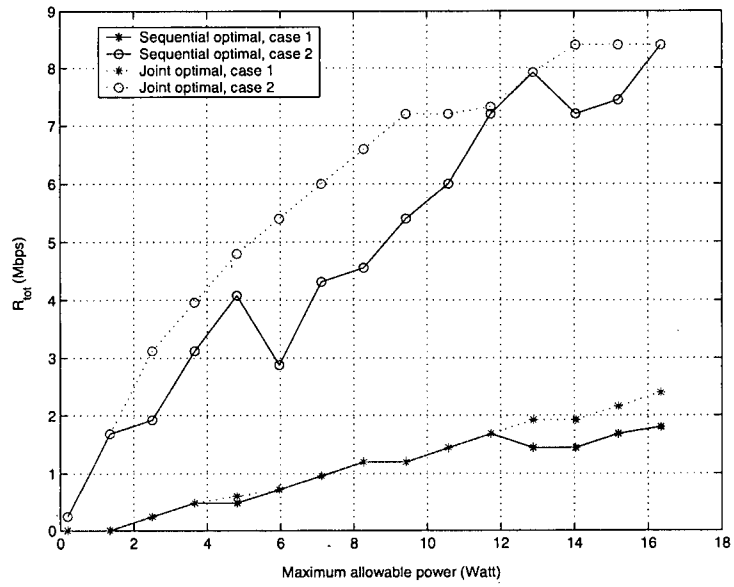

Figure 2.12: Total bit rate R_{tot} as a function of the maximum allowable power P_{max} for joint and sequential optimization. (case 1) $\mathbf{v_1}$ = [0.8 0.8 0.8] and (case 2) $\mathbf{v_1}$ = [0.005 0.005 0.005].

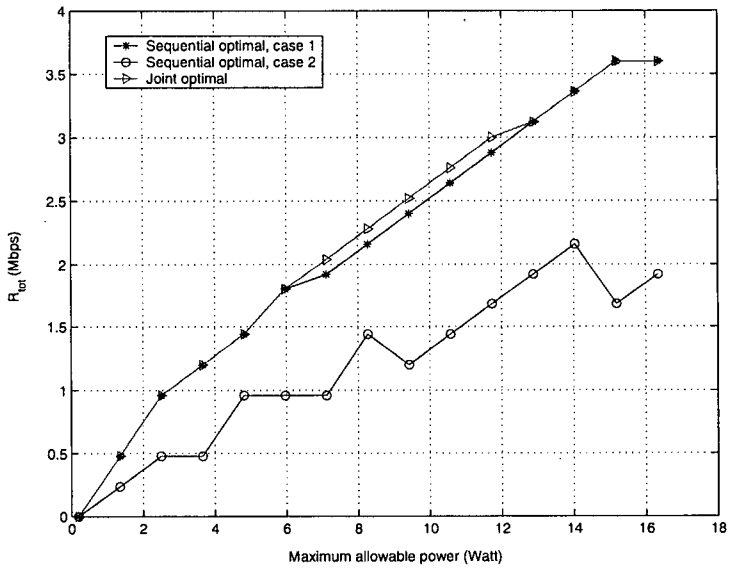

Figure 2.13: Total bit rate R_{tot} as a function of the maximum allowable power P_{max} with $\mathbf{v_1}$ = [0.2 0.6 0.9] for joint optimization, and (case 1) $\mathbf{v_1}$ = [0.2 0.6 0.9] and (case 2) $\mathbf{v_1}$ = [0.9 0.6 0.2] for sequential optimization.

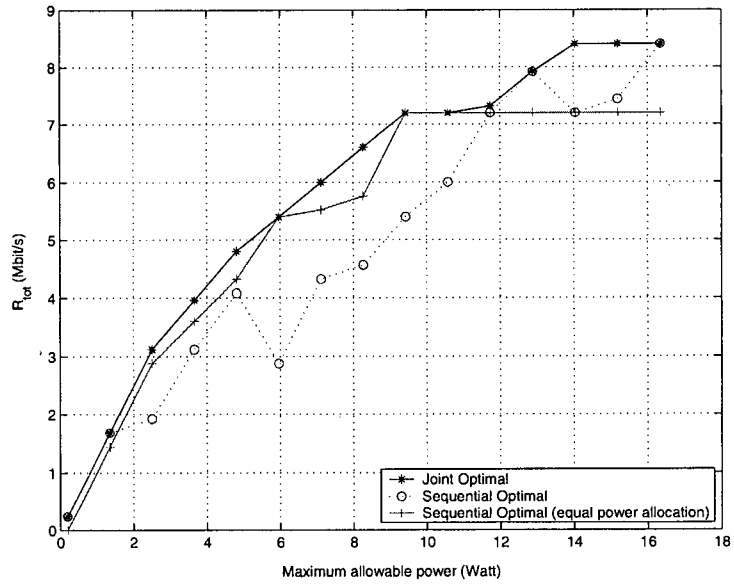

Figure 2.14: Total bit rate R_{tot} as a function of the maximum allowable power P_{max} with $\mathbf{v_1}$ = [0.005 0.006 0.007] for joint optimization, sequential optimization, and sequential optimization with equal power allocation, given that $N_{i,max} = 5$.

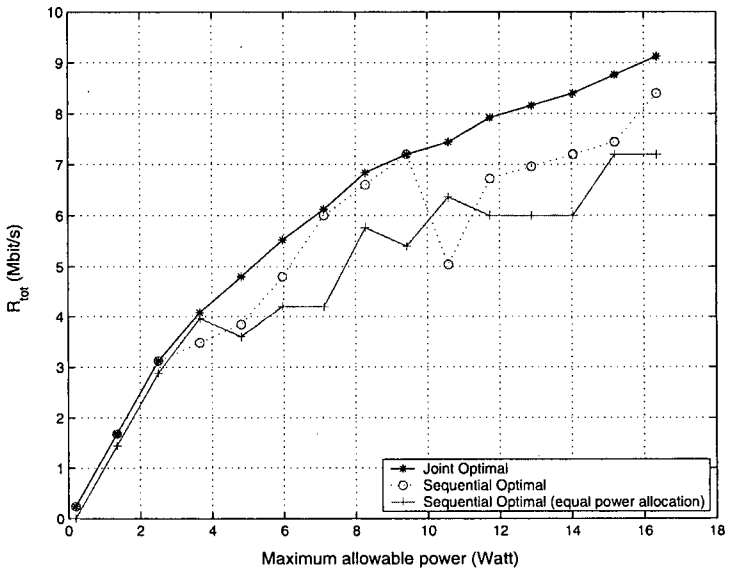

Figure 2.15: Total bit rate R_{tot} as a function of the maximum allowable power P_{max} with $\mathbf{v_1}$ = [0.005 0.006 0.007] for joint optimization, sequential optimization, and sequential optimization with equal power allocation, given that $N_{i,max} = 10$.

Load-Based Model

Using the default parameter values listed in Table 2.1, we now provide some numerical results for the joint and sequential load-based optimizations. The results also assume $\mathbf{v_1} = [v_{1,1}\ v_{1,2}\ v_{1,3}] = [0.15\ 0.010\ 0.0015]$, and $N_{i,max} = 10$. Figure 2.16 shows the total bit rate R_{tot} as a function of P_{max} for JO and SO with and without optimal ordering, with $\mathbf{D}$ = (2.0 0.8 0.5). The value of R_{tot} for the joint and sequential models can be obtained using (2.18) and (2.62) respectively. In this case the MS with the largest buffer content size experiences the worst channel condition and vice versa. The result shows that JO provides a higher total allocated bit rate than SO. It can also be seen that with SO, optimal ordering can provide a significant improvement. With JO, R_{tot} increases monotonically with P_{max}. However, with sequential optimization, a higher P_{max} may allow more resources to be allocated to the first MS, leaving less resources for other MS's. As a result, a higher P_{max} does not guarantee a higher R_{tot} for SO. The assumption that the number of multicode

is continuous leads to a slightly higher R_{tot} for JO. The reason is due to the more relaxed constraint. In the case of SO with optimal ordering, a greater increase in R_{tot} can be observed when the number of multicodes is assumed to be continuous.

Figure 2.17 shows the power efficiency, η_p, as a function of P_{max} for JO as well as SO with and without optimal ordering. A higher bit rate can be achieved using higher order MCS's at the expense of a higher transmit power. The figure shows that η_p generally decreases with increasing P_{max}. Note that since η_p is not the optimization objective function, η_p for JO can be lower than that for SO.

Figure 2.18 shows the total bit rate, R_{tot}, as a function of the total normalized buffer size $D = \sum_{i=1}^{L} D_i$ for JO and SO with and without optimal ordering, with $\mathbf{D}/D_3 = [3.5,\ 2.5,\ 1.0]$, and $P_{max} = 10$ W.. At low traffic loads, radio resources are not a limiting factor and there is little difference among the three schemes. As the traffic load increases, JO exhibits a significant improvement over SO with no optimal ordering. Since R_{tot} is sensitive to the combination of channel condition and buffer content size, the first MS with a bad combination can leave little resources for subsequent MS's resulting in a poor overall performance. Figure 2.18 suggests that SO with optimal ordering can provide a relatively good performance.

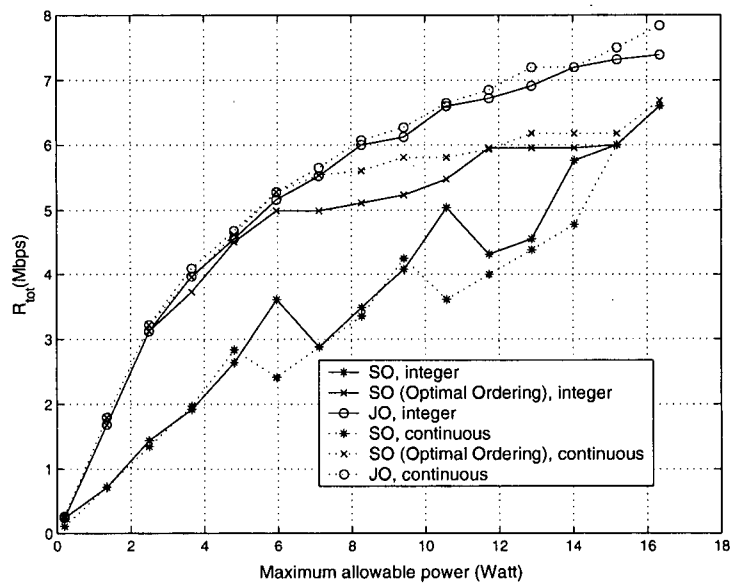

Figure 2.16: Total bit rate R_{tot} as a function of the maximum allowable power P_{max} for joint optimization and sequential optimization with and without optimal ordering, with $\mathbf{D} = [2.0,\ 0.8,\ 0.5]$.

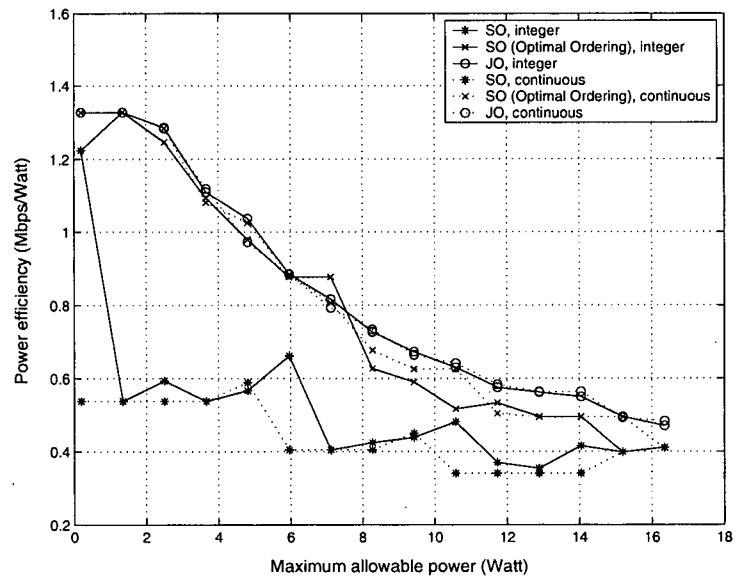

Figure 2.17: Power efficiency η_p as a function of the maximum allowable power P_{max} for joint optimization and sequential optimization with and without optimal ordering, with $\mathbf{D} = [2.0,\ 0.8,\ 0.5]$.

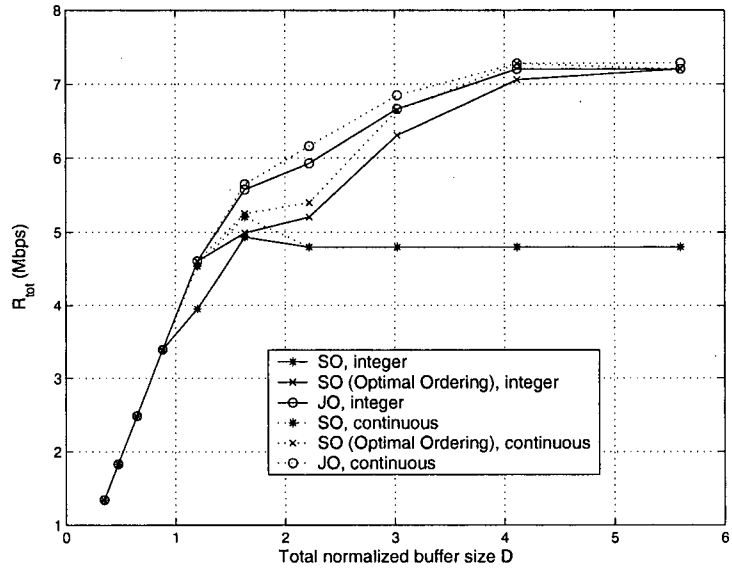

Figure 2.18: Total bit rate R_{tot} as a function of the total normalized buffer size $D = \sum_{i=1}^{L} D_i$ for joint optimization and sequential optimization with and without optimal ordering, with $\mathbf{D}/D_3 = [3.5,\ 2.5,\ 1.0]$, and $P_{max} = 10$ W.

2.5 Conclusions

The allocation of radio resources for the downlink of a CDMA network has been formulated as a mixed-integer nonlinear programming problem in which resources allocated to MS's are jointly optimized. It is shown that due to the non-linear nature of AMC as well as the maximum number of multicodes which can be assigned to an MS, an optimal allocation generally involves simultaneous transmissions to several mobiles. An optimal scheduling scheme which takes into account the amount of traffic destined for the different MS's was also proposed and studied. The results show that such a scheduler provides significant performance gains over schedulers which ignore MS traffic loads.

In order to reduce computational complexity, a sequential optimization procedure was presented in which resource allocation is performed successively for each MS. For the channel-based model, numerical results show that when the interference level is low, joint optimization can provide a significant improvement in total bit rate over sequential optimization.

When the interference level is high, the improvement is smaller. It is shown that the order of allocation plays an important role for sequential optimization. For the load-based model, it is found that the total bit rate is quite sensitive to the order in which MS's are allocated resources. Numerical results further show that sequential optimization with proper ordering can be an attractive sub-optimal alternative to the more computationally complex joint optimization.

References

[1] "Physical Layer Aspects of UTRA High Speed Downlink Packet Access," 3rd Generation Partnership Project, Technical Report 3G TR25.858, 2002.

[2] H. Holma and A. Toskala, Eds., *WCDMA for UMTS Radio Access for Third Generation Mobile Communications.* John Wiley & Sons, 2002.

[3] Y. Zhao, "Theoretical Study of Link Adaptation Algorithms for Adaptive Modulation in Wireless Mobile Communication Systems," in *IEEE Proc. of Universal Personal Communications, ICUPC'98*, vol. 1, October 1998, pp. 587 – 591.

[4] S. A. Jafar and A. Goldsmith, "Optimal Rate and Power Adaptation for Multirate CDMA," in *Proc. of 52th IEEE Vehicular Technology Conference, Fall*, vol. 3, Sept. 2000, pp. 994 –1000.

[5] R. Kwan, P. Chong, and M. Rinne, "Analysis of the adaptive modulation and coding algorithm with the multicode transmission," in *Proc. of 56th IEEE Vehicular Technology Conference VTC'02*, vol. 4, September 2002, pp. 2007 – 2011.

[6] ——, "The Effect of Code-Multiplexing on the High Speed Downlink Packet Access (HSDPA) in a WCDMA Network," in *Wireless Communication and Networking Conference WCNC*, vol. 3, March 2003, pp. 1728 – 1732.

[7] A. Bedekar, S. C. Borst, K. Ramanan, P. A. Whiting, and E. M. Yeh, "Downlink Scheduling in CDMA Data Network," Centrum Voor Wiskunde en Informatica, Probability, Networks, and Algorithms (PNA) PNA-R9910, Oct. 1999.

[8] C. A. Floudas, *Nonlinear and Mixed-Integer Optimization.* Oxford University Press, Inc, 1995.

[9] E. A. Eiselt and C.-L. Sandblom, *Integer Programing and Network Models.* Springer, 2000.

Chapter 3

Scheduling for the Downlink in a CDMA Network with Imperfect Channel Estimation

3.1 Introduction

In third generation (3G) multimedia CDMA networks, a variety of techniques are used to meet the quality of service (QoS) requirements for different types of traffic. With adaptive modulation and coding (AMC) [1], performance is improved by adapting the employed modulation and coding scheme (MCS) to changing channel conditions. A mobile station (MS) with favorable channel condition can be assigned a higher order modulation with a higher channel coding rate whereas a lower order modulation with a lower channel coding rate is assigned when channel conditions are unfavorable. For example, AMC is used in the High Speed Downlink Packet Access (HSDPA) enhancement adopted for the 3GPP cellular standard [2]. Multicode transmission [3] is a technique which can be used to provide higher bit rates to MS's.

It is well known that adapting the transmission parameters in a wireless system to changing channel conditions can be beneficial. In the case of the fast power control [1], the transmission power is adjusted based on the channel fading. Thus, transmission over a good channel requires less power to maintain the target signal quality at the receiver. The process of changing transmission parameters to compensate for variations in channel condition is known as *link adaptation.*

[1]The material in this chapter is largely based on R. Kwan and C. Leung, "Scheduling for the Downlink in a CDMA Network with Imperfect Channel Estimation." *Proc. of IEEE International Workshop on Adaptive Wireless Networks (AWIN), IEEE Global Telecommunication Conference (Globecom'04)*, Dallas, Texas, Dec. 2004.

Besides power control, AMC is also used for link adaptation [1, 2, 4]. A higher order modulation provides better spectral efficiency at the expense of a worse bit error rate (BER) performance. A lower channel coding rate provides greater error correction capability at the expense of information transmission rate. Thus, with a proper combination of the modulation order and channel coding rate, it is possible to design a set of MCS, from which an adaptive selection is made per transmission-time-interval (TTI) so that an improved spectral efficiency can be achieved under good channel conditions. At each selection of the MCS, the criterion is to keep the probability of erroneous decoding of a transmission block below a threshold value.

Multicode transmission can be employed [1, 5] to increase the bit rate by splitting the bits of a transmission block to more than one channelization code at each TTI. In this scheme, a high rate data stream is divided into a number of lower rate data sub-streams, which are transmitted in parallel synchronous orthogonal multicode channels. An algorithm for jointly selecting the MCS and number of multicodes to maximize the *assigned* bit rate given power and code constraints has been proposed in [6] in the context of HSDPA. An analytical formulation for this problem is given in [7].

Since the selection of MCS and the number of multicodes is based on knowledge of the channel condition, an incorrect estimation of the channel condition can degrade the system throughput. In this chapter, an analytical formulation is provided for jointly selecting the MCS and number of multicodes to maximize the *effective* bit rate in the presence of signal-to-interference ratio (SIR) estimation errors. This is then used to study the impact of SIR estimation errors on the performance. The formulation is also extended to take into account the actual MS traffic load.

3.2 System Model

Let the downlink received signal-to-interference ratio (SIR) of MS i be given by

$$\gamma_i = \frac{h_i P_i}{I_i} \tag{3.1}$$

where P_i is the downlink power transmitted to MS i from the target base station BS **A**, h_i is the path gain from BS **A** to MS i, and I_i is the total received interference for MS i. In addition, let $\Lambda_{i,j}$ be the required SIR for achieving the target error rate of $\varepsilon_{i,j}$ for MS i and MCS j when a single code is used.

Assuming that multicode transmission is used, the number of multicodes is continuous, and all codes share the power equally, the number, n_i, of codes that can be transmitted while achieving an error rate of $\epsilon_{i,j}$ is given by

$$n_i = \min\left(\frac{\gamma_i}{\lambda_{i,j}}, N_{i,max}\right), \tag{3.2}$$

where $N_{i,max}$ is the maximum number of multicodes that can be assigned to MS i and $\lambda_{i,j}$ is the SIR per code for MS i and MCS j which achieves an error rate of $\epsilon_{i,j}$.

The effective bit rate[2] for MS i with MCS j given γ_i would be

$$\tilde{R}_{i,j} = r_{i,j} n_i (1 - \epsilon_{i,j}(\lambda_{i,j})) \tag{3.3}$$

$$= \begin{cases} r_{i,j}\frac{\gamma_i}{\lambda_{i,j}}(1 - \epsilon_{i,j}(\lambda_{i,j})), & \text{if } \gamma_i < \lambda_{i,j} N_{i,max} \\ r_{i,j} N_{i,max}(1 - \epsilon_{i,j}(\lambda_{i,j})), & \text{if } \gamma_i \geq \lambda_{i,j} N_{i,max}, \end{cases} \tag{3.4}$$

where the basic bit rate $r_{i,j}$ is given by

$$r_{i,j} = \frac{W}{g} R_c^{(j)} \log_2(M_j). \tag{3.5}$$

[2]It is also used interchangeably with the term 'throughput' in this thesis.

In (3.5), W is the chip rate, g is the spreading factor, $R_c^{(j)}$ is the code rate for MCS j, and M_j is the number of points in the modulation constellation for MCS j. In the model, it is assumed that $\{r_{i,j} < r_{i,j+1},\ j = 1, ..., J-1\}$, and $\{\epsilon_{i,j}(\gamma_i) < \epsilon_{i,j+1}(\gamma_i),\ j = 1, ..., J-1\}$, which are realistic in practical applications of adaptive modulation and coding.

3.3 Optimal Bit Rate Allocation with Adaptive Modulation and Coding and Multicodes

Assume that $\epsilon_{i,j}(\lambda_{i,j})$ is a continuous, monotonically decreasing function of $\lambda_{i,j}$, and approaches zero as $\lambda_{i,j} \rightarrow \infty$. From (3.4), it can be seen that the choice of $\lambda_{i,j}$ (which depends on $\epsilon_{i,j}$) has a direct impact upon the effective bit rate $\tilde{R}_{i,j}$. Since $\epsilon_{i,j}$ decreases monotonically with $\lambda_{i,j}$, a smaller value of $\epsilon_{i,j}$ requires a higher value of $\lambda_{i,j}$. The maximum bit rate $r_{i,j}N_{i,max}(1 - \epsilon_{i,j}(\lambda_{i,j}))$ can be achieved if $\gamma_i \geq \lambda_{i,j}N_{i,max}$, but cannot be attained if $\gamma_i < \lambda_{i,j}N_{i,max}$. Increasing $\lambda_{i,j}$ results in a lower $\epsilon_{i,j}$ but a lower number, n_i, of multicodes. This suggests that there exists a value of $\lambda_{i,j}^{(opt)}$ which maximizes $\tilde{R}_{i,j}$ in the region $\gamma_i < \lambda_{i,j}N_{i,max}$. The following theorems provide optimality conditions in the region $\gamma_i < \lambda_{i,j}N_{i,max}$.

Theorem 3.1: The effective bit rate $\tilde{R}_{i,j}$ is maximized at $\lambda_{i,j}^{(opt)}$ given by $\epsilon_{i,j}(\lambda_{i,j}^{(opt)}) - \lambda_{i,j}^{(opt)}\epsilon'_{i,j}(\lambda_{i,j}^{(opt)}) - 1 = 0$ if $\epsilon''_{i,j}(\lambda_{i,j}^{(opt)}) > 0$.

Proof: See Appendix B.1.

Theorem 3.1 provides the conditions to be satisfied by $\lambda_{i,j}^{(opt)}$. However, it is possible that these conditions are also satisfied by other local extrema. By assuming that $\epsilon_{i,j}(x)$ takes the form of a sigmoid function, it can be shown that any $\lambda_{i,j}$ that satisfies the conditions in theorem 3.1 is a unique optimal solution.

Theorem 3.2: Assume that the error rate curve $\epsilon_{i,j}(x)$ can be modelled by a sigmoid function. Then any SIR $\lambda_{i,j}$ that satisfies the conditions in Theorem 3.1 is a unique solution that maximizes the effective bit rate $\tilde{R}_{i,j}$.

Proof: See Appendix B.2.

Although the sigmoid function model in Theorem 3.2 is not exact, it is a very good approximation to the error curves in [8]. According to Theorem 3.2, the optimal value of $\lambda_{i,j}^{(opt)}$ can be expressed in terms of the Lambert W function [9] as given by (B.31). If $\lambda_{i,j}^{(opt)} < \Lambda_{i,j}$, the chosen SIR requirement per code must be at least $\Lambda_{i,j}$ in order to satisfy the QoS requirement. In this case, using Theorem 3.3, we can conclude that the optimal value of $\lambda_{i,j}$ is $\Lambda_{i,j}$. Thus, in order to satisfy the QoS requirement, the optimal value, $\lambda_{i,j}^{*}$, of the SIR per code is given by

$$\lambda_{i,j}^{*} = \max(\lambda_{i,j}^{(opt)}, \Lambda_{i,j}). \tag{3.6}$$

Theorem 3.3: Assuming that the error rate curve $\epsilon_{i,j}(x)$ can be modelled by a sigmoid function, the effective bit rate $\tilde{R}_{i,j}$ decreases monotonically with $\lambda_{i,j}$ in the region $[\lambda_{i,j}^{(opt)}, \infty)$.

Proof: See Appendix B.3.

With the combination of AMC and multicodes, at a given γ_i, the effective MS bit rate $\tilde{R}_i(\gamma_i)$ is the maximum bit rate that can be provided among all MCS's. In other words,

$$\tilde{R}_i(\gamma_i) = \max_j(\{\tilde{R}_{i,j}(\gamma_i), \forall j = 1, ..., J\}), \tag{3.7}$$

where $\tilde{R}_{i,j}(\gamma_i)$ is the effective bit rate for MCS j at $\lambda_{i,j}^{*}$. A rough plot of $\tilde{R}_i(\gamma_i)$ is shown in Fig. 3.1.

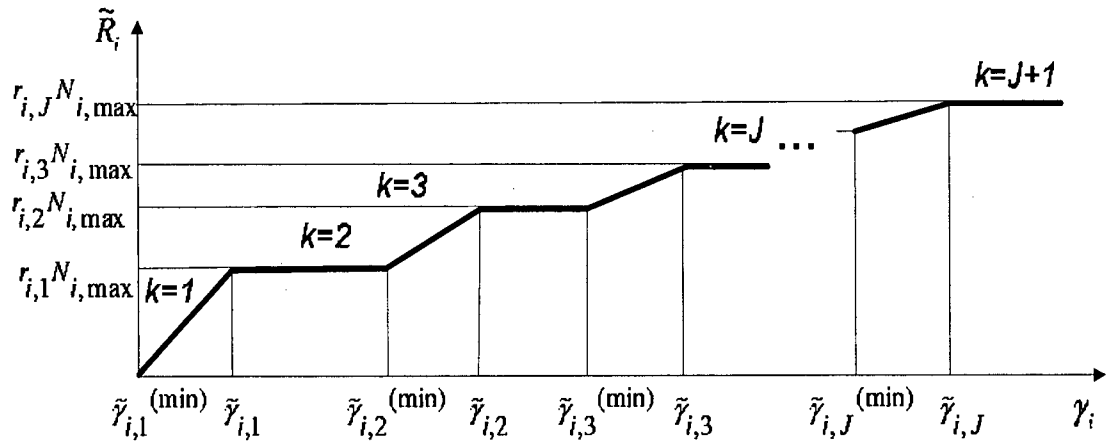

Figure 3.1: MS bit rate and γ_i relationship with MCS's.

As γ_i increases from 0, an increasing number of multicodes can be utilized, resulting in an increase of $\tilde{R}_i(\gamma_i)$. In this case, $\tilde{R}_{i,1}(\gamma_i) = \max(\tilde{R}_{i,j}(\gamma_i), \forall j = 1, ...J)$, since the effective bit rate is lower for $j > 1$ due to poorer error performance. As γ_i reaches $\tilde{\gamma}_{i,1}$, the maximum number, $N_{i,max}$, of multicodes allowed for MS i is used and a further increase in γ_i will not allow a higher number of multicodes to be allocated. At this stage, the next higher order MCS still gives a lower effective bit rate due to the poorer error performance. As γ_i reaches $\tilde{\gamma}_{i,2}^{(min)}$, MCS 2 is selected, and $\tilde{R}_i(\gamma_i) = \tilde{R}_{i,2}(\gamma_i)$. In a similar way, $\tilde{R}_i(\gamma_i)$ increases with increasing γ_i until $j = J$ and $N_{i,max}$ multicodes are used. Given γ_i, the problem of evaluating $\tilde{R}_i(\gamma_i)$ reduces to the determination of the set of thresholds $\{\tilde{\gamma}_{i,j}, \forall j = 1, ...J\}$ and $\{\tilde{\gamma}_{i,j}^{(min)}, \forall j = 1, ...J\}$.

Let $\tilde{\gamma}_{i,j}$ be

$$\tilde{\gamma}_{i,j} = \lambda_{i,j}^* N_{i,max}, \ \forall j = 1, ..., J \tag{3.8}$$

By definition, $\tilde{\gamma}_{i,j}^{(min)}$ can be obtained by solving the equation relating the highest effective bit rate of the MCS $j-1$ with the lowest effective bit rate of the MCS j. Thus,

$$N_{i,max} r_{i,j-1} \left(1 - \epsilon_{i,j-1}(\frac{\tilde{\gamma}_{i,j}^{(min)}}{N_{i,max}})\right) =$$

$$r_{i,j} n_i \left(1 - \epsilon_{i,j}(\frac{\tilde{\gamma}_{i,j}^{(min)}}{n_i})\right), \ \forall j = 2, ...J \tag{3.9}$$

$$= r_{i,j} \frac{\tilde{\gamma}_{i,j}^{(min)}}{\lambda_{i,j}^*} \left(1 - \epsilon_{i,j}(\lambda_{i,j}^*)\right), \ \forall j = 2, ...J. \tag{3.10}$$

Assuming the difference between $\lambda_{i,j}^{(min)}$ and $\lambda_{i,j+1}^{(min)}$ is reasonably large, and since

$$\tilde{\gamma}_{i,j}^{(min)} > \lambda_{i,j-1}^* N_{i,max}, \ \forall j = 2, ..., J, \tag{3.11}$$

the quantity $\epsilon_{i,j-1}(\tilde{\gamma}_{i,j}^{(min)}/N_{i,max})$ is negligibly small, and $\tilde{\gamma}_{i,j}^{(min)}$ can be well approximated as

$$\tilde{\gamma}_{i,j}^{(min)} = \frac{N_{i,max} r_{i,j-1}}{r_{i,j}\left(1 - \epsilon_{i,j}(\lambda_{i,j}^*)\right)} \lambda_{i,j}^*, \quad \forall j = 2, ..., J. \tag{3.12}$$

Without the loss of generality, we set $\tilde{\gamma}_{i,1}^{(min)} = 0$ and $\tilde{\gamma}_{i,J+1}^{(min)} = \infty$. The corresponding minimum number of multicodes for the j^{th} MCS is then given by

$$\tilde{n}_{i,j}^{(min)} = \frac{\tilde{\gamma}_{i,j}^{(min)}}{\lambda_{i,j}^*}, \ \forall j = 1, ..., J. \tag{3.13}$$

Let $\mathcal{C}_{i,j}^{(1)}(\gamma_i)$ and $\mathcal{C}_{i,j}^{(2)}(\gamma_i)$ take the truth values of the conditions $\tilde{\gamma}_{i,j}^{(min)} \leq \gamma_i \leq \tilde{\gamma}_{i,j}$ and $\tilde{\gamma}_{i,j} \leq \gamma_i \leq \tilde{\gamma}_{i,j+1}^{(min)}$ respectively. With the constraint on the number of multicodes, the optimal effective bit rate $\tilde{R}_i(\gamma_i)$ is given by

$$\tilde{R}_i(\gamma_i) = \begin{cases} r_{i,j} \frac{\gamma_i}{\lambda_{i,j}^*} \left(1 - \epsilon_{i,j}(\lambda_{i,j}^*)\right) & , \text{ if } \mathcal{C}_{i,j}^{(1)}(\gamma_i) \\ r_{i,j} N_{i,max} \left(1 - \epsilon_{i,j}(\lambda_{i,j}^*)\right) & , \text{ if } \mathcal{C}_{i,j}^{(2)}(\gamma_i) \end{cases}$$

$$\forall j = 1, ..., J. \tag{3.14}$$

3.4 Effect of Estimation Error

In reality, some error in estimating γ_i is inevitable. Let $\hat{\gamma}_i$ be the estimated value of γ_i, and is given by

$$\hat{\gamma}_i = \gamma_i + \varepsilon_{\gamma_i}, \tag{3.15}$$

where ε_{γ_i} is the estimation error for γ_i. As a result of the estimation error, the number of multicodes and the MCS may be allocated sub-optimally. Let j' and n_i' be the assigned MCS and the number of multicodes based on $\hat{\gamma}_i$, where n_i' is given by

$$n_i' = \min\left(\frac{\hat{\gamma}_i}{\lambda^*_{i,j'}}, N_{i,max}\right) \tag{3.16}$$

Let $\mathcal{C}^{(1)}_{i,j'}(\hat{\gamma}_i)$ and $\mathcal{C}^{(2)}_{i,j'}(\hat{\gamma}_i)$ take the truth values of the conditions $\tilde{\gamma}^{(min)}_{i,j'} \leq \hat{\gamma}_i \leq \tilde{\gamma}_{i,j'}$ and $\tilde{\gamma}_{i,j'} \leq \hat{\gamma}_i \leq \tilde{\gamma}^{(min)}_{i,j'+1}$ respectively. The sub-optimal effective bit rate $R_i(\gamma_i|\hat{\gamma}_i)$ is given by

$$R_i(\gamma_i|\hat{\gamma}_i) = \begin{cases} r_{i,j'} n_i' \left(1 - \epsilon_{i,j'}(\frac{\gamma_i}{n_i'})\right) & \text{if } \mathcal{C}^{(1)}_{i,j'}(\hat{\gamma}_i) \\ r_{i,j'} N_{i,max} \left(1 - \epsilon_{i,j'}(\frac{\gamma_i}{n_i'})\right) & \text{if } \mathcal{C}^{(2)}_{i,j'}(\hat{\gamma}_i) \end{cases} \quad \forall j' = 1, ..., J, \tag{3.17}$$

$$= \begin{cases} r_{i,j'} \frac{\hat{\gamma}_i}{\lambda^*_{i,j'}} \left(1 - \epsilon_{i,j'}(\frac{\gamma_i \lambda^*_{i,j'}}{\hat{\gamma}_i})\right) & \text{if } \mathcal{C}^{(1)}_{i,j'}(\hat{\gamma}_i) \\ r_{i,j'} N_{i,max} \left(1 - \epsilon_{i,j'}(\frac{\gamma_i}{N_{i,max}})\right) & \text{if } \mathcal{C}^{(2)}_{i,j'}(\hat{\gamma}_i) \end{cases} \quad \forall j' = 1, ..., J. \tag{3.18}$$

It is convenient to express the estimated SIR $\hat{\gamma}_i$ in terms of a multiplicative factor of the actual SIR γ_i, i.e.

$$\hat{\gamma}_i = \gamma_i(1+\beta_{\gamma_i}), \quad \beta_{\gamma_i} \geq -1 \tag{3.19}$$

where $\beta_{\gamma_i} = \varepsilon_{\gamma_i}/\gamma_i$ is typically a sample of some random variable. From (3.18) and (3.19), we can observe that as β_{γ_i} increases from 0, more multicodes would be allocated, but at the expense of a lower SIR per code. On the other hand, as β_{γ_i} decreases from 0, the SIR per code improves, but at the expense of fewer allocated multicodes. From a practical point of view, the former typically results in a rapid decrease in bit rate due to the fact that an over-estimation of γ_i generally results in a rapid increase in $\epsilon_{i,j}$. In the latter case, the effect upon the bit rate due to a small improvement in $\epsilon_{i,j}$ is generally small compared to that of the reduced multicode allocation. In other words, while an under-estimation of γ_i roughly translates in a reduction in bit rate due to under-allocation of multicodes or allocation of a lower order MCS, over-estimation of γ_i gives rise to the same effect due to the degradation in error performance (in the physical layer[3]). However, the impact upon bit rate due to under or over-estimation of γ_i is asymmetrical: while under-estimation has a roughly linear effect upon the bit rate, over-estimation usually has a much more detrimental impact due to the nonlinear nature of the physical layer error performance as a function of the channel condition.[4]

The above observation suggests that if $\hat{\gamma}_i$ is intentionally assumed to be lowered by a conservative factor Δ_i than what is observed, the chance of over-estimation can be reduced. In this case, (3.19) is modified to

$$\hat{\gamma}_i = \gamma_i(1+\beta_{\gamma_i})(1-\Delta_i), \quad \beta_{\gamma_i} \geq -1, \; 0 \leq \Delta_i \leq 1. \tag{3.20}$$

[3]The term 'physical layer' is used to distinguish the error performance at the physical layer from that of the estimation error.

[4]For example, with turbo codes, the error performance generally improves very rapidly once the SIR exceeds a certain threshold [10].

Since it would be more harmful to allow over-estimation than vice versa, the introduction of such conservative factor Δ_i is, on average, expected to provide gain in the presence of estimation errors. Note that in the region $\tilde{\gamma}_{i,j} \leq \gamma_i \leq \tilde{\gamma}_{i,j+1}^{(min)}$ where the bit rate is code-limited, over-estimation would be less harmful, since more multicodes are not allowed to further reduce the SIR per code, and, hence, decreasing the chance of further transmission error.

Using (3.20), (3.18) can be re-written as

$$\tilde{R}_i(\gamma_i|\hat{\gamma}_i) = \tilde{R}_i(\gamma_i|\Delta_i, \beta_{\gamma_i}), \tag{3.21}$$

and the average effective bit rate given Δ_i is given by

$$\overline{R_i(\gamma_i|\Delta_i)} = \int_{-\infty}^{\infty} \tilde{R}_i(\gamma_i|\Delta_i, \beta_{\gamma_i}) f_{\mathcal{B}}(\beta_{\gamma_i}) d\beta_{\gamma_i}, \tag{3.22}$$

where $f_{\mathcal{B}}(\beta_{\gamma_i})$ is the probability density function (pdf) of $\mathcal{B}_{\gamma_i}$.

3.5 Load-Based Scheduling with Estimation Error

In the case when the MS traffic is not back-logged, and the amount of data, B_i, in the buffer (i.e. the buffer content size) is known for each MS i, the code and power resources can be allocated more efficiently. Let $D_i = B_i/(WT_a)$ be the ratio of the buffer content size in bits to the number of bits that a full bandwidth W can carry over the scheduling period T_a. Thus, the required bit rate can be defined as $R_{req} = D_i W$. Furthermore, let $\mathcal{C}_i^{(r)} = \{C_{i,k}^{(r)}, 1 \leq k \leq J+1\}$ be the set of conditions for MS i such that $D_i W$ falls into one

of $J+1$ bit rate regions as shown in Fig. 3.1, where $\mathcal{C}_{i,k}^{(r)}$ is given by

$$\mathcal{C}_{i,k}^{(r)} = \begin{cases} r_{i,k-1}N_{i,max}(1-\epsilon_{i,k}(\lambda_{i,k}^*)) < D_iW \\ \leq r_{i,k}N_{i,max}(1-\epsilon_{i,k}(\lambda_{i,k}^*)),\ 1 \leq k \leq J, \\ r_{i,J}N_{i,max}(1-\epsilon_{i,J}(\lambda_{i,J}^*)) < D_iW,\ k = J+1. \end{cases} \tag{3.23}$$

where $r_{i,0} = 0$. The basic idea behind load-sensitive scheduling is to tailor the number of multicodes and power depending upon the bit rate region where the buffer content size D_i resides. Thus, the required MS bit rate $r_i^{(r)}$ and the corresponding SIR $\gamma_i^{(r)}$ are given by

$$r_i^{(r)} = \begin{cases} \frac{D_iW}{1-\epsilon_{i,k}(\lambda_{i,k}^*)}, & \text{if } \mathcal{C}_{i,k}^{(r)},\ 1 \leq k \leq J, \\ r_{i,J}N_{i,max}, & \text{if } \mathcal{C}_{i,J+1}^{(r)} \end{cases} \tag{3.24}$$

$$\gamma_i^{(r)} = \begin{cases} \lambda_{i,k}^* \left(\frac{D_iW}{r_{i,k}(1-\epsilon_{i,k}(\lambda_{i,k}^*))} \right), & \text{if } \mathcal{C}_{i,k}^{(r)},\ 1 \leq k \leq J, \\ \lambda_{i,J}^* N_{i,max}, & \text{if } \mathcal{C}_{i,J+1}^{(r)}. \end{cases} \tag{3.25}$$

Ideally, when the multicode and power resources are unlimited, (3.24) is optimal given the buffer content size B_i. However, in reality, it is possible that B_i is too large or γ_i is too small to support $\gamma_i^{(r)}$ due to the undesirable channel condition. Thus, the allocation of resources should reflect not only the buffer content size B_i, but also the current SIR γ_i. Let $\mathcal{C}_{i,j}^{(1)}(\gamma_i)$ and $\mathcal{C}_{i,j}^{(2)}(\gamma_i)$ take the truth values of the conditions $\tilde{\gamma}_{i,j}^{(min)} \leq \gamma_i \leq \tilde{\gamma}_{i,j}$ and $\tilde{\gamma}_{i,j} \leq \gamma_i \leq \tilde{\gamma}_{i,j+1}^{(min)}$ respectively. The resulting effective bit rate $R_i^{(lb)}(\gamma_i|\hat{\gamma}_i)$ is given by

$$R_i^{(lb)}(\gamma_i|\hat{\gamma}_i) = \begin{cases} r_i^{(r)}(1-\epsilon_{i,j''}(\gamma_i\lambda_{i,j''}^*/\gamma_i^{(r)})), & \text{if } \gamma_i^{(r)} \leq \hat{\gamma}_i,\ \mathcal{C}_{i,k}^{(r)}, \quad 1 \leq k \leq J+1 \\ r_{i,j'}\frac{\hat{\gamma}_i}{\lambda_{i,j'}^*}\left(1-\epsilon_{i,j'}(\gamma_i\lambda_{i,j'}^*/\hat{\gamma}_i)\right), & \text{if } \gamma_i^{(r)} > \hat{\gamma}_i,\ \mathcal{C}_{i,j'}^{(1)}(\hat{\gamma}_i), \quad 1 \leq j' \leq J, \\ r_{i,j'}N_{i,max}\left(1-\epsilon_{i,j'}(\gamma_i/N_{i,max})\right), & \text{if } \gamma_i^{(r)} > \hat{\gamma}_i,\ \mathcal{C}_{i,j'}^{(2)}(\hat{\gamma}_i), \quad 1 \leq j' \leq J, \end{cases} \tag{3.26}$$

where j' is the selected MCS when $C_{i,j'}^{(1)}(\hat{\gamma}_i)$ or $C_{i,j'}^{(2)}(\hat{\gamma}_i)$ is true, and $j'' = \min(k, J)$ is the selected MCS when $C_{i,k}^{(r)}$ is true. The average effective bit rate given Δ_i is given by

$$\overline{R_i^{(lb)}(\gamma_i|\Delta_i)} = \int_{-\infty}^{\infty} R_i^{(lb)}(\gamma_i|\Delta_i, \beta_{\gamma_i}) f_{\mathcal{B}}(\beta_{\gamma_i}) d\beta_{\gamma_i}, \tag{3.27}$$

where $R_i^{(lb)}(\gamma_i|\Delta_i, \beta_{\gamma_i})$ is the effective bit rate as a function of γ_i given the conservative factor Δ_i and the relative estimation error β_{γ_i}.

3.6 Numerical Results

Numerical results are now provided to show the impact of estimation errors upon the system performance. The estimation error β_{γ_i} is assumed to have a truncated Gaussian distribution

$$f_{\mathcal{B}}(\beta_{\gamma_i}) = \begin{cases} \frac{1}{\sqrt{2\pi}\sigma_i} e^{-\beta_{\gamma_i}^2/2\sigma_i^2} & , \text{ if } \beta_{\gamma_i} > -1 \\ C_\beta \delta(\beta_{\gamma_i} + 1) & , \text{ if } \beta_{\gamma_i} = -1 \end{cases} \tag{3.28}$$

where C_β is a normalizing constant, δ is the Dirac delta function, and σ_i is the standard deviation of the untruncated Gaussian distribution[5]. The simulations assume g=16, $N_{i,max}$=5, and the MCS's consist of QPSK 1/2, QPSK 3/4, 16-QAM 1/2, and 16-QAM 3/4. The link-level results are taken from [8]. Also, let $\eta_R = \tilde{R}_i(\gamma_i|\Delta_i, \beta_{\gamma_i})/\tilde{R}_i(\gamma_i)$ and $\overline{\eta_R} = \overline{R_i(\gamma_i|\Delta_i)}/\tilde{R}_i(\gamma_i)$ be the effective bit rate ratio and the averaged effective bit rate ratio respectively, which quantify the relative degradation of the effective bit rate due to estimation errors.

Figure 3.2 shows the averaged normalized effective bit rate $\overline{R_i(\gamma_i|\Delta_i)}/W$ as a function of γ_i with $\sigma_i^{(t)} = 0.1$ for various $\Delta_i's$, where $\sigma_i^{(t)}$[6] is the standard deviation of (3.28). As expected, when $\Delta_i = 0$ and in the presence of estimation errors, a significant degradation in bit rate can be observed compared to the case without estimation errors. However, by selecting an

[5]Note that the standard deviation of $f_{\mathcal{B}}(\beta_{\gamma_i})$ is slightly different from σ_i due to the truncation. However, when σ_i is small, the difference is negligible.

[6]See appendix B.4 for the relationship between $\sigma_i^{(t)}$ and σ_i.

appropriate conservative factor Δ_i, the effect of estimation errors can be reduced, especially in the region $\tilde{\gamma}_{i,j}^{(min)} \leq \gamma_i \leq \tilde{\gamma}_{i,j}$.

Figure 3.3 shows the normalized effective bit rate η_R as a function of the relative estimation error β_{γ_i} with $\sigma_i^{(t)} = 0.1$ and $\Delta_i = 0$. The results clearly show the asymmetrical effect of the estimation error upon the effective bit rate. The bit rate generally decreases much more rapidly as β_{γ_i} increases from 0 than as β_{γ_i} decreases from 0. The curve for $\gamma_i = 2$ is flat because it falls in a flat region of the bit rate vs. γ_i curve, i.e. in the range $(\tilde{\gamma}_{i,3}, \tilde{\gamma}_{i,4}^{(min)})$ as can be seen in Fig. 3.2.

Figure 3.4 shows the averaged effective bit rate ratio $\overline{\eta_R}$ as a function of the conservative factor Δ_i with $\sigma_i^{(t)} = 0.1$. The cases $\gamma_i = 0.2$ and 2.5 fall within the sloped regions of the "no error, $\Delta_i = 0$" curve in Fig. 3.1. In these cases, the system can only achieve about 70% of the estimation-error-free bit rate with no conservative factor, i.e. $\Delta_i = 0$. However, by an appropriate selection of Δ_i, approximately equal to $\sigma_i^{(t)}$, a significant increase in $\overline{\eta_R}$ can be obtained. The cases $\gamma_i = 1.8, 3.2$ and 4.5 lie in the flat regions of the "no error, $\Delta_i = 0$" curve in Fig. 3.1. As a result, $\overline{\eta_R}$ is relatively less sensitive to the estimation error and a small value of Δ_i has little effect on the bit rate.

Figures 3.5 and 3.6 show the averaged effective bit rate ratio $\overline{\eta_R}$ as a function of the standard deviation $\sigma_i^{(t)}$ with $\gamma_i = 2.5$ (sloped region) and 1.8 (flat region) respectively. The results show that for $\gamma_i = 2.5$, $\overline{\eta_R}$ decreases quite rapidly with $\sigma_i^{(t)}$ when $\Delta_i = 0$. However, with an appropriate value of Δ_i, $\overline{\eta_R}$ can be made much less sensitive to estimation errors. For $\gamma_i = 1.8$, $\overline{\eta_R}$ does not vary much with small values of $\sigma_i^{(t)}$.

In the case of the load-based model, it is convenient to quantify performance degradation by comparing the effective bit rate to the requested bit rate. Let the averaged effective-to-requested bit rate ratio $\eta_R^{(lb)}$ be $\overline{R_i^{(lb)}(\gamma_i|\Delta_i)}/(D_iW)$. Figure 3.7 shows $\eta_R^{(lb)}$ as a function of $\sigma_i^{(t)}$ with $D_i = 0.85$, $\Delta_i = 0$ and four different values of γ_i. It can be seen that when γ_i is small, the effective bit rate cannot support the requested bit rate D_iW, resulting in a low value of $\eta_R^{(lb)}$ even when no error is present. It can be observed that even a small error can

cause a big decrease in $\eta_R^{(lb)}$ when γ_i lies in the sloped regions (i.e. $\gamma_i = 0.25, 1.25$ and 2.5.

Figure 3.8 shows the averaged effective-to-requested bit rate ratio $\eta_R^{(lb)}$ as a function of the conservative factor Δ_i with $\sigma_i^{(t)} = 0.1$, $D_i = 0.85$ and different values of γ_i. The results show that generally a good choice of Δ_i can improve $\eta_R^{(lb)}$. As a rule of thumb, a good choice of Δ_i is in the range $\sigma_i^{(t)}$ to $1.5\sigma_i^{(t)}$.

Figure 3.9 shows the averaged effective-to-requested bit rate ratio $\eta_R^{(lb)}$ as a function of the standard deviation $\sigma_i^{(t)}$ with $\gamma_i = 2.5$, $D_i = 0.85$ for four different values of Δ_i. It can be seen that a good choice of Δ_i can greatly reduce the effect of channel estimation errors on $\eta_R^{(lb)}$.

3.7 Conclusions

In this chapter, the problem of optimal scheduling for a single MS on the downlink of a WCDMA network was studied. Analytical expressions were derived for the optimal effective bit rate when adaptive modulation and coding and multicode transmission are employed. For link adaptation, the selection of the MCS and the number of multicodes is based on an estimation of the downlink SIR. It was shown that a small estimation error can result in a bad selection of MCS and number of multicodes leading to a significant degradation in the effective bit rate. It was shown that the impact of SIR estimation errors can be greatly reduced by using a conservative margin with the estimated SIR value.

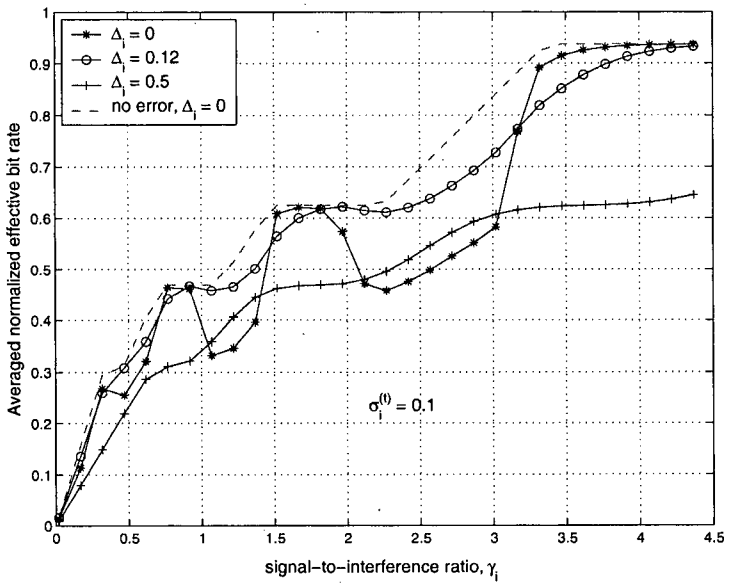

Figure 3.2: Averaged normalized effective bit rate $\overline{R_i(\gamma_i|\Delta_i)}/W$ as a function of γ_i with $\sigma_i^{(t)} = 0.1$.

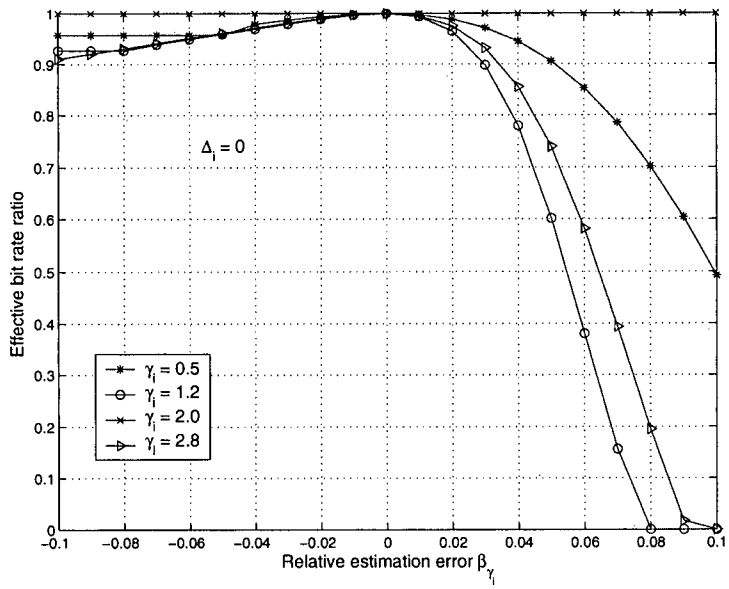

Figure 3.3: Normalized effective bit rate η_R as a function of the relative estimation error β_{γ_i} with $\sigma_i^{(t)} = 0.1$.

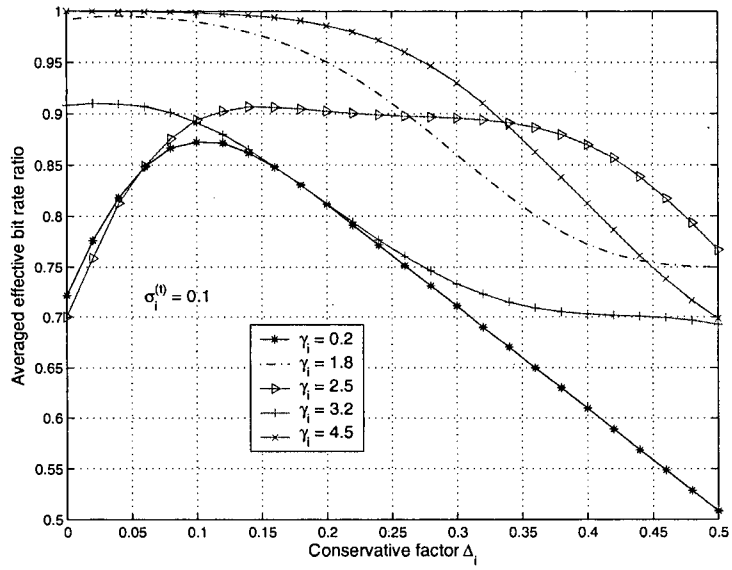

Figure 3.4: Averaged effective bit rate ratio $\overline{\eta_R}$ as a function of the conservative factor Δ_i with $\sigma_i^{(t)} = 0.1$.

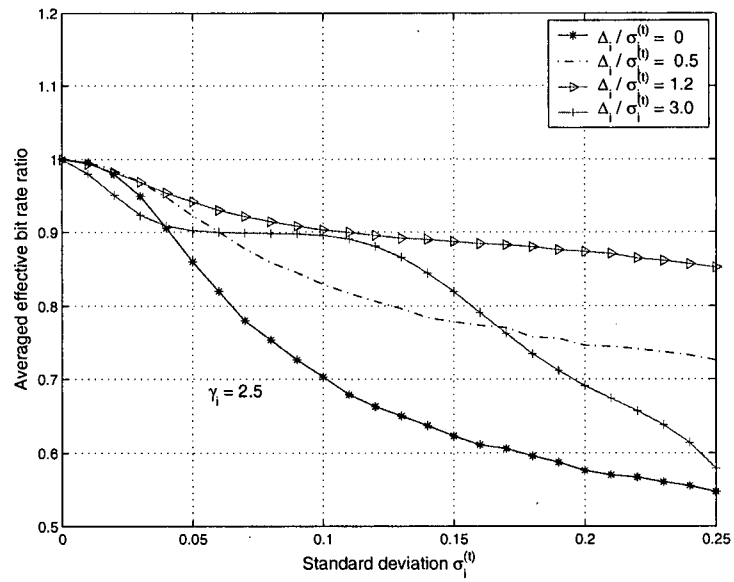

Figure 3.5: Averaged effective bit rate ratio $\overline{\eta_R}$ as a function of the standard deviation $\sigma_i^{(t)}$ with $\gamma_i = 2.5$.

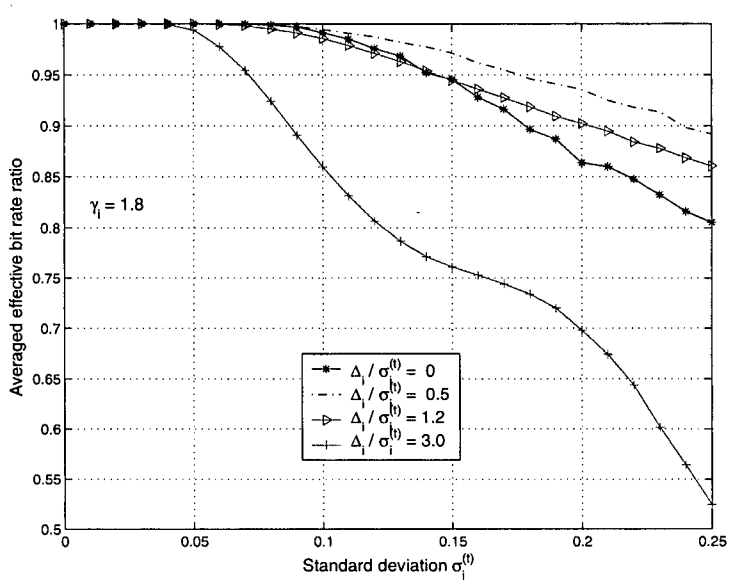

Figure 3.6: Averaged effective bit rate ratio $\overline{\eta_R}$ as a function of the standard deviation $\sigma_i^{(t)}$ with $\gamma_i = 1.8$.

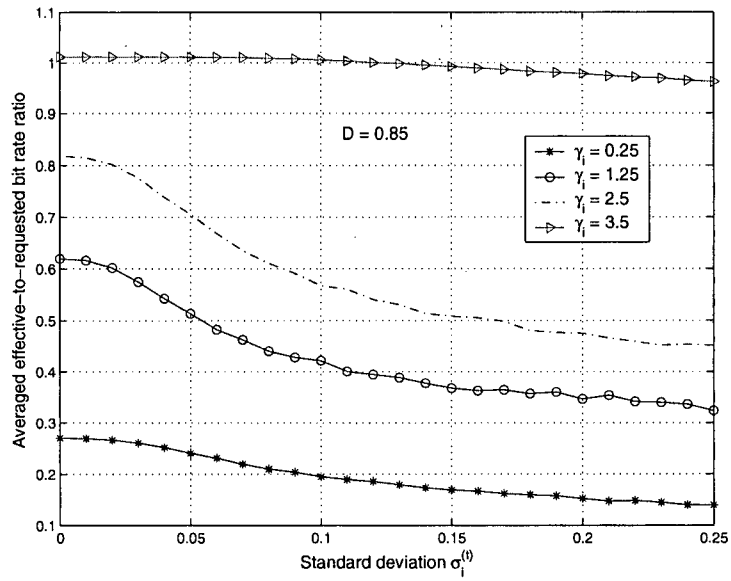

Figure 3.7: Averaged effective-to-requested bit rate ratio as a function of the standard deviation $\sigma_i^{(t)}$ with $D_i = 0.85$, $\Delta_i = 0$ and different values of γ_i.

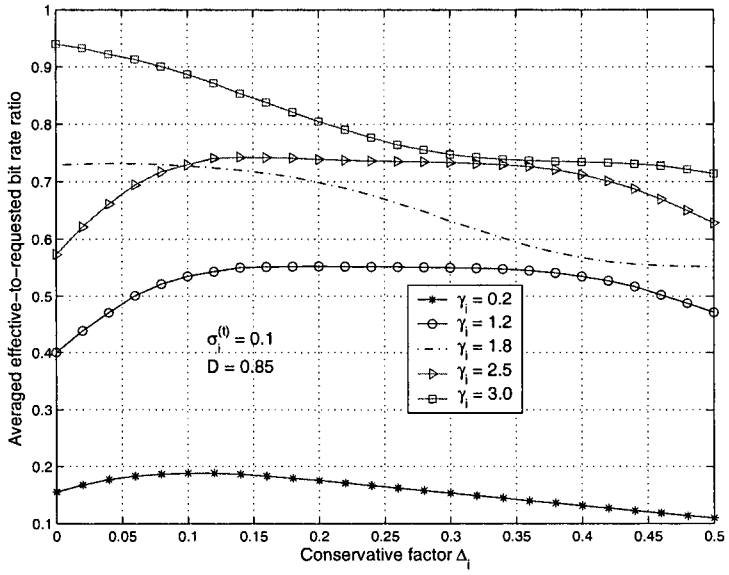

Figure 3.8: Averaged effective-to-requested bit rate ratio as a function of the conservative factor Δ_i with $\sigma_i^{(t)} = 0.1$, $D_i = 0.85$ and different values of γ_i.

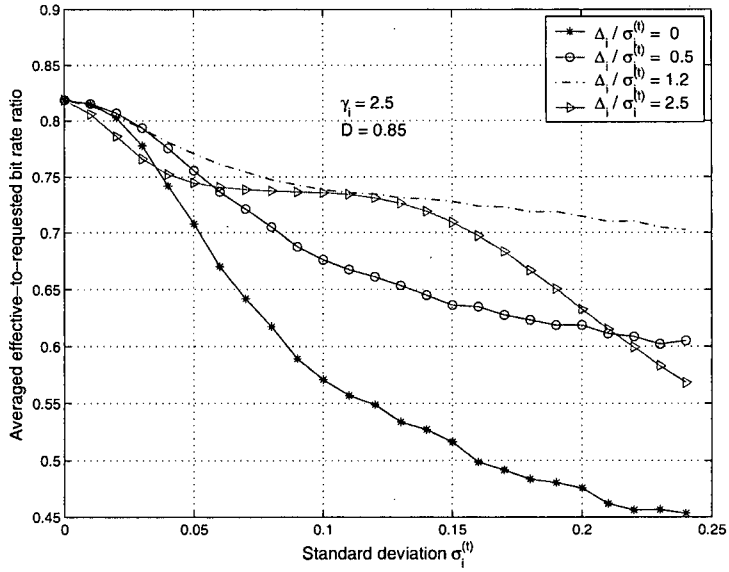

Figure 3.9: Averaged effective-to-requested bit rate ratio as a function of the standard deviation $\sigma_i^{(t)}$ with $\gamma_i = 2.5$, $D_i = 0.85$ and different values of Δ_i.

References

[1] H. Holma and A. Toskala, Eds., *WCDMA for UMTS Radio Access for Third Generation Mobile Communications.* John Wiley & Sons, 2002.

[2] "Physical Layer Aspects of UTRA High Speed Downlink Packet Access," 3rd Generation Partnership Project, Technical Report 3G TR25.858, 2002.

[3] S. J. Lee, H. W. Lee, and D. K. Sung, "Capacities of Single-Code and Multicode DS-CDMA Systems Accommodating Multiclass Service," *IEEE Trans. on Vehicular Technology*, vol. 48, no. 2, pp. 376 –384, March 1999.

[4] Y. Zhao, "Theoretical Study of Link Adaptation Algorithms for Adaptive Modulation in Wireless Mobile Communication Systems," in *IEEE Proc. of Universal Personal Communications, ICUPC'98*, vol. 1, October 1998, pp. 587 – 591.

[5] S. A. Jafar and A. Goldsmith, "Optimal Rate and Power Adaptation for Multirate CDMA," in *Proc. of 52th IEEE Vehicular Technology Conference, Fall*, vol. 3, Sept. 2000, pp. 994 –1000.

[6] R. Kwan, P. Chong, and M. Rinne, "Analysis of the adaptive modulation and coding algorithm with the multicode transmission," in *Proc. of 56th IEEE Vehicular Technology Conference VTC'02*, vol. 4, September 2002, pp. 2007 – 2011.

[7] R. Kwan and C. Leung, "Channel-Based Downlink Scheduling Schemes for CDMA Networks," in *Proc. of IEEE Vehicular Technology Conference (VTC)*, Los Angeles, California, September 2004.

[8] M. Döttling, J. Michel, and B. Raaf, "Hybrid ARQ and Adaptive Modulation and Coding Schemes for High Speed Downlink Packet Access," in *Proc. of IEEE International Symposium on Personal, Indoor and Mobile Radio Communications (PIMRC)*, September 2002.

[9] R. M. Corless, G. H. Gonnet, D. E. G. Hare, D. J. Jeffrey, and D. E. Knuth, "On the Lambert W Function," *Adv. Comput. Math.*, vol. 5, pp. 329 – 359, 1996.

[10] C. Berrou, A. Glavieux, and P. Thitimajshima, "Near Shannon limit error-correcting coding and decoding: Turbo-codes. 1," in *Proc. of IEEE International Conference on Communications (ICC)*, vol. 2, May 1993, pp. 1064 – 1070.

Chapter 4

Adaptive Modulation and Coding with Multicodes over Nakagami Fading Channels

4.1 Introduction

Third generation (3G) cellular networks allow a wide variety of traffic to be carried over the wireless channel. Radio resource allocation algorithms are needed which make efficient use of resources while at the same time satisfying the quality of service (QoS) requirements of each type of traffic. It is expected that downlink traffic will be especially important since most of the high speed internet access and broadcast services traffic is in the downlink direction. In order to support broadband packet data services, a high speed downlink packet access (HSDPA) channel has been incorporated in the 3GPP standard [1, 2].

Link adaptation refers to the process of changing transmission parameters to account for changes in channel conditions. Power control and adaptive modulation (AM) are two methods for implementing link adaptation [2]-[6]. In AM, the modulation scheme is changed according to the channel condition so as to improve the spectral efficiency. In [4], the impact of channel estimation delay on the bit error rate (BER) is analyzed for adaptive quadrature amplitude modulation (AQAM) over Nakagami fading channels. In [5], the design of an optimum AM scheme is studied for the flat Rayleigh fading channel when channel prediction is employed. The goal is to choose optimal thresholds for modulation selection using the second-order statistics of the channel prediction error. In [6], the impact of channel estimation errors on AM performance in flat fading is examined. The adaptation

[1]The material in this chapter is largely based on R. Kwan and C. Leung, "Adaptive Modulation and Coding with Multicodes over Nakagami Fading Channels." *Proc. of IEEE Wireless Communications and Networking Conference (WCNC'05)*, vol. 2, New Orleans, Louisiana, March, 2005.

schemes in [4, 5, 6], are based on uncoded quadrature amplitude modulation (QAM).

The 3GPP HSDPA channel uses adaptive modulation and coding in which channel coding is applied on top of each modulation scheme to improve power efficiency [1] and multicode transmission is employed to increase bit rate [2]. The advantages of using multicodes are discussed in [7]. In [8], the problem of code and power allocation in the downlink of a CDMA network is studied. The modulation and coding schemes (MCS) and the number of multicodes are jointly optimized based on the given power and multicode constraints. Also, the effects of imperfect channel state estimation are considered.

In contrast to the QAM case, no known analytical expressions are available for the error rates of the MCS's used in HSDPA. In this chapter, these error rate curves are approximated using sigmoid functions. Based on this error rate model, an analysis of the bit rate performance of AMC combined with multicodes over Nakagami fading channels is carried out. In Section 4.2, the bit rate model with AMC and multicode is described, followed by the performance analysis in Section 4.3. Numerical results are presented in Section 4.4 and the main findings are summarized in Section 4.5.

4.2 Adaptive Modulation and Coding with Multicodes

Let the downlink received signal-to-noise ratio (SNR) for mobile station (MS) i, be

$$\gamma_i = h_i P_i / I_i \tag{4.1}$$

where h_i is the path gain from the base station, BS **A**, to MS i, P_i is the power that BS **A** has allocated for the traffic channel to MS i, and I_i is the total received interference and noise power at MS i. Since we will only consider a single MS, the subscript i will henceforth be dropped.

With AMC and orthogonal multicodes, the optimal effective bit rate $R_j(\gamma)$ for MCS j for a given value of γ is [8]

$$\tilde{R}(\gamma) \;=\; r_j n_j(\gamma)(1-\varepsilon_j(\lambda_j^*)), \tag{4.2}$$

where λ_j^* is the required SNR for a single code with MCS j to meet a pre-defined error requirement $\varepsilon_j(\lambda_j^*)$. For simplicity, it is assumed that the number, $n_j(\gamma)$, of multicodes is continuous, i.e. can take on any real value, in which case the optimal value is given by [8]

$$n_j(\gamma) \;=\; \begin{cases} \gamma/\lambda_j^* \;,\; \tilde{\gamma}_j^{(min)} \le \gamma < \tilde{\gamma}_j,\; 1 \le j \le J \\ N_{max} \;,\; \tilde{\gamma}_j \le \gamma < \tilde{\gamma}_{j+1}^{(min)},\; 1 \le j \le J, \end{cases} \tag{4.3}$$

where J is the number of available MCS's, and N_{max} is the maximum number of multicodes that can be assigned to the MS. The basic bit rate r_j in (4.2) is given by

$$r_j \;=\; \frac{W}{g} R_c^{(j)} \log_2 M_j,\; 1 \le j \le J, \tag{4.4}$$

where W is the chip rate, $R_c^{(j)}$ is the code rate for MCS j, M_j is the number of points in the modulation constellation for MCS j and g is the spreading factor. As shown in Fig. 4.1,

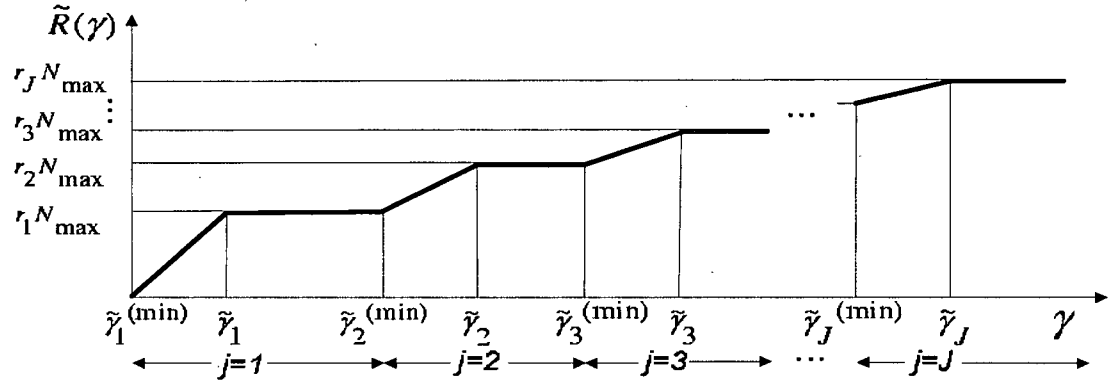

Figure 4.1: Allocated MS bit rate as a function of γ.

the terms $\tilde{\gamma}_j^{(min)}$ and $\tilde{\gamma}_j$ correspond to a set of decision thresholds which specify the optimal

MCS and number of multicodes for a given value of γ. The decision thresholds $\tilde{\gamma}_j^{(min)}$ and $\tilde{\gamma}_j$ can be obtained as [8]

$$\tilde{\gamma}_j = \lambda_j^* N_{max}, \quad 1 \leq j \leq J \tag{4.5}$$

$$\tilde{\gamma}_j^{(min)} = \lambda_j^* \frac{r_{j-1}}{r_j(1-\varepsilon_j(\lambda_j^*))} N_{max}, \quad 2 \leq j \leq J. \tag{4.6}$$

It might be noted that $\tilde{\gamma}_1^{(min)} = 0$ and $\tilde{\gamma}_{J+1}^{(min)} = \infty$.

4.3 Performance Analysis over Nakagami Fading Channels

In practice, the actual received SNR, γ, may not be identical to the estimated version, $\hat{\gamma}$. Thus, instead of λ_j^*, the actual SNR per (multi)code, $\lambda(\hat{\gamma}, \gamma)$ would be

$$\lambda(\hat{\gamma}, \gamma) = \frac{\gamma}{n_j(\hat{\gamma})} \tag{4.7}$$

$$= \begin{cases} \lambda_j^* \gamma/\hat{\gamma} & , \ \tilde{\gamma}_j^{(min)} \leq \hat{\gamma} < \tilde{\gamma}_j, \ 1 \leq j \leq J \\ \gamma/N_{max} & , \ \tilde{\gamma}_j \leq \hat{\gamma} < \tilde{\gamma}_{j+1}^{(min)}, \ 1 \leq j \leq J. \end{cases} \tag{4.8}$$

The probability density function (pdf) of the channel gain A for Nakagami-m fading is given by [9]

$$p_A(a) = \frac{2}{\Gamma(m)} \left(\frac{m}{\Omega}\right)^m a^{2m-1} e^{-ma^2/\Omega}, \tag{4.9}$$

where $\Omega = E(A^2)$ is the average power gain, m is the Nakagami fading parameter ($m \geq 1/2$), and $\Gamma(.)$ is the gamma function. The pdf $p_\Gamma(\gamma)$ of the received SNR Γ is given by

$$p_\Gamma(\gamma) = \left(\frac{m}{\bar{\Gamma}}\right)^m \frac{\gamma^{m-1}}{\Gamma(m)} e^{-m\gamma/\bar{\Gamma}} \tag{4.10}$$

where $\bar{\Gamma}$ is the average received SNR. Let A and $\hat{A}$ be the actual and estimated channel gains. Assuming that these two channel gains are correlated with the same average power, their joint pdf $p_{A,\hat{A}}(a,\hat{a})$ is given by [10]

$$\begin{aligned} p_{A,\hat{A}}(a,\hat{a}) &= \frac{4(a\hat{a})^m}{(1-\rho)\Gamma(m)\rho^{(m-1)/2}}\left(\frac{m}{\Omega}\right)^{m+1} \times \\ & I_{m-1}\left(\frac{2m\sqrt{\rho}a\hat{a}}{(1-\rho)\Omega}\right)\exp\left(-\frac{m(a^2+\hat{a}^2)}{(1-\rho)\Omega}\right). \end{aligned} \tag{4.11}$$

In (4.11), ρ is the correlation coefficient of A^2 and $\hat{A}^2$. Using (4.9) and (4.11), the conditional pdf of Γ given $\hat{\Gamma}$ can be obtained as [4]

$$\begin{aligned} p_{\Gamma|\hat{\Gamma}}(\gamma|\hat{\gamma}) &= \frac{m}{(1-\rho)\bar{\Gamma}}\left(\frac{\gamma}{\rho\hat{\gamma}}\right)^{(m-1)/2} \times \\ & I_{m-1}\left(\frac{2m\sqrt{\rho\gamma\hat{\gamma}}}{(1-\rho)\bar{\Gamma}}\right)\exp\left(-\frac{m(\rho\gamma+\hat{\gamma})}{(1-\rho)\bar{\Gamma}}\right). \end{aligned} \tag{4.12}$$

Due to the nature of the selected MCS's, it is difficult to obtain the corresponding error rates analytically [11]. Instead, we approximate them using sigmoid functions. Such an approximation is quite accurate, as depicted in Fig. 4.2, where the simulated frame error rates of the selected MCS's are obtained from the first transmission results in [11].

Let the error rate $\varepsilon_j(x)$ for MCS j be

$$\varepsilon_j(x) = \frac{1}{1+a_1^{(j)}\exp(a_2^{(j)}x)},\ a_1^{(j)},\ a_2^{(j)} > 0. \tag{4.13}$$

The effective bit rate, $\tilde{R}(\gamma|\hat{\gamma})$, at γ given $\hat{\gamma}$ is given by

$$\tilde{R}(\gamma|\hat{\gamma}) = r_j n_j(\hat{\gamma})\phi_j(\lambda(\hat{\gamma},\gamma)) \tag{4.14}$$

where

$$\phi_j(\lambda(\hat{\gamma},\gamma)) = 1-\varepsilon_j(\lambda(\hat{\gamma},\gamma)) \tag{4.15}$$

$$= \frac{a_1^{(j)}\exp(c_1^{(j)}(\hat{\gamma})\gamma/\hat{\gamma})}{1+a_1^{(j)}\exp(c_1^{(j)}(\hat{\gamma})\gamma/\hat{\gamma})} \tag{4.16}$$

and

$$c_1^{(j)}(\hat{\gamma}) = \begin{cases} a_2^{(j)}\lambda_j^*, & \text{if } \tilde{\gamma}_j^{(min)} \le \hat{\gamma} < \tilde{\gamma}_j \quad (4.17a) \\ a_2^{(j)}\hat{\gamma}/N_{max}, & \text{if } \tilde{\gamma}_j \le \hat{\gamma} < \tilde{\gamma}_{j+1}^{(min)}. \quad (4.17b) \end{cases}$$

The average conditional bit rate, $\tilde{R}(\hat{\gamma})$, at a given $\hat{\gamma}$, is given by

$$\tilde{R}(\hat{\gamma}) = \int_0^\infty \tilde{R}(\gamma|\hat{\gamma})p_{\Gamma|\hat{\Gamma}}(\gamma|\hat{\gamma})d\gamma. \tag{4.18}$$

The term $\phi_j(\lambda(\hat{\gamma},\gamma))$ in (4.16) can be written as a power series as follows

$$\phi_j^* = \begin{cases} \sum_{n=0}^{\infty}(-1)^n(a_1^{(j)}e^{c_1^{(j)}(\hat{\gamma})\gamma/\hat{\gamma}})^{-n}, & \text{if } \gamma > K_j \quad (4.19a) \\ 1/2, & \text{if } \gamma = K_j \quad (4.19b) \\ \sum_{n=1}^{\infty}(-1)^{n-1}(a_1^{(j)}e^{c_1^{(j)}(\hat{\gamma})\gamma/\hat{\gamma}})^n, & \text{if } \gamma < K_j \quad (4.19c) \end{cases}$$

where

$$K_j = -\hat{\gamma}\ln a_1^{(j)}/c_1^{(j)}(\hat{\gamma}). \tag{4.20}$$

It can be seen that (4.19a) converges for $\gamma \in (K_j,\infty)$, and diverges for $\gamma \in [0,K_j]$, whereas (4.19c) converges for $\gamma \in [0,K_j)$ and diverges for $\gamma \in [K_j,\infty)$.

Let $\tilde{R}^-(\gamma|\hat{\gamma})$ and $\tilde{R}^+(\gamma|\hat{\gamma})$ be the effective bit rates given $\hat{\gamma}$ when the parameter γ lies in the regions $[0,K_j)$ and (K_j,∞) respectively. The resulting average conditional bit rates

$\tilde{R}^-(\hat{\gamma})$ and $\tilde{R}^+(\hat{\gamma})$ given $\hat{\gamma}$ for the lower and upper regions are respectively given by

$$\tilde{R}^-(\hat{\gamma}) = \lim_{\epsilon \to 0} \int_0^{K_j - \epsilon} \tilde{R}^-(\gamma|\hat{\gamma}) p_{\Gamma|\hat{\Gamma}}(\gamma|\hat{\gamma}) d\gamma \tag{4.21}$$

$$\tilde{R}^+(\hat{\gamma}) = \lim_{\epsilon \to 0} \int_{K_j + \epsilon}^{\infty} \tilde{R}^+(\gamma|\hat{\gamma}) p_{\Gamma|\hat{\Gamma}}(\gamma|\hat{\gamma}) d\gamma \tag{4.22}$$

For $\gamma = K_j$, the conditional bit rate $\tilde{R}^=(\hat{\gamma})$ given $\hat{\gamma}$ is given by

$$\tilde{R}^=(\hat{\gamma}) = \lim_{\epsilon \to 0} \int_{K_j - \epsilon}^{K_j + \epsilon} \frac{1}{2} r_j n_j(\hat{\gamma}) p_{\Gamma|\hat{\Gamma}}(\gamma|\hat{\gamma}) d\gamma \tag{4.23}$$

$$= \begin{cases} \lim_{\epsilon \to 0} \frac{1}{2} r_j n_j(\hat{\gamma}) \int_{K_j - \epsilon}^{K_j + \epsilon} \delta(\gamma - \hat{\gamma}) d\gamma, & \text{if } \rho = 1 \\ 0, & \text{if } \rho < 1. \end{cases} \tag{4.24}$$

Note that K_j defined in (4.20) is generally different from $\hat{\gamma}$, and (4.24) most likely vanishes even at $\rho = 1$. Finally, $\tilde{R}(\hat{\gamma})$ is given by

$$\tilde{R}(\hat{\gamma}) = \tilde{R}^-(\hat{\gamma}) + \tilde{R}^=(\hat{\gamma}) + \tilde{R}^+(\hat{\gamma}). \tag{4.25}$$

4.3.1 The case $\gamma > K_j$

Using (4.14) and (4.19a), the term $\tilde{R}_j^+(\hat{\gamma})$ given in (4.22) can be expressed as

$$\tilde{R}^+(\hat{\gamma}) = \lim_{\epsilon \to 0} \int_{K_j + \epsilon}^{\infty} r_j n_j(\hat{\gamma}) \times \sum_{n=0}^{\infty} (-1)^n (a_1^{(j)} e^{c_1^{(j)}(\hat{\gamma})\gamma/\hat{\gamma}})^{-n} p_{\Gamma|\hat{\Gamma}}(\gamma|\hat{\gamma}) d\gamma \tag{4.26}$$

$$= r_j n_j(\hat{\gamma}) \sum_{n=0}^{\infty} (-1)^n (a_1^{(j)})^{-n} \Phi_n(\hat{\gamma}) \tag{4.27}$$

where $\Phi_n(\hat{\gamma})$ is given by

$$\Phi_n(\hat{\gamma}) = \lim_{\epsilon \to 0} \int_{K_j + \epsilon}^{\infty} e^{-n c_1^{(j)}(\hat{\gamma})\gamma/\hat{\gamma}} p_{\Gamma|\hat{\Gamma}}(\gamma|\hat{\gamma}) d\gamma. \tag{4.28}$$

Using the Generalized Marcum Q-function [9, 12],

$$Q_m(\alpha,\beta) = \frac{1}{\alpha^{m-1}}\int_\beta^\infty x^m I_{m-1}(\alpha x)\times \exp\left[-\left(\frac{x^2+\alpha^2}{2}\right)\right]dx, \tag{4.29}$$

the term $\Phi_n(\hat{\gamma})$ can be expressed as

$$\Phi_n(\hat{\gamma}) = \lim_{\epsilon\to 0}\left(\frac{m\hat{\gamma}}{c_3^{(j)}(\hat{\gamma})}\right)^m \exp\left(-\frac{\rho n c_1^{(j)}(\hat{\gamma}) m\hat{\gamma}}{c_3^{(j)}(\hat{\gamma})}\right)\times Q_m\left(\sqrt{\frac{2\rho m^2\hat{\gamma}^2}{\bar{\Gamma}(1-\rho)c_3^{(j)}(\hat{\gamma})}}, \sqrt{2c_2^{(j)}(\hat{\gamma})(K_j+\epsilon)}\right), \tag{4.30}$$

and the details of the derivation are given in the Appendix C. The terms $c_2^{(j)}(\hat{\gamma})$ and $c_3^{(j)}(\hat{\gamma})$ are given by

$$c_2^{(j)}(\hat{\gamma}) = \left(\frac{n c_1^{(j)}(\hat{\gamma})}{\hat{\gamma}} + \frac{m}{\bar{\Gamma}(1-\rho)}\right) \tag{4.31}$$

$$c_3^{(j)}(\hat{\gamma}) = m\hat{\gamma} + \bar{\Gamma}(1-\rho) n c_1^{(j)}(\hat{\gamma}) \tag{4.32}$$

Due to the rapid convergence of the series in (4.27), $\tilde{R}^+(\hat{\gamma})$ can be accurately computed using a limited number, N^+, of terms so that

$$\tilde{R}^+(\hat{\gamma}) \simeq r_j n_j(\hat{\gamma}) \sum_{n=0}^{N^+} (-1)^n (a_1^{(j)})^{-n} \Phi_n(\hat{\gamma}) \tag{4.33}$$

4.3.2 The case $\gamma < K_j$

Using (4.14) and (4.19c), the term $\tilde{R}^-(\hat{\gamma})$ in (4.21) can be expressed as

$$\tilde{R}^-(\hat{\gamma}) = \lim_{\epsilon\to 0}\int_0^{K_j-\epsilon} r_j n_j(\hat{\gamma})\times \sum_{n=1}^{\infty}(-1)^{n-1}(a_1^{(j)} e^{c_1^{(j)}(\hat{\gamma})\gamma/\hat{\gamma}})^n p_{\Gamma|\hat{\Gamma}}(\gamma|\hat{\gamma})d\gamma \tag{4.34}$$

$$= r_j n_j(\hat{\gamma}) \sum_{n=1}^{\infty} (-1)^{n-1} (a_1^{(j)})^n \times \lim_{\epsilon \to 0} \int_0^{K_j - \epsilon} e^{n c_1^{(j)}(\hat{\gamma})\gamma/\hat{\gamma}} p_{\Gamma|\hat{\Gamma}}(\gamma|\hat{\gamma}) d\gamma \quad (4.35)$$

Unfortunately, no closed-form solution was found for the integral in (4.35). Instead, we approximate $\phi_j(\lambda(\hat{\gamma}, \gamma))$ in (4.14) by a piece-wise constant function. Then, from (4.21), $\tilde{R}^-(\hat{\gamma})$ can be approximated as

$$\tilde{R}^-(\hat{\gamma}) \simeq r_j n_j(\hat{\gamma}) \sum_{k=0}^{\lfloor (K_j/\delta)-1 \rfloor} \phi_j(\lambda_j(\hat{\gamma}, K_j - k\delta)) \times \int_{K_j-(k+1)\delta}^{K_j - k\delta} p_{\Gamma|\hat{\Gamma}}(\gamma|\hat{\gamma}) d\gamma \quad (4.36)$$

$$= r_j n_j(\hat{\gamma}) \sum_{k=0}^{\lfloor (K_j/\delta-1) \rfloor} \phi_j(\lambda_j(\hat{\gamma}, K_j - k\delta)) \times (Q_m(\alpha, \beta_k^-) - Q_m(\alpha, \beta_k^+)) \quad (4.37)$$

where

$$\alpha = \sqrt{\frac{2m\rho\hat{\gamma}}{(1-\rho)\bar{\Gamma}}} \quad (4.38)$$

$$\beta_k^- = \sqrt{\frac{2m(K_j - (k+1)\delta)}{(1-\rho)\bar{\Gamma}}} \quad (4.39)$$

$$\beta_k^+ = \sqrt{\frac{2m(K_j - k\delta)}{(1-\rho)\bar{\Gamma}}} \quad (4.40)$$

Due to the nature of the sigmoid function defined in (4.16), and since $\tilde{R}_j^-(\hat{\gamma})$ is defined in the region $\gamma \in [0, K_j)$, the weight of (4.37) lies mainly in the region near $\gamma = K_j$, and (4.37) decreases rapidly as γ decreases from K_j. Thus, (4.37) can be approximated using finite number of terms, N^-, as

$$\tilde{R}^-(\hat{\gamma}) \simeq r_j n_j(\hat{\gamma}) \sum_{k=0}^{N^-} \phi_j(\lambda_j(\hat{\gamma}, K_j - k\delta)) \times (Q_m(\alpha, \beta_k^-) - Q_m(\alpha, \beta_k^+)) \quad (4.41)$$

The average effective bit rate[2], $\overline{R}$, is then given by

$$\overline{R} = \int_0^\infty \tilde{R}(\hat{\gamma}) p_{\hat{\Gamma}}(\hat{\gamma}) d\hat{\gamma} \tag{4.42}$$

where $\tilde{R}(\hat{\gamma})$ and $p_{\hat{\Gamma}}(\hat{\gamma})$ are given by (4.25) and (4.10) respectively.

4.4 Results and Discussion

The performance analysis presented in the previous section of AMC with multicodes in a CDMA system over Nakagami fading channels can be used to provide some numerical results for $\tilde{R}(\hat{\gamma})$ and $\overline{R}$ given in (4.25) and (4.42) respectively. These results are compared against the numerical results obtained by applying (4.14) and (4.16) directly to (4.18) in Fig. 4.3. In order to distinguish between the two set of results, the former will be referred to as approximate and the latter as exact. In Figs. 4.5 and 4.6, the numerical results are compared against simulations for numerical convenience. The parameter values which were used are listed in Table 4.1. The values of $a_1^{(j)}$ and $a_2^{(j)}$ are obtained using the first transmission error rates of the selected MCS's in [11]. For computational efficiency, the Marcum Q-function was approximated using the results in [12].

Fig. 4.3 shows the normalized average conditional bit rate $\tilde{R}(\hat{\gamma})/W$ for $\rho = 0.001$ and $\rho = 0.3$ as a function of the estimated SNR, $\hat{\gamma}$, with $m = 15$ and $\bar{\Gamma} = 2.5$. It can be seen that $\tilde{R}(\hat{\gamma})/W$ varies a lot with $\hat{\gamma}$. Due to the rapid increase (from nearly 0 to nearly 1) in the error rate curve for MCS j as a certain SNR threshold T_j is crossed, a high penalty in bit rate is incurred if the actual SNR, γ, is lower than the estimated value, $\hat{\gamma}$. When $\hat{\gamma} < \bar{\Gamma}$, $\tilde{R}(\hat{\gamma})$ does not always increase with ρ. This somewhat surprising result is due to the fact that when $\hat{\gamma} < \bar{\Gamma}$, the probability that $\Gamma > \hat{\gamma}$ is higher when ρ is small. On the other hand, when $\hat{\gamma}$ exceeds $\bar{\Gamma}$, the probability that $\Gamma > \hat{\gamma}$ is higher when ρ is larger. In the region $3 < \hat{\gamma} < 4.5$, where the bit rate is limited by the maximum number of multicodes, N_{max}, an increase in

[2]It is also used interchangeably with the term 'average throughput' in this thesis.

$\hat{\gamma}$ implies an increase in Γ when $\rho = 0.3$. As a result, $\tilde{R}(\hat{\gamma})$ increases due to the increased value of $\lambda(\hat{\gamma}, \gamma)$. It can be observed that $\tilde{R}(\hat{\gamma})$ decreases to almost zero when $\hat{\gamma} > 4.7$. The reason is because the actual channel SNR is being significantly over-estimated.

Fig. 4.4 shows the conditional pdf, $p(\gamma|\hat{\gamma})$, of the actual SNR, γ, given the estimated SNR, $\hat{\gamma}$, for $\bar{\Gamma} = 2.5$, $m = 5$, and (top) $\rho = 0.001$, (bottom) $\rho = 0.5$. This figure illustrates that when ρ is small (top), the actual SNR, γ, distribution is more or less independent of the estimated SNR, $\hat{\gamma}$. On the other hand, when ρ is large (bottom), the change in the distribution of Γ with $\hat{\gamma}$ is evident. The figure also shows that when $\hat{\gamma} < \bar{\Gamma}$, the probability that $\Gamma > \hat{\gamma}$ is higher for $\rho = 0.001$ than for $\rho = 0.5$.

Fig. 4.5 shows the normalized average bit rate $\overline{R}/W$ as a function of the average SNR, $\bar{\Gamma}$, for $\rho = 0.001$ and $\rho = 0.3$ with $m = 15$. The figure indicates that $\overline{R}/W$ may not increase monotonically with $\bar{\Gamma}$ when the channel estimation error is large. It can also be seen that the average bit rate drops severely as ρ decreases from 1 to 0.3. A decrease in ρ from 0.3 to 0.001 results in only a slight degradation in average bit rate.

Fig. 4.6 shows the normalized average bit rate $\overline{R}/W$ as a function of the channel correlation ρ, when $m = 35$, and $\bar{\Gamma} = 2.5$. Note that when ρ approaches 1, the approximated results become numerically unstable. In such cases, only simulation results are shown. It can be seen that ρ has to be close to 1 for the degradation on average bit rate to be small.

4.5 Conclusions

In this chapter, the average bit rate performance of AMC with multicodes is analyzed for a CDMA system experiencing Nakagami fading and channel estimation errors. Efficiently computable approximations are obtained and shown to be fairly accurate. Numerical results show that significant performance degradations can occur in the presence of fading when the estimated channel state is erroneous.

Parameter	Value
MCS	QPSK 1/2, 16-QAM 1/2, QPSK 3/4, 16-QAM 3/4
Channel Coding	Turbo Code
Spreading Factor (g)	16
N_{max}	10
N^+	8
N^-	15
δ	0.001

Table 4.1: List of parameter values.

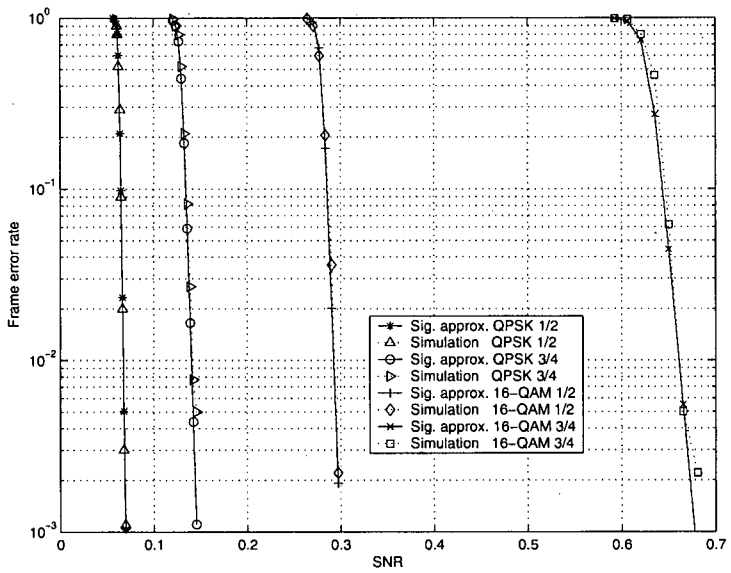

Figure 4.2: Frame error rate as a function of SNR for 4 MCS's.

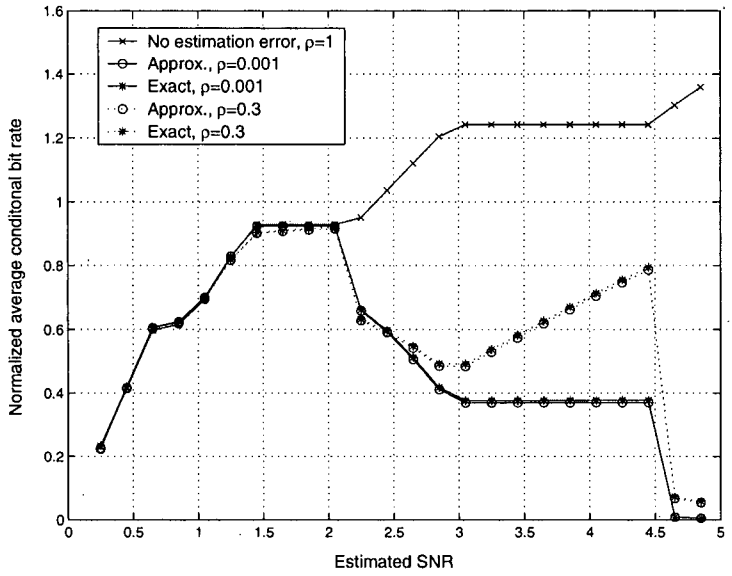

Figure 4.3: Normalized average conditional bit rate $\tilde{R}(\hat{\gamma})/W$ as a function of the estimated SNR, $\hat{\gamma}$, with $m = 15$, and $\bar{\Gamma} = 2.5$, at $\rho = 0.001$ and $\rho = 0.3$.

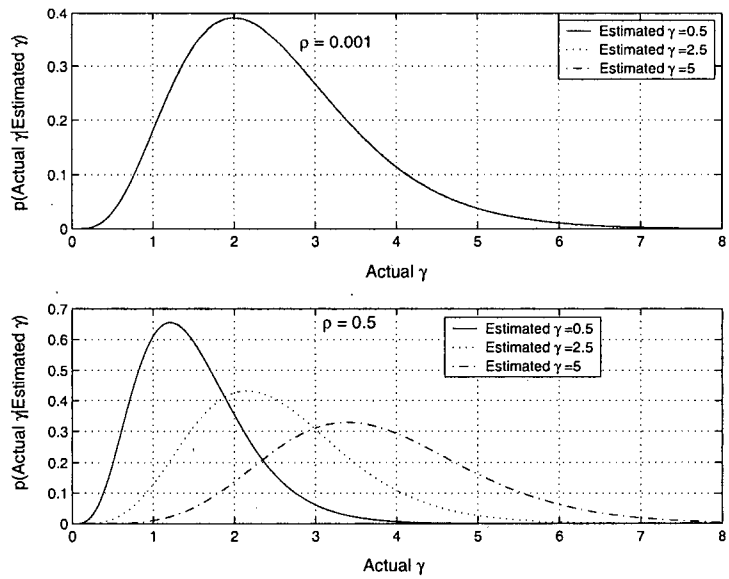

Figure 4.4: Conditional pdf $p(\gamma|\hat{\gamma})$ of the actual SNR, Γ, given the estimated SNR, $\hat{\gamma}$, with $\bar{\Gamma} = 2.5$, $m = 5$, and (top) $\rho = 0.001$, (bottom) $\rho = 0.5$.

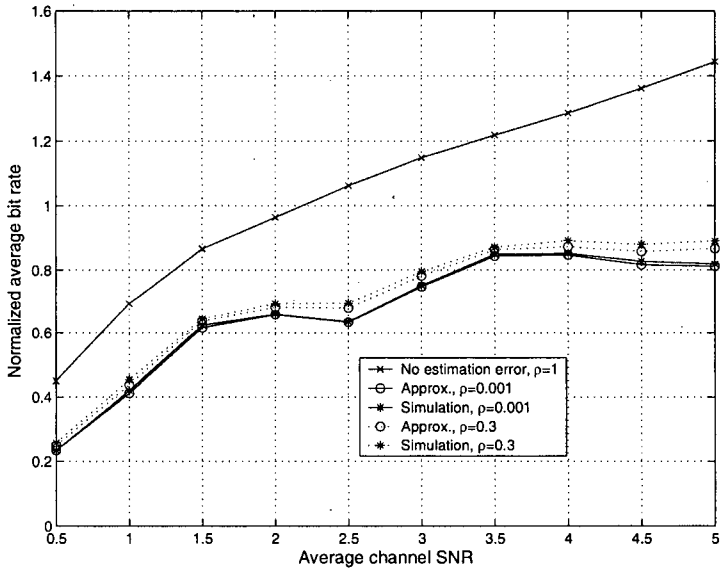

Figure 4.5: Normalized average bit rate $\overline{R}/W$ as a function of the average channel SNR, $\bar{\Gamma}$, with $\rho = 0.001$ and $\rho = 0.3$ when $m = 15$.

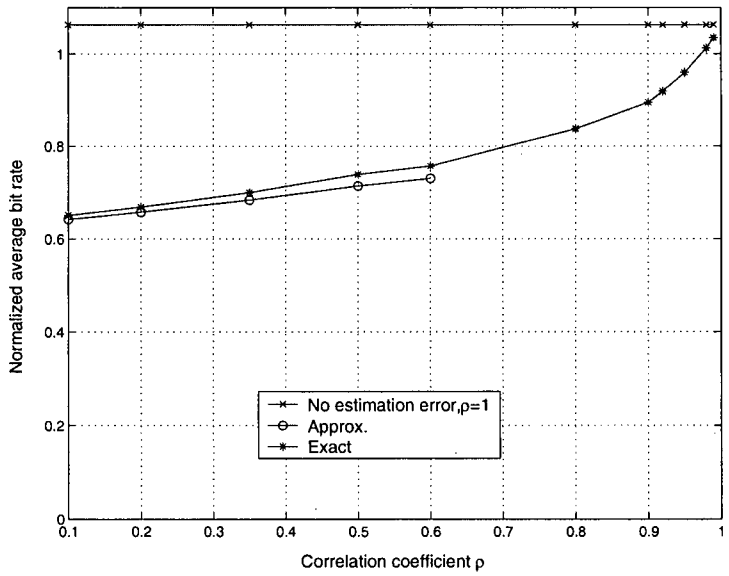

Figure 4.6: Normalized average bit rate $\overline{R}/W$ as a function of the correlation coefficient ρ, with $m = 35$, and $\bar{\Gamma} = 2.5$.

References

[1] "Physical Layer Aspects of UTRA High Speed Downlink Packet Access," 3rd Generation Partnership Project, Technical Report 3G TR25.858, 2002.

[2] H. Holma and A. Toskala, Eds., *WCDMA for UMTS Radio Access for Third Generation Mobile Communications.* John Wiley & Sons, 2002.

[3] N. C. Ericsson, "Adaptive Modulation and Scheduling for Fading Channels," in *Proc. of IEEE Global Telecommunications Conference, Globecom'99*, vol. 5, December 1999, pp. 2668–2672.

[4] S. A. Jafar and A. Goldsmith, "Adaptive Multicode CDMA for Uplink Throughput Maximization," in *Proc. of IEEE Vehicular Technology Conference, Spring*, vol. 1, May 2001, pp. 6–9.

[5] S. Falahati, "Adaptive Modulation systems for Predicted Wireless Channels," *IEEE Transactions on Communications*, vol. 52, no. 2, pp. 307 – 316, Feb. 2004.

[6] J. F. Paris, M. C. Aguayo-Torres, and J. T. Entrambasaguas, "Impact of Channel Estimation Error on Adaptive Modulation Performance in Flat Fading," *IEEE Transactions on Communications*, vol. 52, no. 5, pp. 716 – 720, May 2004.

[7] S. J. Lee, H. W. Lee, and D. K. Sung, "Capacities of Single-Code and Multicode DS-CDMA Systems Accommodating Multiclass Service," *IEEE Trans. on Vehicular Technology*, vol. 48, no. 2, pp. 376 –384, March 1999.

[8] R. Kwan and C. Leung, "Scheduling for the Downlink in a CDMA Network with Imperfect Channel Estimation," in *Proc. of IEEE Global Telecommunications Conference - Adaptive Wireless Network Workshop*, Dallas, Texas, December 2004, pp. 469–476.

[9] J. G. Proakis, *Digital Communications*, 4th ed. McGraw-Hill, 2001.

[10] M. Nakagami, "The m-Distribution: A General Formula of Intensity Distribution of Rapid Fading," in *Statistical Methods in Radio Wave Propagation.* Oxford, U.K.: Pergamon Press, 1960, pp. 3–36.

[11] M. Döttling, J. Michel, and B. Raaf, "Hybrid ARQ and Adaptive Modulation and Coding Schemes for High Speed Downlink Packet Access," in *Proc. of IEEE International Symposium on Personal, Indoor and Mobile Radio Communications (PIMRC)*, September 2002.

[12] G. E. Corazza and G. Ferrari, "New Bounds for the Marcum Q-Function," *IEEE Transactions on Information Theory*, vol. 48, no. 11, pp. 3003 – 3008, Nov. 2002.

Chapter 5

Performance of a CDMA system employing AMC in the Presence of Channel Estimation Errors

5.1 Introduction

Adaptive Modulation and Coding (AMC) has been adopted in the 3GPP standard in order to improve spectral efficiency [1]. In order to increase the granularity of the adaptation and to provide higher bit rates, multicode transmission [2] is employed. Multicode transmission increases the bit rate by dividing a high rate data stream into a number of lower rate sub-streams. These sub-streams are transmitted in parallel synchronous multicode channels so that inter-stream interference is avoided in the absence of multipath.

On the downlink to a target mobile station **MS A**, the base station (BS) typically acquires the channel state information (CSI) from **MS A** via an uplink feedback channel. Based on the newly acquired CSI, the BS assigns an appropriate modulation and coding scheme (MCS) and number of multicodes to **MS A** for use in the next scheduling period. Since the use of AMC requires knowledge of the channel state, it is important to assess the performance degradation which would result from inaccuracies in estimating the channel state.

This chapter examines the performance of using (1) a simple averaging filter (2) a hidden Markov model (HMM) based filter in a CDMA system employing AMC and multicodes. An HMM formulation of the system is presented in Section 5.2. The performance evaluation measures are discussed in Section 5.4. Some numerical results are presented in Section 5.5.

[1]The material in this chapter is largely based on R. Kwan and C. Leung, "An HMM Approach to Adaptive Modulation and Coding with Multicodes for Fading Channels." *Proc. of IEEE Canadian Conference on Electrical and Computer Engineering (CCECE'05)*, Saskatoon, Saskatchewan, May, 2005.

5.2 HMM Formulation

The assigned bit rate for any given scheduling period can take on one of a finite set of values, depending on the MCS and the number of multicodes which are selected. We choose to associate a channel state with each possible value of the assigned bit rate. The channel is then modelled as a finite state Markov Chain (FSMC) [3]. Since the true channel state is not available at the BS, a HMM formulation is appropriate [4].

It is shown in [5] that the average throughput[2] for a CDMA system with AMC and multicodes can be written as

$$\overline{R} \approx \sum_{j=1}^{J} \left(\phi_2(j) + \sum_{k=\lfloor \tilde{\gamma}_j^{(min)}/\lambda_j \rfloor}^{N_{max}-1} \phi_1(j,k) \right) \tag{5.1}$$

where

$$\phi_1(j,k) = r_j k(1-\varepsilon_0)\left[F_\Gamma((k+1)\lambda_j) - F_\Gamma(k\lambda_j)\right] \tag{5.2}$$

$$\phi_2(j) = r_j N_{max}(1-\varepsilon_0)\left[F_\Gamma(\tilde{\gamma}_{j+1}^{(min)}) - F_\Gamma(\tilde{\gamma}_j)\right] \tag{5.3}$$

and $F_\Gamma(\gamma)$ is the cumulative distribution function (cdf) of the signal-to-noise ratio (SNR), Γ. The terms $\tilde{\gamma}_j^{(min)}$ and $\tilde{\gamma}_j$ correspond to a set of decision thresholds which specify the MCS and number of multicodes for the near-optimal throughput for a given value of γ [5], and ε_0 denotes the maximum tolerable frame error rate (FER). The basic bit rate, r_j, for MCS j is given by

$$r_j = \frac{W}{g} R_c^{(j)} \log_2 M_j, \ 1 \le j \le J, \tag{5.4}$$

where W is the chip rate, g is the spreading factor, $R_c^{(j)}$ is the code rate for MCS j and M_j is the number of points in the modulation constellation for MCS j, N_{max} is the maximum

[2]It is used interchangeably with the term 'average effective bit rate' in this thesis.

number of multicodes that can be assigned to an MS, and λ_j is the minimum required SNR per code for MCS j to achieve an FER of ε_0.

This allows us to determine a near-optimal mapping from a given value of γ to an assigned bit rate, based on [5], as follows. Let $\mathcal{C}$ be the set of possible assigned bit rates such that

$$\mathcal{C} = \begin{cases} 0 & , \text{ if } 0 \leq \gamma < \lambda_1 \\ r_j k_j & , \text{ if } k_j \lambda_j \leq \gamma < (k_j + 1)\lambda_j \\ r_j N_{max} & , \text{ if } \tilde{\gamma}_j \leq \gamma < \tilde{\gamma}_{j+1}^{(min)} \end{cases} \tag{5.5}$$

where $\lfloor \tilde{\gamma}_j^{(min)} / \lambda_j \rfloor \leq k_j \leq N_{max} - 1$.

For notational convenience, let the set $\mathcal{C}$ be expressed as

$$\mathcal{C} = \{C_1, C_2, \ldots, C_N\} \tag{5.6}$$

where $C_1 < C_2 < \cdots < C_N$, and N is the number of possible assigned bit rates. For any value of γ which maps to an assigned bit rate of C_i, we say that the channel is in state i.

The throughput $\overline{R}$ in (5.1) can then be written as

$$\overline{R} \approx (1 - \varepsilon_0) \sum_{i=1}^{N} C_i p(i) \tag{5.7}$$

where $p(i)$ is the probability that the channel is in state i.

Let $x_k \in \{1, 2, \ldots, N\}$ denote the channel state at time k. Also, let $\pi_k(i) = P(X_k = i)$ be the probability that the channel is in state i at time k, and $\underline{\pi}_k = [\pi_k(1), \ldots, \pi_k(N)]$. For small values of the normalized Doppler rate (defined as the product of the Doppler rate of the channel and the scheduling period), the sequence of channel states can be modelled as a first order Markov process. Then, the probability vector at time $k + 1$ is given by

$$\underline{\pi}_{k+1} = \underline{\pi}_k \mathbf{A} \tag{5.8}$$

where $\mathbf{A} = \{a_{i,j}\}$, $i, j = 1, \ldots, N$ is the state transition probability matrix, and $a_{i,j}$ is the probability that $X_k = j$ given that $X_{k-1} = i$.

We model the observed channel state as

$$y_k = x_k + v_k \tag{5.9}$$

where v_k represents the observation noise and is the outcome of an independent random variable (rv) V with pdf $f_V(v)$. Denote the conditional pdf of Y_k by

$$b_i(y_k) = f_{Y_k}(y_k|X_k = i). \tag{5.10}$$

We are interested in minimizing the variance of the state estimate, i.e. $E[(\hat{X}_k - X_k)^2]$, where $\hat{X}_k$ is the estimated state and X_k is the actual state.

Given a sequence of observations $\underline{y}^{(k)} = [y_1, y_2, \ldots, y_k]$, up to time k, the *minimum variance state estimate* is given by [6]

$$\hat{x}_k = E[X_k|\underline{y}^{(k)}]. \tag{5.11}$$

Let the *forward probability* be $\alpha_k(j) = P(X_k = j, \underline{y}^{(k)})$. From (5.11), the optimal filter is given by

$$\hat{x}_k = \frac{\sum_{j=1}^{N} j\alpha_k(j)}{\sum_{j=1}^{N} \alpha_k(j)}, \tag{5.12}$$

where $\alpha_k(j)$ can be computed recursively as [6]

$$\alpha_k(j) = b_j(y_k) \sum_{i=1}^{N} a_{i,j}\alpha_{k-1}(i) \tag{5.13}$$

with $\alpha_1(m) = b_m(y_1)P(X_1 = m), m = 1, \ldots, N$ as the initial distribution.

5.3 Transition Probabilities Estimation

In section 5.2, the transition probabilities $\{a_{i,j}\}$ are assumed to be known. In practice, these probabilities can be estimated using the expectation-maximization (EM) algorithm. The idea behind the EM algorithm is as follows.

Let $\underline{X}^{(K)} = [X_1, X_2, \ldots, X_K]$, where K is the number of observation samples. Also, let θ and $\theta^{(0)}$ be the true parameters and the initial estimate of the parameters respectively. Using $\theta^{(0)}$, the EM algorithm iteratively generates a sequence of estimates $\{\theta^{(l)},\ l = 1, 2, \ldots, L\}$ based on the following steps:

- *Expectation:* To obtain the auxiliary[3] likelihood

$$Q(\theta|\theta^{(l)}) = E\left[\ln\left(p(\underline{X}^{(K)}, \underline{y}^{(K)}|\theta)\right)|\underline{y}^{(K)}, \theta^{(l)}\right]; \tag{5.14}$$

- *Maximization:* To maximize the auxiliary likelihood such that

$$\theta^{(l+1)} = \max_{\theta} Q(\theta|\theta^{(l)}). \tag{5.15}$$

If $b_j(y_k)$ is known, the estimated transition probabilities $\{\hat{a}_{i,j}^{(l)}\}$ after l iterations can be obtained using standard constrained optimization techniques, and are given by [6]

$$\hat{a}_{i,j}^{(l+1)} = \frac{\sum_{k=2}^{K} \alpha_{k-1}^{(l)}(i)\hat{a}_{i,j}^{(l)} b_j(y_k)\beta_k^{(l)}(j)}{\sum_{k=2}^{K} \alpha_{k-1}^{(l)}(i)\beta_{k-1}^{(l)}(i)}, \tag{5.16}$$

where

$$\alpha_k^{(l)}(j) = b_j(y_k)\sum_{i=1}^{N} \hat{a}_{i,j}^{(l)}\alpha_{k-1}^{(l)}(i) \tag{5.17}$$

$$\beta_k^{(l)}(j) = \sum_{j=1}^{N} a_{i,j}^{(l)} b_j(y_{k+1})\beta_{k+1}^{(l)}(j) \tag{5.18}$$

[3]The auxiliary likelihood $Q(\theta|\theta^{(l)})$ is used instead of the true likelihood $L(\theta, K) = p(\underline{y}^{(K)}|\theta)$ because the former is easier to optimize, and maximizing the former has the same effect as maximizing the latter [6].

and $\beta_k^{(l)}(j)$ is known as the *backward probability*, with $\beta_{K+1}^{(l)}(j) = 1$.

5.4 Performance Measures

In general, the estimated state $\hat{x}_k$ in (5.12) takes on continuous values. However, $\hat{x}_k$ should take on one of the allowed discrete values as described earlier. Thus, $\hat{x}_k$ can be modified according to the following mapping:

$$\tilde{x}_k = \begin{cases} N \text{ , if } \hat{x}_k > \frac{2N-1}{2} \\ i \text{ , if } \frac{2i-1}{2} \leq \hat{x}_k \leq \frac{2i+1}{2} \\ 1 \text{ , if } \hat{x}_k < \frac{3}{2} \end{cases}, \quad i = 2, ..., N-1. \tag{5.19}$$

As discussed in [7], the effect of estimation error is asymmetrical. Over-estimation typically gives rise to a worse throughput degradation than under-estimation. Thus, the instantaneous throughput $\tilde{R}_k(\tilde{x}_k)$ can be approximated as

$$\tilde{R}_k(\tilde{x}_k) \approx \begin{cases} (1-\varepsilon_0)C_i & , \text{ if } x_k \geq \tilde{x}_k = i \\ 0 & , \text{ if } x_k < \tilde{x}_k \end{cases} \tag{5.20}$$

The average throughput is then given by

$$\overline{R} = \lim_{M_s \to \infty} \frac{1}{M_s} \sum_{k=1}^{M_s} \tilde{R}_k(\tilde{x}_k) \tag{5.21}$$

Let $\overline{R'}$ be the average throughput for the case when no filtering is performed, and is given by (5.21) except that the instantaneous throughput is modified to be $\tilde{R}_k(\tilde{y}_k)$, where $\tilde{y}_k$ can be obtained from (5.19), with $\hat{x}_k$ and $\tilde{x}_k$ replaced by $\hat{y}_k$ and $\tilde{y}_k$ respectively. The average

improvement factor η_f is given by

$$\eta_f = \left(\frac{\overline{R} - \overline{R'}}{\overline{R'}}\right) \times 100 \tag{5.22}$$

where M_s is the total number of observation instances.

5.5 Numerical Results

The MCS set consists of turbo coded QPSK and 16-QAM with code rates of 1/2 or 3/4. A maximum of 2 multicodes can be assigned to each user; the spreading factor is 16 as specified in [8] and a target frame error rate of 1% is assumed. The values of $\tilde{\gamma}_j^{(min)}$ and $\tilde{\gamma}_j$ are obtained using the first transmission error rates of the selected MCS's in [9]. The MCS and number of multicodes assignment is performed at the BS once every scheduling period, during which the channel is assumed to be constant. The signal amplitude is assumed to follow a Rayleigh fading distribution and the average signal SNR is normalized to unity. For simplicity, the observation noise $V \sim N(0, \sigma_V^2)$ is assumed. The estimate of noise variance, σ_V^2 can be computed as [6]

$$(\hat{\sigma}_V^{(l+1)})^2 = \frac{\sum_{k=1}^{K}\sum_{j=1}^{N}\alpha_k^{(l)}(j)\beta_k^{(l)}(j)(y_k - j)^2}{\sum_{k=1}^{K}\sum_{j=1}^{N}\alpha_k^{(l)}(j)\beta_k^{(l)}(j)} \tag{5.23}$$

The number of iterations, L, for the EM algorithm is set to 5. Using a higher value for L resulted in little change in the normalized throughput. For the results presented in this section, the 95% confident interval lies within 3% of the values shown.

Fig. 5.1 shows the improvement factor, η_f, as a function of the observation noise standard deviation for the normalized doppler frequencies $f_dT = 0.005$ and $f_dT = 0.025$ respectively. For comparisons, the improvement for a system employing a linear averaging filter (LAF) with a window size Z is also shown. The results show that the improvements of both systems over the unfiltered system increase with the observation noise. In all cases, the performance

of the HMM system is always superior to that of the LAF system. The results also suggest that both systems provide greater improvement when the channel changes more slowly. However, it can be seen that the performance of a LAF system is very sensitive to the choice of Z, i.e. a reasonably good value of Z for a given value of f_dT can be in fact unacceptable for another value of f_dT. As shown in Fig. 5.2, an appropriate value of Z has to be chosen for a LAF system to achieve a reasonable improvement η_f. However, such value of Z is not always available in practice.

5.6 Conclusions

In this chapter, the impact of channel state estimation errors in a system employing AMC and multicodes was studied. An HMM filter was employed to alleviate the effects of estimation errors. It was shown that HMM filtering can significantly reduce the state estimation error, and improve the system throughput.

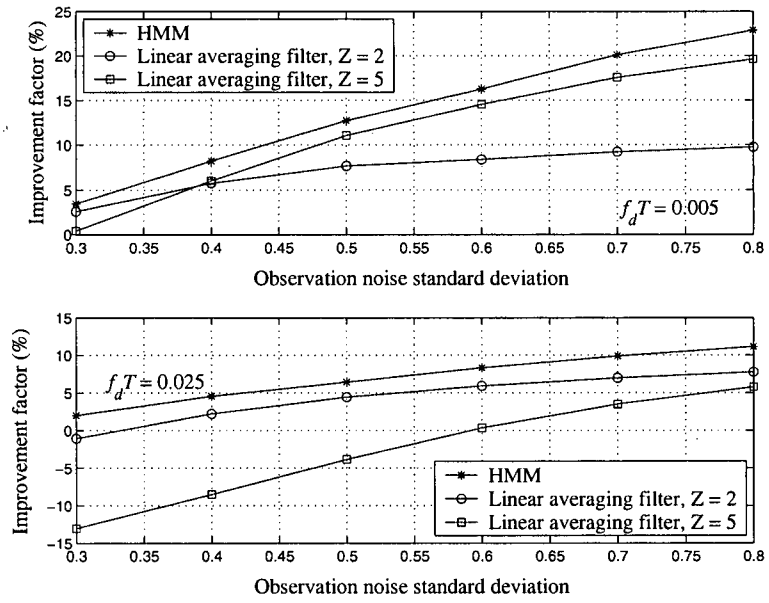

Figure 5.1: Improvement factor, η_f, as a function of the observation noise standard deviation.

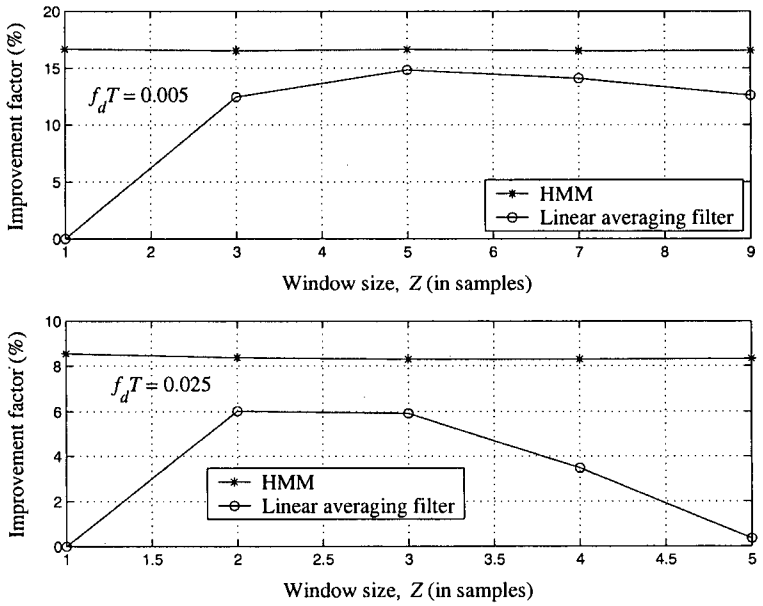

Figure 5.2: Improvement factor, η_f, as a function of the LAF window size, Z, with $\sigma_V = 0.6$.

References

[1] H. Holma and A. Toskala, Eds., *WCDMA for UMTS Radio Access for Third Generation Mobile Communications.* John Wiley & Sons, 2002.

[2] S. J. Lee, H. W. Lee, and D. K. Sung, "Capacities of Single-Code and Multicode DS-CDMA Systems Accommodating Multiclass Service," *IEEE Trans. on Vehicular Technology*, vol. 48, no. 2, pp. 376 –384, March 1999.

[3] C.-D. Iskander and P. T. Mathiopoulos, "Fast Simulation of Diversity Nakagami Fading Channels Using Finite-State Markov Models," *IEEE Transactions on Broadcasting*, vol. 49, no. 3, pp. 269 – 277, September 2003.

[4] R. J. Elliott, L. Aggoun, and J. B. Moore, *Hidden Markov Models, Estimation and Control.* New York: Springer-Verlag, 1995.

[5] R. Kwan and C. Leung, "Order Statistics for Non-Identically Distributed Nakagami Fading Channels with An Application," in *Proc. of IEEE Vehicular Technology Conference (VTC)*, September 2005.

[6] T. K. Moon and W. C. Stirling, *Mathematical Methods and Algorithms for Signal Processing.* New Jersey: Prentice Hall, 2000.

[7] R. Kwan and C. Leung, "Scheduling for the Downlink in a CDMA Network with Imperfect Channel Estimation," in *Proc. of IEEE Global Telecommunications Conference - Adaptive Wireless Network Workshop*, Dallas, Texas, December 2004, pp. 469–476.

[8] "Physical Layer Aspects of UTRA High Speed Downlink Packet Access," 3rd Generation Partnership Project, Technical Report 3G TR25.858, 2002.

[9] M. Döttling, J. Michel, and B. Raaf, "Hybrid ARQ and Adaptive Modulation and Coding Schemes for High Speed Downlink Packet Access," in *Proc. of IEEE International Symposium on Personal, Indoor and Mobile Radio Communications (PIMRC)*, September 2002.

Chapter 6

Gamma Variate Ratio Distribution with Application to CDMA Performance Analysis

6.1 Introduction

In wireless communication systems, interference is usually considered undesirable since it corrupts the desired signal and generally lowers the probability of correct reception. On the downlink of a cellular network employing Code Division Multiple Access (CDMA) the interference experienced by a mobile station (MS) is dominated by the signal transmitted by the same cell base station (BS) and signals from BS's in neighboring cells [1]. Typically, both the desired and interfering signals undergo *multipath fading* [2]. In the performance analyses of CDMA systems, the total interference often modelled as Gaussian noise with a time invariant power. While this Gaussian approximation facilitates the analysis, it may yield inaccurate results [3]. The reason is that the Gaussian approximation, which is based on the central limit theorem, relies on statistical independence among all the signals. However, this assumption may not be valid, especially on the downlink of a CDMA system.

In this chapter, a model for the received signal-to-interference ratio (SIR) on the downlink of a CDMA network is studied. Statistical characterizations of the SIR are derived. To illustrate their usefulness, the results are applied to assess the performance of a CDMA system which employs adaptive modulation and coding (AMC).

[1]The material in this chapter is largely based on R. Kwan and C. Leung, "Gamma Variate Ratio Distribution with Application to CDMA Performance Analysis." *Proc. of IEEE Sarnoff Symposium on Advances in Wired and Wireless Communication*, Princeton, New Jersey, April, 2005.

6.2 System Model and SIR Statistics

Let the downlink received SIR at the target MS be

$$\Gamma = \frac{\zeta hGP}{\alpha hG(1-\zeta)P + \alpha' h'G'P + h''G''I} \tag{6.1}$$

where P is the total power transmitted by the home cell BS, BS **A**, ζ is the fraction of P allocated to target MS, and I is the power transmitted by the dominant interfering BS, BS **B**. The terms h and h'' are the long-term path gains from BS **A** to the MS and from BS **B** to the MS respectively. The terms G and G'' represent the corresponding short-term path gains. The terms h' and G' correspond to the long-term and short-term path gains of the second strongest multipath component due to BS **A**'s transmission[2]. The term $\alpha \in [0,1]$ is used to model the effect of intra-cell interference due to the possible use of non-orthogonal codes, and $\alpha' \in [0,1]$ is used to model the effect of non-orthogonality due to multipath interference. In the case when orthogonal codes are used, $\alpha = 0$.

The numerator in (6.1) is the power of the desired signal in the strongest multipath; the first term in the denominator is the interference power in the strongest multipath due to multicode non-orthogonality; the second term is the interference power due to the second strongest multipath, and the third term is interference due to BS **B**.

In this chapter, we study the effects of short-term fading[3] and assume that the long-term path gains are constant [4]. Also, we assume that the relative delay between the first and second strongest multipath components are much smaller than the channel coherence time, so that $G \approx G'$. Then (6.1) reduces to

$$\Gamma = \frac{X_1}{a_1 X_1 + a_2 X_2} \tag{6.2}$$

[2]We assume that the interfering effect due to the weaker multipath components are negligible.

[3]Note that since G, G', and G'' denote the random variables corresponding to the respective short-term path gains, the term Γ is also a random variable, with the corresponding outcome denoted by γ.

where $a_1 = (\alpha h(1-\zeta)+\alpha^{'}h^{'})/(\zeta h)$, $a_2 = h^{''}/(\zeta h)$, $X_1 = GP$, and $X_2 = G^{''}I$. Assuming that the short-term signal amplitude follows a Nakagami-m distribution [2], the random variables (rv) X_1 and X_2 have gamma distributions $\mathcal{G}(\bar{X}_i, \alpha_i)$, given by

$$f_{X_i}(x_i) = \left(\frac{\alpha_i}{\bar{X}_i}\right)^{\alpha_i} \frac{x_i^{\alpha_i - 1}}{\Gamma(\alpha_i)} e^{-\alpha_i x_i/\bar{X}_i}, \; x_i > 0, \; i = 1, 2 \tag{6.3}$$

where $\bar{X}_i$ is the average value of X_i, and $\alpha_i > 0$ is a shaping parameter, and $\Gamma(.)$ is the Gamma function.

The pdf and m^{th} moment of the rv Γ in (6.2) are derived in Theorems 2.1 and 2.2 respectively. Statistical characteristics of Γ have been studied for the special cases of $a_1 = 0$ and $a_1 = a_2$ in [5, 6]. It might be noted that the results can be applied to the case involving multiple interfering BS's since the pdf of the sum of gamma rv's can be well approximated by another gamma pdf [7].

Theorem 2.1: Let $\Gamma = X_1/(a_1X_1 + a_2X_2)$, where a_1 and a_2 are positive constants, and X_1 and X_2 are gamma distributed with pdf $\mathcal{G}(\bar{X}_1, \alpha_1)$ and $\mathcal{G}(\bar{X}_2, \alpha_2)$ respectively. Then the pdf of the rv Γ is given by

$$f_\Gamma(\gamma) = K_{12}\gamma^{\alpha_1 - 1}(1 - a_1\gamma)^{\alpha_2 - 1}(c_1 + c_2\gamma)^{-(\alpha_1+\alpha_2)}, \; 0 \le \gamma \le 1/a_1 \tag{6.4}$$

where

$$K_{12} = \left(\frac{\alpha_1}{\bar{X}_1}\right)^{\alpha_1} \left(\frac{\alpha_2}{\bar{X}_2}\right)^{\alpha_2} \left(\frac{1}{B(\alpha_1, \alpha_2)}\right) \left(\frac{1}{a_2}\right)^{\alpha_2} \tag{6.5}$$

$$c_1 = \frac{\alpha_2}{\bar{X}_2 a_2} \tag{6.6}$$

$$c_2 = \frac{\alpha_1}{\bar{X}_1} - \frac{\alpha_2 a_1}{\bar{X}_2 a_2}, \tag{6.7}$$

and $B(\alpha_1, \alpha_2)$ is the beta integral, which is defined as [8]

$$B(\alpha_1, \alpha_2) = \frac{\Gamma(\alpha_1)\Gamma(\alpha_2)}{\Gamma(\alpha_1 + \alpha_2)}. \tag{6.8}$$

Proof: The joint pdf of two independent gamma rv's, X_1 and X_2, with pdf given in (6.3) is

$$f_{X_1,X_2}(x_1, x_2) = \left(\frac{\alpha_1}{\bar{X}_1}\right)^{\alpha_1} \left(\frac{\alpha_2}{\bar{X}_2}\right)^{\alpha_2} \left(\frac{1}{\Gamma(\alpha_1)\Gamma(\alpha_2)}\right) x_1^{\alpha_1 - 1} x_2^{\alpha_2 - 1} \exp\left(-\left(\frac{\alpha_1 x_1}{\bar{X}_1} + \frac{\alpha_2 x_2}{\bar{X}_2}\right)\right) \tag{6.9}$$

Defining

$$\Gamma = \frac{X_1}{a_1 X_1 + a_2 X_2} \tag{6.10}$$

$$S = a_1 X_1 + a_2 X_2 \tag{6.11}$$

we have

$$X_1 = \Gamma S \tag{6.12}$$

$$X_2 = \frac{1}{a_2} S(1 - a_1 \Gamma). \tag{6.13}$$

From (6.10), it can be seen that as the term $a_2 X_2$ approaches zero, Γ attains its maximum value of $1/a_1$.

Using a standard result on the functional transformation of rv's [9], the joint pdf, $f_{\Gamma,S}(\gamma, s)$, of Γ and S is given by

$$f_{\Gamma,S}(\gamma, s) = \left. \frac{f_{X_1,X_2}(x_1, x_2)}{\left| J\left(\frac{x_1, x_2}{\gamma, s}\right) \right|} \right|_{x_1 = \gamma s, x_2 = \frac{1}{a_2} s(1 - a_1 \gamma)} \tag{6.14}$$

where $J\left(\frac{x_1,x_2}{\gamma,s}\right)$ is the Jacobian of the transformation from (x_1, x_2) to (γ, s), i.e.

$$J\left(\frac{x_1,x_2}{\gamma,s}\right) = \begin{vmatrix} \frac{\partial x_1}{\partial \gamma} & \frac{\partial x_1}{\partial s} \\ \frac{\partial x_2}{\partial \gamma} & \frac{\partial x_2}{\partial s} \end{vmatrix} \tag{6.15}$$

$$= \begin{vmatrix} s & \gamma \\ -\frac{a_1}{a_2}s & \frac{1}{a_2}(1-a_1\gamma) \end{vmatrix} \tag{6.16}$$

$$= \frac{s}{a_2}. \tag{6.17}$$

We then have

$$\begin{aligned} f_{\Gamma,S}(\gamma,s) &= \left(\frac{\alpha_1}{\bar{X}_1}\right)^{\alpha_1}\left(\frac{\alpha_2}{\bar{X}_2}\right)^{\alpha_2}\left(\frac{1}{\Gamma(\alpha_1)\Gamma(\alpha_2)}\right)\times \\ &\quad \frac{1}{a_2}\left[s(\gamma s)^{\alpha_1-1}\left(\frac{1}{a_2}s(1-a_1\gamma)\right)^{\alpha_2-1}\right. \\ &\quad \left.\exp\left(-(\frac{\alpha_1}{\bar{X}_1}\gamma s+\frac{\alpha_2}{\bar{X}_2 a_2}s(1-a_1\gamma)\right)\right] \qquad (6.18) \\ &= \left(\frac{\alpha_1}{\bar{X}_1}\right)^{\alpha_1}\left(\frac{\alpha_2}{\bar{X}_2}\right)^{\alpha_2}\left(\frac{1}{\Gamma(\alpha_1)\Gamma(\alpha_2)}\right)\times \\ &\quad \left(\frac{1}{a_2}\right)^{\alpha_2}\left[s^{\alpha_1}\gamma^{\alpha_1-1}s^{\alpha_2-1}(1-a_1\gamma)^{\alpha_2-1}\times\right. \\ &\quad \left.\exp\left(-(\frac{\alpha_1}{\bar{X}_1}\gamma s+\frac{\alpha_1}{\bar{X}_2}\frac{1}{a_2}s-\frac{\alpha_2}{\bar{X}_2}\frac{a_1}{a_2}\gamma s)\right)\right] \qquad (6.19) \\ &= \left(\frac{\alpha_1}{\bar{X}_1}\right)^{\alpha_1}\left(\frac{\alpha_2}{\bar{X}_2}\right)^{\alpha_2}\left(\frac{1}{\Gamma(\alpha_1)\Gamma(\alpha_2)}\right)\left(\frac{1}{a_2}\right)^{\alpha_2}\times \\ &\quad s^{\alpha_1+\alpha_2-1}\gamma^{\alpha_1-1}(1-a_1\gamma)^{\alpha_2-1}e^{-s(c_1+c_2\gamma)}. \qquad (6.20) \end{aligned}$$

Using (6.20) and the identity [8]

$$\int_0^\infty x^{\nu-1}e^{-\mu x}dx = \frac{1}{\mu^\nu}\Gamma(\nu),\ \mu>0,\ \nu>0, \tag{6.21}$$

the pdf of Γ can be written as

$$f_\Gamma(\gamma) = \int_0^\infty f_{\Gamma,S}(\gamma,s)ds \tag{6.22}$$

$$= K_{12}\gamma^{\alpha_1-1}(1-a_1\gamma)^{\alpha_2-1}(c_1+c_2\gamma)^{-(\alpha_1+\alpha_2)}, \quad (6.23)$$

where K_{12}, c_1, and c_2 are given by (6.5), (6.6), and (6.7) respectively. ■

In the special case of $\alpha_1/\bar{X}_1 = \alpha_2/\bar{X}_2$, and $a_1 = a_2 = 1$, the pdf reduces to the standard beta distribution [5], i.e.

$$f_\Gamma(\gamma) = \frac{\gamma^{\alpha_1-1}(1-\gamma)^{\alpha_2-1}}{B(\alpha_1,\alpha_2)}, 0 \le \gamma \le 1. \quad (6.24)$$

On the other hand, if $\alpha_1/\bar{X}_1 = \alpha_2/\bar{X}_2$, $a_1 = 0$, and $a_2 = 1$, the pdf reduces to a beta prime distribution [5]

$$f_\Gamma(\gamma) = \frac{\gamma^{\alpha_1-1}(1+\gamma)^{-(\alpha_1+\alpha_2)}}{B(\alpha_1,\alpha_2)}, \gamma \ge 0. \quad (6.25)$$

The case $\alpha_1/\bar{X}_1 \neq \alpha_2/\bar{X}_2$, and $a_1 = a_2 = 1$ is treated in [6].

We now derive the m^{th} moment of Γ.

Theorem 2.2: The m^{th} moment of Γ is given by

$$E[\Gamma^m] = K_{12}c_1^{-(\alpha_1+\alpha_2)}a_1^{-(\alpha_1+m)}B(\alpha_2,\alpha_1+m) \times {}_2F_1(\alpha_1+\alpha_2,\alpha_1+m;\alpha_2+\alpha_1+m;-\frac{c_2}{c_1}a_1^{-1}), \quad (6.26)$$

where ${}_2F_1()$ is the *hypergeometric function* [8], given by

$${}_2F_1(a,b;c;t) = \frac{1}{B(b,c-b)}\int_0^1 x^{b-1}(1-x)^{c-b-1}(1-xt)^{-a}dx, \text{ Re } c > \text{Re } b > 0. \quad (6.27)$$

Proof: Expressing the density function $f_\Gamma(\gamma)$ in the form

$$f_\Gamma(\gamma) = K_{12}a_1^{\alpha_2-1}c_2^{-(\alpha_1+\alpha_2)}\gamma^{\alpha_1-1}(a_1^{-1}-\gamma)^{\alpha_2-1}\left(\frac{c_1}{c_2}+\gamma\right)^{-(\alpha_1+\alpha_2)}, \quad (6.28)$$

we can write

$$E[\Gamma^m] = \int_0^{a_1^{-1}} \gamma^m f_\Gamma(\gamma) d\gamma \tag{6.29}$$

$$= K_{12} a_1^{\alpha_2 - 1} c_2^{-(\alpha_1+\alpha_2)} \times$$

$$\int_0^{a_1^{-1}} \gamma^{\alpha_1+m-1} (a_1^{-1} - \gamma)^{\alpha_2 - 1} \left(\frac{c_1}{c_2} + \gamma\right)^{-(\alpha_1+\alpha_2)} d\gamma. \tag{6.30}$$

Using the identity [8],

$$\int_0^u x^{\nu-1}(x+\alpha)^\lambda (u-x)^{\mu-1} dx =$$

$$\alpha^\lambda u^{\mu+\nu-1} B(\mu,\nu) {}_2F_1(-\lambda, \nu; \mu_\nu; -u/\alpha), \ \nu > 0, \ \mu > 0 \tag{6.31}$$

(6.30) can be expressed as (6.26). ■

The central moments can be evaluated using the following result.

Theorem 2.3: The m^{th} central moment of Γ is given by

$$E[(\Gamma - \mu_\Gamma)^m] = K_{12} \sum_{k=0}^{m} \binom{m}{k} (-\mu_\Gamma)^{m-k} c_2^{-(\alpha_1+\alpha_2)} \times$$

$$\left(\frac{c_1}{c_2}\right)^{-(\alpha_1+\alpha_2)} a_1^{-(\alpha_1+k)} B(\alpha_2, \alpha_1 + k) \times$$

$${}_2F_1(\alpha_1+\alpha_2, \alpha_1+k; \alpha_2+\alpha_1+k; -\frac{c_2}{c_1} a_1^{-1}), \tag{6.32}$$

where $\mu_\Gamma = E[\Gamma]$.

Proof: Using (6.31), (6.28) and the binomial expansion, we can write

$$E[(\Gamma - \mu_\Gamma)^m] = \int_0^{a_1^{-1}} (\gamma - \mu_\Gamma)^m f_\Gamma(\gamma) d\gamma \tag{6.33}$$

$$= K_{12} \sum_{k=0}^{m} \binom{m}{k} (-\mu_\Gamma)^{m-k} c_2^{-(\alpha_1+\alpha_2)} \times$$

$$a_1^{\alpha_2-1}\int_0^{a_1^{-1}}\gamma^{\alpha_1+k-1}(a_1^{-1}-\gamma)^{\alpha_2-1}\left(\frac{c_1}{c_2}+\gamma\right)^{-(\alpha_1+\alpha_2)}d\gamma \qquad (6.34)$$

which can be put in the form of (6.32). ■

An expression for the moment generating function (MGF) of Γ is derived in Theorem 2.4.

Theorem 2.4: The MGF of Γ is given by

$$\begin{aligned}\Phi_\Gamma(s) &= K_{12}c_1^{-(\alpha_1+\alpha_2)}\sum_{k=0}^{\infty}\frac{s^k}{k!}a_1^{-(\alpha_1+k)}B(\alpha_2,\alpha_1+k)\times \\ &\quad {}_2F_1(\alpha_1+\alpha_2,\alpha_1+k;\alpha_2+\alpha_1+k;-a_1^{-1}c_2/c_1) \qquad (6.35)\end{aligned}$$

Proof: Using (6.28) and expanding the exponential term as an infinite series, we have

$$\begin{aligned}\Phi_\Gamma(s) &= \int_{-\infty}^{\infty}f_\Gamma(\gamma)e^{s\gamma}d\gamma \qquad (6.36)\\ &= K_{12}a_1^{\alpha_2-1}c_2^{-(\alpha_1+\alpha_2)}\int_0^{a_1^{-1}}\gamma^{\alpha_1-1}(a_1^{-1}-\gamma)^{\alpha_2-1}\times \\ &\quad \left(\frac{c_1}{c_2}+\gamma\right)^{-(\alpha_1+\alpha_2)}\sum_{k=0}^{\infty}\frac{(s\gamma)^k}{k!}d\gamma \qquad (6.37)\\ &= K_{12}a_1^{\alpha_2-1}c_2^{-(\alpha_1+\alpha_2)}\sum_{k=0}^{\infty}\frac{s^k}{k!}\int_0^{a_1^{-1}}\gamma^{\alpha_1+k-1}(a_1^{-1}-\gamma)^{\alpha_2-1}\times \\ &\quad \left(\frac{c_1}{c_2}+\gamma\right)^{-(\alpha_1+\alpha_2)}d\gamma \qquad (6.38)\end{aligned}$$

Using (6.31), the last expression can be reduced to (6.35). ■

The m^{th} derivative of $\Phi_\Gamma(s)$ is given by

$$\begin{aligned}\Phi_\Gamma^{(m)}(s) &= K_{12}c_1^{-(\alpha_1+\alpha_2)}\sum_{k=m}^{\infty}\frac{s^{(k-m)}}{(k-m)!}B(\alpha_2,\alpha_1+k)\times \\ &\quad a_1^{-(\alpha_1+k)}{}_2F_1(\alpha_1+\alpha_2,\alpha_1+k;\alpha_2+\alpha_1+k;-a_1^{-1}c_2/c_1) \qquad (6.39)\end{aligned}$$

and the m^{th} moment of Γ can also be obtained as

$$E[\Gamma^m] = \Phi_\Gamma^{(m)}(0). \tag{6.40}$$

An expression for the cumulative distribution function (cdf) of Γ is given by Theorem 2.5.

Theorem 2.5: If α_2 is an integer, the cdf of Γ can be expressed as

$$F_\Gamma(\gamma) = K_{12}c_1^{-(\alpha_1+\alpha_2)} \sum_{q=0}^{\alpha_2-1} (-1)^q \binom{\alpha_2-1}{q} \frac{a_1^q \gamma^{\alpha_1+q}}{\alpha_1+q} \times {}_2F_1(\alpha_1+\alpha_2, \alpha_1+q; 1+\alpha_1+q; -\frac{c_2}{c_1}\gamma). \tag{6.41}$$

Proof: Using the binomial expansion

$$(a+x)^n = \sum_{k=0}^{n} \binom{n}{k} x^k a^{n-k}, \tag{6.42}$$

the term $(1-a_1\gamma)^{\alpha_2-1}$ in (6.4) can be expressed as

$$(1-a_1\gamma)^{\alpha_2-1} = \left(a_1(\frac{1-a_1\gamma}{a_1})\right)^{\alpha_2-1} \tag{6.43}$$

$$= a_1^{\alpha_2-1}(b_1-\gamma)^{\alpha_2-1} \tag{6.44}$$

$$= a_1^{\alpha_2-1} \sum_{q=0}^{\alpha_2-1} (-1)^q \binom{\alpha_2-1}{q} \gamma^q b_1^{\alpha_2-1-q}. \tag{6.45}$$

where $b_1 = 1/a_1$. Using (6.45), the pdf of Γ in (6.4) can be written as

$$f_\Gamma(\gamma) = K_{12}a_1^{\alpha_2-1}c_1^{-(\alpha_1+\alpha_2)} \sum_{q=0}^{\alpha_2-1} (-1)^q \binom{\alpha_2-1}{q} b_1^{\alpha_2-1-q}\gamma^{\alpha_1+q-1}\left(1+\frac{c_2}{c_1}\gamma\right)^{-(\alpha_1+\alpha_2)} \tag{6.46}$$

Using the identity [8]

$$\int_0^u x^{\mu-1}(1+\beta x)^{-\nu}dx = \frac{u^\mu}{\mu}\,{}_2F_1(\nu,\mu;1+\mu,-\beta u), \quad |\arg(1+\beta u)|<\pi,\ \mathrm{Re}\,\mu>0, \tag{6.47}$$

and (6.46), $F_\Gamma(\gamma_1)$ can be written as

$$F_\Gamma(\gamma_1) = \int_0^{\gamma_1} f_\Gamma(\gamma)d\gamma \tag{6.48}$$

$$= K_{12}a_1^{\alpha_2-1}c_1^{-(\alpha_1+\alpha_2)}\sum_{q=0}^{\alpha_2-1}(-1)^q\begin{pmatrix}\alpha_2-1\\ q\end{pmatrix}b_1^{\alpha_2-1-q}\times \int_0^{\gamma_1}\gamma^{\alpha_1+q-1}\left(1+\frac{c_2}{c_1}\gamma\right)^{-(\alpha_1+\alpha_2)}d\gamma \tag{6.49}$$

$$= K_{12}c_1^{-(\alpha_1+\alpha_2)}\sum_{q=0}^{\alpha_2-1}(-1)^q\begin{pmatrix}\alpha_2-1\\ q\end{pmatrix}\frac{a_1^q}{\alpha_1+q}\gamma_1^{\alpha_1+q}\times {}_2F_1(\alpha_1+\alpha_2,\alpha_1+q;1+\alpha_1+q;-\frac{c_2}{c_1}\gamma_1). \tag{6.50}$$

Note that in obtaining (6.50), the condition

$$|\arg(1+\frac{c_2}{c_1}\gamma_1)|<\pi \tag{6.51}$$

must be satisfied. This can be verified by substituting (6.6) and (6.7) into (6.51), and realizing that $|\arg(1+c_2\gamma_1/c_1)| \le |\arg(1+(c_2/c_1)(1/a_1))|$. Thus, we have

$$|\arg(1+\frac{c_2}{c_1}\frac{1}{a_1})| = \left|\arg\left(1+\left(\frac{\alpha_1}{\bar{X}_1}-\frac{\alpha_2 a_1}{\bar{X}_2 a_2}\right)\left(\frac{\bar{X}_2 a_2}{\alpha_2}\right)\frac{1}{a_1}\right)\right| \tag{6.52}$$

$$= \left|\arg\left(\frac{\alpha_1\bar{X}_2 a_2}{\alpha_2\bar{X}_1 a_1}\right)\right| < \pi. \tag{6.53}$$

■

6.3 Application in Adaptive Modulation and Coding and Multicodes

It is well known that adapting the transmission parameters in a wireless system to changing channel conditions can be advantageous. In the case of fast power control [10], the transmission power is adjusted based on channel fading. Under good channel conditions a relatively low transmission power is required to maintain the target signal quality at the receiver. The process of changing transmission parameters to compensate for variations in channel conditions is known as link adaptation. Besides power control, adaptive modulation and coding (AMC) is another means for performing link adaptation [11, 12], and is used in the 3GPP High Speed Downlink Packet Access (HSDPA) channel. The goal of AMC is to change the modulation and channel coding according to the varying channel conditions. In order to increase the bit rate, multicode transmission is also used in the 3GPP standard [10, 11].

The multicode scheme [13] increases the bit rate by splitting the bits of a Transmission Block to more than one channelization code in a scheduling period. In this scheme, high rate data stream is divided into a number of lower rate data sub-streams. All the sub-streams are transmitted in parallel synchronous multicode channels so that interchannel interference is avoided.

Some scheduling issues regarding AMC and orthogonal multicodes have been studied in [14]. The model in [14] mainly addresses the throughput performance on a per scheduling period basis. In contrast, the analysis presented below examines the average throughput performance by taking into account the time-varying nature of the channel.

With AMC and orthogonal multicodes, the effective bit rate, $\tilde{R}(\gamma)$, at a given SIR, γ, is given by [14]

$$\tilde{R}(\gamma) = r_j n_j(\gamma)(1 - \varepsilon_j(\gamma)),\ j = 1, \ldots, J \tag{6.54}$$

where $\varepsilon_j(\gamma)$ is the frame error rate of modulation and coding scheme (MCS) j and J is the number of available MCS's. For a given maximum number, N_{max}, of multicodes, the number, $n_j(\gamma)$, of multicodes that can be assigned to the MS is given by [14]

$$n_j(\gamma) = \begin{cases} \lfloor \gamma/\lambda_j \rfloor, & \tilde{\gamma}_j^{(min)} \leq \gamma \leq \tilde{\gamma}_j \\ N_{max}, & \tilde{\gamma}_j \leq \gamma \leq \tilde{\gamma}_{j+1}^{(min)} \end{cases} \tag{6.55}$$

where λ_j is the minimum SIR required per code for MCS j to achieve its target frame error rate. The basic bit rate r_j in (6.54) is given by

$$r_j = \frac{W}{g} R_c^{(j)} \log_2 M_j, \quad 1 \leq j \leq J, \tag{6.56}$$

where W is the chip rate, $R_c^{(j)}$ is the code rate for MCS j, M_j is the number of points in the modulation constellation for MCS j and g is the spreading factor. As shown in Fig. 6.1, the terms $\tilde{\gamma}_j^{(min)}$ and $\tilde{\gamma}_j$ correspond to a set of decision thresholds which yield near-optimal choice of the MCS and number of multicodes for a given value of γ[4] Following a procedure similar to that in [14], the set of decision thresholds $\tilde{\gamma}_j$ and $\tilde{\gamma}_{i,j}^{(min)}$ can be obtained as

$$\tilde{\gamma}_j = \lambda_j N_{max}, \quad 1 \leq j \leq J \tag{6.57}$$

$$\tilde{\gamma}_j^{(min)} = \begin{cases} \lambda_j \text{ ,. } j = 1 \\ \beta_j \text{ , } 1 < j \leq J \\ \infty \text{ , } j = J+1 \end{cases} \tag{6.58}$$

where $\beta_j \in (0, \infty)$ is the smallest value such that

$$r_j \left\lfloor \frac{\beta_j}{\lambda_j} \right\rfloor (1 - \varepsilon_j(\lambda_j)) \geq r_{j-1} N_{max}, \quad 2 \leq j \leq J. \tag{6.59}$$

[4]For illustration purposes, Fig. 4.1 assumes that the number of multicodes is a real number. In this case the proposed scheme is bit rate optimal [14]. For an integer number of multicodes, the rising slopes are replaced by staircases. The effect on optimality is discussed in Appendix D.

For simplicity, the reasonable assumption that $\varepsilon_{j-1}(\beta_j/N_{max})$ is negligible is made in (6.59).

The average bit rate $\overline{R}$ over γ is then given by

$$\overline{R} = \sum_{j=1}^{J} \int_{\tilde{\gamma}_j^{(min)}}^{\tilde{\gamma}_{j+1}^{(min)}} r_j n_j(\gamma)(1-\varepsilon_j(\gamma)) f_\Gamma(\gamma) d\gamma, \tag{6.60}$$

where

$$\varepsilon_j(\gamma) = \zeta_j(\gamma/n_j(\gamma)) \tag{6.61}$$

$$= \begin{cases} \zeta_j(\frac{\gamma}{\lfloor \gamma/\lambda_j \rfloor}), & \tilde{\gamma}_j^{(min)} \le \gamma \le \tilde{\gamma}_j \\ \zeta_j(\frac{\gamma}{N_{max}}), & \tilde{\gamma}_j \le \gamma \le \tilde{\gamma}_{j+1}^{(min)} \end{cases} \tag{6.62}$$

and $\zeta_j(\gamma)$ is the frame error rate of MCS j at an SIR value of γ. The SIR per code for $\tilde{\gamma}_j^{(min)} \le \gamma \le \tilde{\gamma}_j$ can be expressed as

$$\frac{\gamma}{\lfloor \gamma/\lambda_j \rfloor} = \begin{cases} \gamma, & \lambda_j \le \gamma < 2\lambda_j \\ \gamma/2, & 2\lambda_j \le \gamma < 3\lambda_j \\ \vdots, & \vdots \\ \gamma/N_{max}, & (N_{max}-1)\lambda_j \le \gamma < N_{max}\lambda_j \end{cases} \tag{6.63}$$

$$= \gamma/k, \quad k\lambda_j \le \gamma < (k+1)\lambda_j, \quad 1 \le k \le N_{max}-1 \tag{6.64}$$

Using (6.62) and (6.64), the average effective bit rate $\overline{R}$ in (6.60) becomes

$$\overline{R} = \sum_{j=1}^{J} \left(\int_{\tilde{\gamma}_j^{(min)}}^{\tilde{\gamma}_j} r_j n_j(\gamma)(1-\varepsilon_j(\gamma)) f_\Gamma(\gamma) d\gamma + \int_{\tilde{\gamma}_j}^{\tilde{\gamma}_{j+1}^{(min)}} r_j n_j(\gamma)(1-\varepsilon_j(\gamma)) f_\Gamma(\gamma) d\gamma \right) \tag{6.65}$$

$$= \sum_{j=1}^{J} r_j \left(\sum_{k=\lfloor \tilde{\gamma}_j^{(min)}/\lambda_j \rfloor}^{N_{max}-1} \phi_1(j,k) + \phi_2(j) \right) \tag{6.66}$$

where the quantities $\phi_1(j,k)$ and $\phi_2(j)$ are given by

$$\phi_1(j,k) = k\int_{k\lambda_j}^{(k+1)\lambda_j}(1-\zeta_j(\frac{\gamma}{k}))f_\Gamma(\gamma)d\gamma \tag{6.67}$$

$$\phi_2(j) = N_{max}\int_{\tilde{\gamma}_j}^{\tilde{\gamma}_{j+1}^{(min)}}(1-\zeta_j(\frac{\gamma}{N_{max}}))f_\Gamma(\gamma)d\gamma. \tag{6.68}$$

Since $\tilde{\gamma}_j^{(min)}$ and $\tilde{\gamma}_j$ are chosen so that $\zeta_j(\frac{\gamma}{k}) \leq \varepsilon_0$ and $\zeta_j(\frac{\gamma}{N_{max}}) \leq \varepsilon_0$, where ε_0 is the target frame error rate, lower bounds to (6.67) and (6.68) can be written as

$$\tilde{\phi}_1(j,k) = k(1-\varepsilon_0)\int_{k\lambda_j}^{(k+1)\lambda_j} f_\Gamma(\gamma)d\gamma \tag{6.69}$$

$$\tilde{\phi}_2(j) = N_{max}(1-\varepsilon_0)\int_{\tilde{\gamma}_j}^{\tilde{\gamma}_{j+1}^{(min)}} f_\Gamma(\gamma)d\gamma \tag{6.70}$$

Using Theorem 2.5, (6.69) and (6.70) can be written as

$$\tilde{\phi}_1(j,k) = k(1-\varepsilon_0)\Big(F_\Gamma((k+1)\lambda_j) - F_\Gamma(k\lambda_j)\Big) \tag{6.71}$$

$$\tilde{\phi}_2(j) = N_{max}(1-\varepsilon_0)\left(F_\Gamma(\tilde{\gamma}_{j+1}^{(min)}) - F_\Gamma(\tilde{\gamma}_j)\right) \tag{6.72}$$

where $F_\Gamma(.)$ is given in (6.41). Thus, a lower bound on the average bit rate is given by

$$\overline{R}_- = \sum_{j=1}^{J} r_j \left(\sum_{k=\lfloor \tilde{\gamma}_j^{(min)}/\lambda_j \rfloor}^{N_{max}-1} \tilde{\phi}_1(j,k) + \tilde{\phi}_2(j) \right) \tag{6.73}$$

An upper bound on the average bit rate is given by

$$\overline{R}_+ = \frac{1}{1-\varepsilon_0}\overline{R}_-. \tag{6.74}$$

6.4 Numerical Results

As shown in (6.2), the received SIR Γ is a ratio involving X_1 and X_2. Thus, the unit for the means of X_1 and X_2 is arbitrary. Fig. 6.2 shows the pdf $f_\Gamma(\gamma)$ for different values of a_1 with $a_2 = 1$, $\alpha_1 = 3$, $\alpha_2 = 2$, $\bar{X}_1 = 1.5$ and $\bar{X}_2 = 1$. As expected, the curve for $a_1 = 0.01$ approaches the beta prime pdf whereas the curve for $a_1 = 0.99$ is close to the beta pdf. It can be seen that as a_1 increases, the pdf $f_\Gamma(\gamma)$ becomes narrower since the influence of X_2 is reduced.

Fig. 6.3 shows the outage probability, $P_O(Z) = \int_0^Z f_\Gamma(\gamma)d\gamma$, as a function of $E[\Gamma]$ for different values of a_1 when $\alpha_1 = 2$, $\alpha_2 = 2$, $\bar{X}_2 = 1.6$, $a_2 = 0.35$ and $Z = 0.2$. The value of $E[\Gamma]$ is changed by varying $\bar{X}_1$. For the chosen value of Z, the outage probability decreases with a_1. However, this may not be the case for other values of Z as indicated in the next paragraph.

Fig. 6.4 shows the outage probability as a function of the outage threshold, Z, for three different values of a_1 (and corresponding values of a_2) with $\alpha_1 = 2$, $\alpha_2 = 2$, $\bar{X}_1 = 0.5$, $\bar{X}_2 = 0.25$ and $E[\Gamma] = 3$ dB. Even though the $E[\Gamma]$'s are the same for all three cases, the outage probabilities are quite different. The outage probability curves grow sharper as a_1 increases (and a_2 decreases). It can also be seen that the outage probability does not necessarily decrease with a_1.

Fig. 6.5 shows the outage probability as a function of the outage threshold, Z, with (a) $E[\Gamma] = 3$ dB and (b) $E[\Gamma] = 5.4$ dB. For the proposed model, $\alpha_1 = 2$, $\alpha_2 = 2$, $\bar{X}_1 = 0.5$, $\bar{X}_2 = 0.25$, $a_2 = 0.25$, with (a) $a_1 = 0.3478$ and (b) $a_1 = 0.1557$. For the Gaussian approximation, $\alpha_1 = 2$, $\bar{X}_1 = 0.5$, with the relative noise power (a) $N_0 = 0.25$ and (b) $N_0 = 0.1429$. Note that for the proposed model, the outage probability is 1 when $Z > 1/a$. The results show that the Gaussian approximation can be quite inaccurate as it ignores the fading of the interfering signal.

Fig. 6.6 shows the average bit rate (normalized to the chip rate) bounds as a function

of a_1 when $\alpha_1 = 5$, $\alpha_2 = 2$, $\bar{X}_1 = 0.2$, $\bar{X}_2 = 0.25$ and $N_{max} = 10$ for different values of a_2, with a target frame error rate, ε_0, of 1%. The spreading factor g is assumed to be 16. The modulation schemes are QPSK and 16-QAM and the codes are of rates 1/2 or 3/4. For simplicity, the SIR thresholds used to achieve ε_0 for each MCS are based on the first transmission results in [15]. As expected, at a given a_2, increasing the value of a_1 effectively increases the home BS interference and results in a poorer bit rate performance. The same observation holds if a_2 is increased while a_1 is kept fixed.

6.5 Conclusions

In this chapter, the pdf of $\Gamma = X_1/(a_1X_1 + a_2X_2)$, where X_1 and X_2 are gamma variates, and a_1 and a_2 are arbitrary constants is derived. The pdf simplifies to the *beta* distribution and the *beta prime* distribution in special cases. Analytical expressions for the moments, the moment generating function and the cumulative distribution function are obtained in terms of the hypergeometric function. Finally, the usefulness of the distribution of R is illustrated for the problem of adaptive modulation and coding with multicode transmission in a CDMA network.

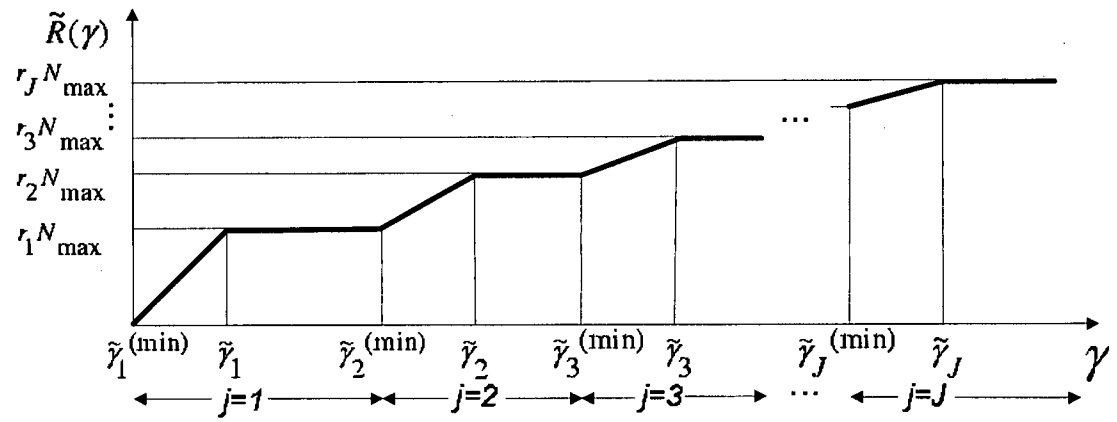

Figure 6.1: Allocated MS bit rate as a function of γ.

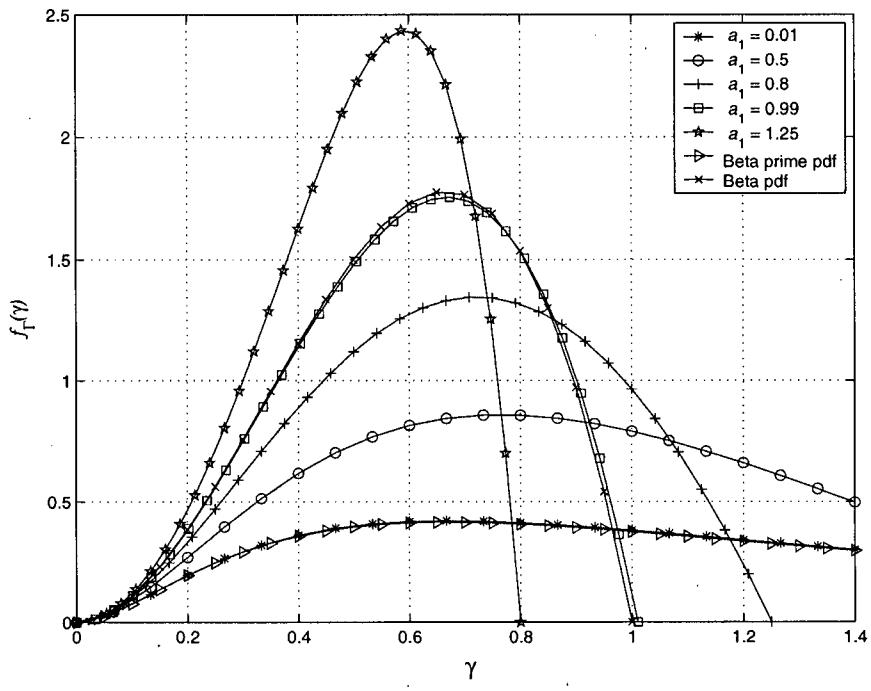

Figure 6.2: The pdf $f_\Gamma(\gamma)$ for five different values of a_1 with $a_2 = 1$, $\alpha_1 = 3$, $\alpha_2 = 2$, $\bar{X}_1 = 1.5$, and $\bar{X}_2 = 1$.

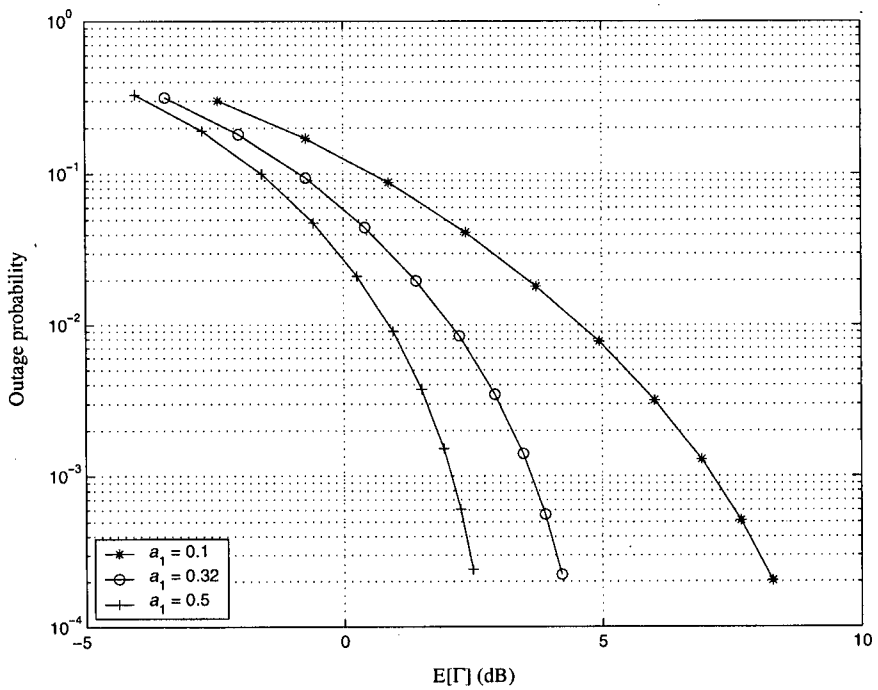

Figure 6.3: Outage probability as a function of $E[\Gamma]$ for different values of a_1 when $\alpha_1 = 2$, $\alpha_2 = 2$, $\bar{X}_2 = 1.6$, $a_2 = 0.35$, and $Z = -7$ dB.

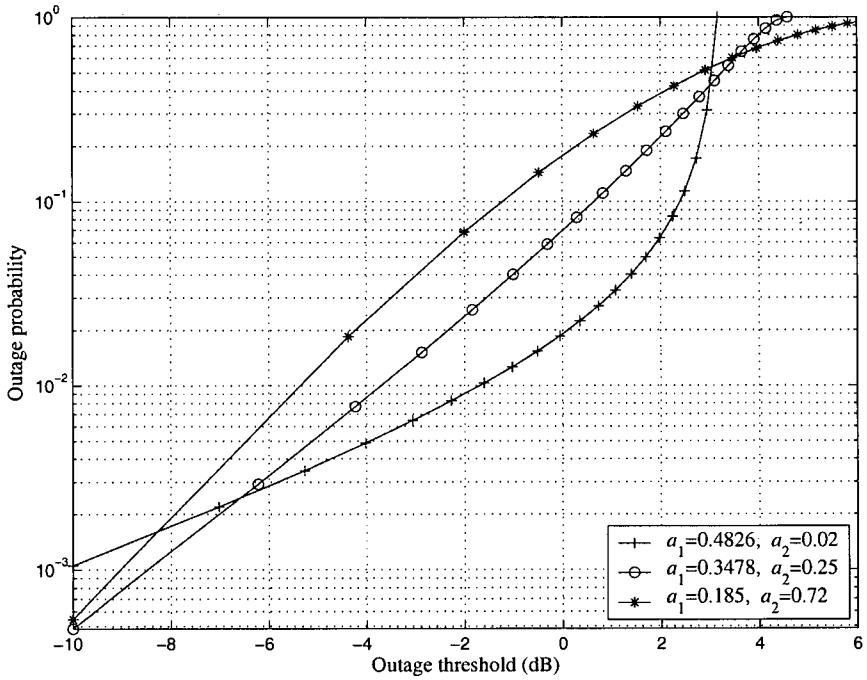

Figure 6.4: Outage probability as a function of the outage threshold, Z, for three different values of a_1 (and corresponding values of a_2) with $\alpha_1 = 2$, $\alpha_2 = 2$, $\bar{X}_1 = 0.5$, $\bar{X}_2 = 0.25$ and $E[\Gamma] = 3.0$ dB.

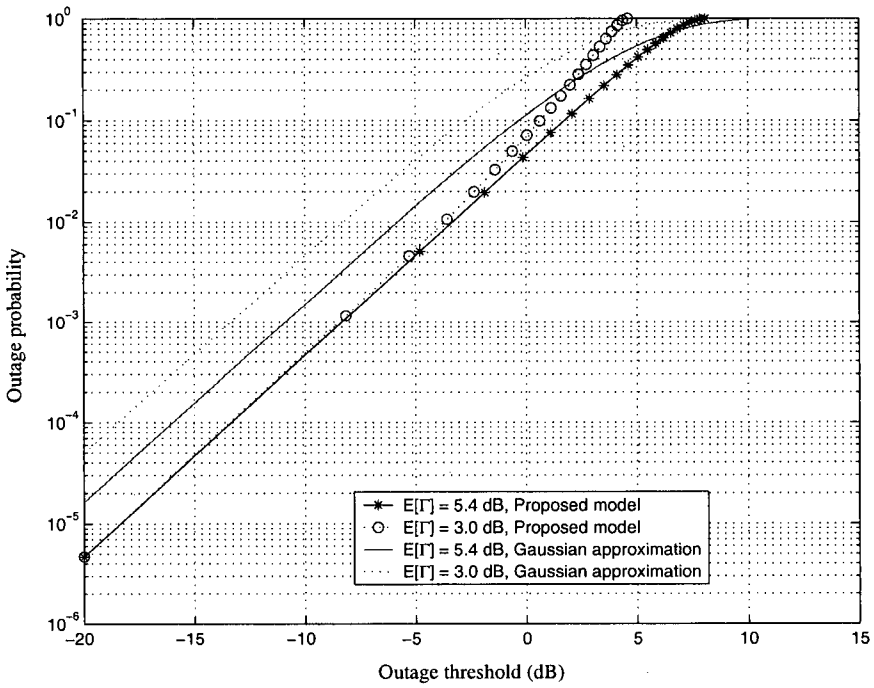

Figure 6.5: Outage probability as a function of the outage threshold, Z, with (a) $E[\Gamma] = 3.0$ dB and (b) $E[\Gamma] = 5.4$ dB. For the proposed distribution, $\alpha_1 = 2$, $\alpha_2 = 2$, $\bar{X}_1 = 0.5$, $\bar{X}_2 = 0.25$, $a_2 = 0.25$, with (a) $a_1 = 0.3478$ and (b) $a_1 = 0.1557$. For the Gaussian approximation, $\alpha_1 = 2$, $\bar{X}_1 = 0.5$, with the relative noise power (a) $N_0 = 0.25$ and (b) $N_0 = 0.1429$.

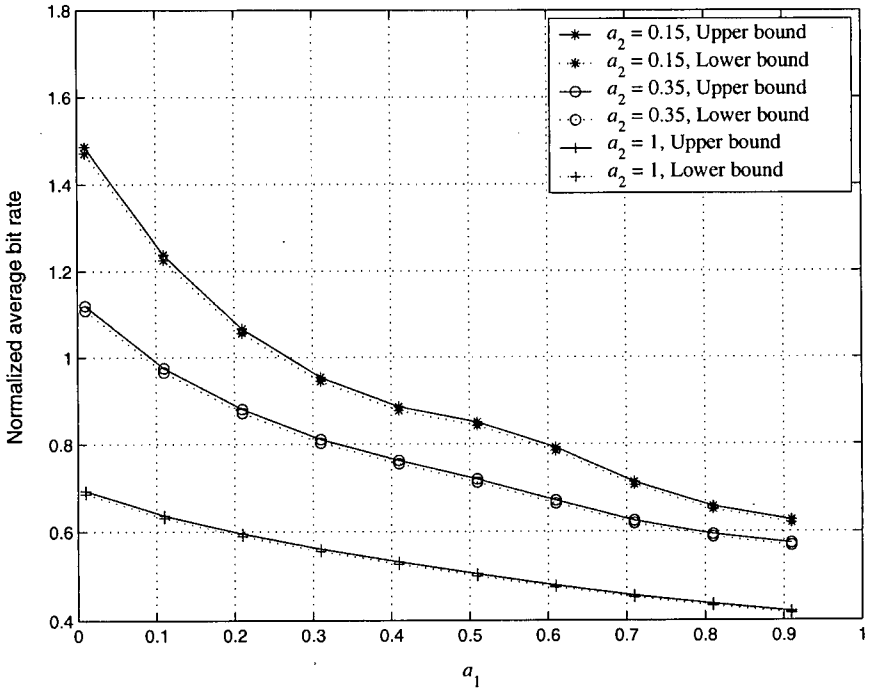

Figure 6.6: Normalized average bit rate bounds as a function of a_1 for three different values of a_2 with $\alpha_1 = 5$, $\alpha_2 = 2$, $\bar{X}_1 = 0.2$, $\bar{X}_2 = 0.25$, $N_{max} = 10$ and a target frame error rate of 1%.

References

[1] A. J. Viterbi, *CDMA - Principles of Spread Spectrum Communication.* Addison-Wesley, 1995.

[2] M. K. Simon and M.-S. Alouini, *Digital Communication over Fading Channels: A Unified Approach to Performance Analysis.* John Wiley & Sons, 2000.

[3] J. O. Sebeni and C. Leung, "Performance of Concatenated Walsh/PN Spreading Sequences for CDMA Systems," in *Proc. of 49th IEEE Vehicular Technology Conference (VTC)*, Houston, Texas, May 1999.

[4] T. S. Rappaport, *Wireless Communications Principles and Practice.* New Jersey: Prentice-Hall PTR, 1996.

[5] A. Zellner, *An Introduction to Bayesian Inference in Econometrics.* John Wiley & Sons, 1971.

[6] K. O. Bowman, L. R. Shenton, and P. C. Gailey, "Distribution of the Ratio of Gamma Variates," in *Commumications in Statistics, Simulation and Compututation.* Texas, USA: Marcel Dekker Inc., 1998, vol. 27, no. 1, pp. 1–19.

[7] C. Mun, C.-H. Kang, and H.-K. Park, "Approximation of SNR Statistics for MRC Diversity Systems in Arbitrarily Correlated Nakagami Fading Channels," *Electronics Letters*, vol. 35, no. 4, pp. 266–267, February 1999.

[8] I. S. Gradshteyn and I. M. Ryzhik, *Table of Integrals, Series, and Products.* Academic Press Inc., 1980.

[9] L. Couch, *Digital and Analog Communication Systems*, 4th ed. New York: Macmillan, 1993.

[10] H. Holma and A. Toskala, Eds., *WCDMA for UMTS Radio Access for Third Generation Mobile Communications.* John Wiley & Sons, 2002.

[11] "Physical Layer Aspects of UTRA High Speed Downlink Packet Access," 3rd Generation Partnership Project, Technical Report 3G TR25.858, 2002.

[12] M.-S. Alouini and A. J. Goldsmith, "Adaptive Modulation over Nakagami Fading Channels," in *Wireless Personal Communications.* Netherlands: Kluwer Academic Publishers, 2000, vol. 13, pp. 119–143.

[13] S. J. Lee, H. W. Lee, and D. K. Sung, "Capacities of Single-Code and Multicode DS-CDMA Systems Accommodating Multiclass Service," *IEEE Trans. on Vehicular Technology*, vol. 48, no. 2, pp. 376 –384, March 1999.

[14] R. Kwan and C. Leung, "Channel-Based Downlink Scheduling Schemes for CDMA Networks," in *Proc. of IEEE Vehicular Technology Conference (VTC)*, Los Angeles, California, September 2004.

[15] M. Döttling, J. Michel, and B. Raaf, "Hybrid ARQ and Adaptive Modulation and Coding Schemes for High Speed Downlink Packet Access," in *Proc. of IEEE International Symposium on Personal, Indoor and Mobile Radio Communications (PIMRC)*, September 2002.

Chapter 7

General Order Selection Combining for Non-Identically Distributed Fading Channels

7.1 Introduction

In performance analyses of selection combining (SC) [1, 2], the statistics of the maximum of a set of random variables (rv's) are needed. In [3], the cumulative distribution function (cdf) of the output signal-to-noise ratio (SNR) for a L-branch SC system over independent, identically distributed (i.i.d.) Nakagami fading channels is derived assuming that the *fading figure* [4] is an integer. In [5], an exact expression for the moment generating function (MGF) is obtained in terms of the Laurecella hypergeometric function. In [1], a unifying MGF based approach is used to study the performance of dual branch SC over correlated slow Rayleigh and Nakagami-m fading channels. In [6], an expression for the average output SNR for SC with three correlated Nakagami fading branches is obtained as an infinite series. In [7], a closed-form expression for the MGF of SC over i.i.d. Weibull fading channels is obtained in terms of the Meijer G function. SC for independent but not necessarily identically distributed (i.n.d.) Weibull fading channels is studied in [8]. In particular, a closed-form expression is derived for the general moment of the SC output SNR and symbol error rate (SER) expressions for a number of modulation schemes are obtained in terms of the Meijer

[1]The material in this chapter is largely based on R. Kwan and C. Leung, "General Order Selection Combining for Non-Identically Distributed Fading Channels." *Proc. of IEEE Wireless Communications and Networking Conference (WCNC'06)*, Las Vegas, April 2006.

G function.

Generalized SC (GSC), in which the signals from the N strongest paths among the L available resolvable paths are combined, represents a compromise between the SC and maximal ratio combining (MRC) techniques [1]. In [9], the performance of GSC over i.i.d. Weibull fading channels is analyzed. In [10], the probability density function (pdf) and cdf for an L-branch GSC system are obtained for i.i.d. Nakagami fading channels. In [11, 12], expressions for the MGF of a L-branch GSC system are derived assuming the L branch gains are i.n.d. More recent analyses of variants of GSC appear in [13, 14, 15].

In studying problems such as multiuser scheduling [16, 17, 18, 19], we are interested in the performance of not only the user with the highest SNR, but also those of other users. The GSC model is not applicable in this case. Rather, we are interested in *general order selection combining* (GOSC), i.e. the statistics of the q^{th} largest SNR.

In this chapter, the q^{th} order statistic of a set of L i.n.d. rv's is examined for both Nakagami and Weibull fading channels. Using a basic result for the pdf of the q^{th} order statistic for independent rv's and transforming this pdf into an appropriate form, exact, closed-form expressions for the MGF and the general moment of the q^{th} largest SNR are derived in section 7.2. Exact closed-form expressions for the SER for a number of modulation schemes are obtained in section 7.3. Numerical results are presented in section 7.4, followed by conclusions in section 7.5.

7.2 General Order Selection Statistics

The following result [20] for the pdf of the q^{th} order statistic for a set of independent rv's will be used in the sequel.

Theorem: Let $X_1, X_2, \ldots, X_L$ be L independent rv's. The corresponding order statistics are obtained by arranging the L X_i's in a non-increasing order, denoted by $X_{1:L}, X_{2:L}, \ldots, X_{L:L}$, or $X_{(1)}, X_{(2)}, \ldots, X_{(L)}$. Thus, $X_{(1)}$ corresponds to the largest of the X_i's. Let $f_j(x)$ and $F_j(x)$

denote the pdf and cdf of X_j respectively. The pdf of the q^{th} order statistic, $X_{q:L}$, is then given by

$$f_{q:L}(y) = \frac{1}{(q-1)!(L-q)!} {}^{+}\left|\begin{array}{ccc} F_1(y) & \cdots & F_L(y) \\ \cdots & \cdots & \cdots \\ F_1(y) & \cdots & F_L(y) \\ f_1(y) & \cdots & f_L(y) \\ 1-F_1(y) & \cdots & 1-F_L(y) \\ \cdots & \cdots & \cdots \\ 1-F_1(y) & \cdots & 1-F_L(y) \end{array}\right|^{+} \quad \begin{array}{l} \left.\begin{array}{l} \\ \\ \end{array}\right\} L-q \text{ identical rows} \\ \} \text{1 row} \\ \left.\begin{array}{l} \\ \\ \end{array}\right\} q-1 \text{ identical rows} \end{array} \tag{7.1}$$

where the symbol ${}^{+}|\mathbf{A}|^{+}$ denotes the permanent of matrix $\mathbf{A}$ [21].

Using this theorem, the statistics of GOSC in Weibull and Nakagami fading channels are studied in sections 7.2.1 and 7.2.2 respectively.

7.2.1 Weibull Fading Channels

The pdf of the Weibull distribution is given by[2]

$$f_R(r) = \begin{cases} \frac{mr^{m-1}}{\omega} \exp\left(-\frac{r^m}{\omega}\right), & m > 0,\ r \geq 0 \\ 0, & r < 0 \end{cases} \tag{7.2}$$

where m is the Weibull fading parameter and ω is a positive, moment-related parameter given by

$$\omega = \left(\frac{E[R^2]}{\Gamma(1+2/m)}\right)^{m/2}. \tag{7.3}$$

In (7.3), $\Gamma(.)$ denotes the Gamma function.

[2]The term R here is conveniently denoted as the envelop of the faded signal, which is different from the bit rate defined earlier in this thesis.

Let $s_i = \rho_i d_i + n_i$, where d_i is the signal component of the i^{th} user, and n_i is the corresponding noise component. The term $\rho_i = R_i e^{\theta_i}$ denotes the complex channel gain for user i. Let E_s/N_0 be the received energy per symbol to noise power spectral density (PSD). Then the received SNR is $X_i = R_i^2(E_s/N_0)$, with pdf

$$f_{X_i}(x_i) = \begin{cases} \alpha_i \beta_i x_i^{\alpha_i - 1} \exp(-\beta_i x_i^{\alpha_i}), & x_i \geq 0, \\ 0, & x_i < 0 \end{cases} \tag{7.4}$$

where $\alpha_i = m_i/2$, and

$$\beta_i = \left(\frac{\overline{X}_i}{\Gamma(1 + \alpha_i^{-1})} \right)^{-\alpha_i} \tag{7.5}$$

are the channel parameters for user i, and $\overline{X}_i$ is the mean of X_i. The cdf of X_i is given by

$$F_{X_i}(x_i) = \begin{cases} 1 - \exp(-\beta_i x_i^{\alpha_i}), & x_i \geq 0 \\ 0, & x_i < 0. \end{cases} \tag{7.6}$$

It might be noted that X_i also has a Weibull distribution [9, 7].

Let $\{X_i, i = 1, 2, \ldots, L\}$ be a set of i.n.d. Weibull distributed rv's and let $Y = X_{(q)}$. For notational convenience, let

$$f_i(x_i) = f_{X_i}(x_i), \; i = 1, \ldots, L. \tag{7.7}$$

The pdf of Y can be obtained from (7.1) as

$$f_Y^{(q)}(y) = \sum_{l_1=1}^{L} f_{l_1}(y) \sum_{S_{L,q,l_1}} \prod_{j=2}^{L-q+1} F_{l_j}(y) \prod_{u=L-q+2}^{L} (1 - F_{l_u}(y)) \tag{7.8}$$

$$= \sum_{l_1=1}^{L} f_{l_1}(y) \sum_{S_{L,q,l_1}} P_2^{L-q+1}(y) Q_{L-q+2}^{L}(y) \tag{7.9}$$

where S_{L,q,l_1} is the set of all combinations of $L-q$ indices chosen from the set $\{1, 2, \ldots, L\} - l_1$.

Assuming $\alpha_1 = \alpha_2 \ldots = \alpha_L = \alpha$[3] and using (7.6), the term $Q_{L-q+2}^{L}(y) = \prod_{u=L-q+2}^{L}(1-F_{l_u}(y))$ is given by

$$Q_{L-q+2}^{L}(y) = \prod_{u=L-q+2}^{L} e^{-\beta_{l_u} y^{\alpha}}. \tag{7.10}$$

After simplification, the term $P_2^{L-q+1}(y) = \prod_{j=2}^{L-q+1} F_{l_j}(y)$ can be expressed as

$$P_2^{L-q+1}(y) = \sum_{k=0}^{L-q}(-1)^k \sum_{2\le n_1<n_2<\ldots<n_k\le L-q+1} \prod_{p=1}^{k} e^{-\beta_{l_{n_p}} y^{\alpha}} \tag{7.11}$$

Following further simplification, the pdf of Y in (7.9) can be written as

$$f_Y^{(q)}(y) = \sum_{l_1=1}^{L} \alpha\beta_{l_1} \sum_{S_{L,q,l_1}} \sum_{k=0}^{L-q}(-1)^k \sum_{2\le n_1<n_2<\ldots<n_k\le L-q+1} y^{\alpha-1} e^{-\xi_k y^{\alpha}} \tag{7.12}$$

with $\xi_k = \sum_{p=1}^{k} \beta_{l_{n_p}} + \sum_{u=L-q+2}^{L} \beta_{l_u} + \beta_{l_1}$. For the special case of SC, i.e. $q = 1$, (7.12) reduces to [8, eq. (5)]. Equation (7.12) shows that the pdf of Y can be written as linear combinations of Weibull pdf's with parameters ξ_k and α. Using [22, eq. (3.478)], the n^{th} moment can be written as

$$E[Y^n] = \sum_{l_1=1}^{L} \beta_{l_1} \sum_{S_{L,q,l_1}} \sum_{k=0}^{L-q}(-1)^k \sum_{2\le n_1<n_2<\ldots<n_k\le L-q+1} \xi_k^{-\frac{\alpha+n}{\alpha}} \Gamma\left(\frac{\alpha+n}{\alpha}\right). \tag{7.13}$$

Using [23, eq. (21)], and the fact that [23, eq. (11)]

$$e^{-x} = G_{0,1}^{1,0}\left(x \,\middle|\, \begin{matrix} \cdot \\ 0 \end{matrix}\right) \tag{7.14}$$

[3]The term α is conveniently denoted as the fading parameter of the distribution in the case when all α_i's are equal, which is different from the orthogonality factor defined earlier in this thesis.

the MGF of Y can be obtained as

$$\mathcal{M}_Y^{(q)}(s) = \sum_{l_1=1}^{L} \alpha\beta_{l_1} \sum_{S_{L,q,l_1}} \sum_{k=0}^{L-q} (-1)^k \sum_{2\le n_1<n_2<\ldots<n_k\le L-q+1} \frac{(\frac{\kappa}{\lambda})^{1/2}\lambda^{\alpha}s^{-\alpha}}{(2\pi)^{\frac{\kappa+\lambda}{2}-1}} \times$$
$$G_{\lambda,\kappa}^{\kappa,\lambda}\left[\xi_k^{\kappa}s^{-\lambda}\frac{\lambda^{\lambda}}{\kappa^{\kappa}}\middle| \begin{matrix} \{\frac{i-\alpha}{\lambda}\},\ i=1,2,\ldots,\lambda \\ \{\frac{i}{\kappa}\},\ i=0,1,\ldots,\kappa-1 \end{matrix}\right] \tag{7.15}$$

where λ and κ are positive integers chosen so that $\lambda/\kappa = \alpha$ and $G_{c,d}^{a,b}(.)$ is the Meijer G function [22].

7.2.2 Nakagami-m Fading Channels

For Nakagami-m channels, the received SNR is gamma distributed, i.e.

$$f_{X_i}(x_i) = \begin{cases} \left(\frac{\alpha_i}{\beta_i}\right)^{\alpha_i} \frac{x_i^{\alpha_i-1}}{\Gamma(\alpha_i)} \exp\left(-\frac{\alpha_i x_i}{\beta_i}\right), & x_i \ge 0 \\ 0, & x_i < 0, \end{cases} \tag{7.16}$$

where α_i is the fading figure and β_i is the mean of X_i[4]. Assuming that α_i takes on integer values, the pdf of Y can be expressed as

$$f_Y^{(q)}(y) = \sum_{k=0}^{L-q}\sum_{l_1=1}^{L}\sum_{S_{L,q,l_1}} \left(\frac{\alpha_{l_1}}{\beta_{l_1}}\right)^{\alpha_{l_1}} \frac{(-1)^k}{\Gamma(\alpha_{l_1})} \sum_{2\le n_1<\ldots<n_k\le L-q+1} \sum_{m_1=0}^{\alpha_{l_{n_1}}-1} \cdots \sum_{m_k=0}^{\alpha_{l_{n_k}}-1}$$
$$\sum_{m_1'=0}^{\alpha_{l_{L-q+2}}-1} \cdots \sum_{m_{q-1}'=0}^{\alpha_{l_L}-1} \left(\prod_{t=1}^{k}\frac{\zeta_{l_{n_t}}^{m_t}}{m_t!}\right)\left(\prod_{t'=1}^{q-1}\frac{\zeta_{l_{L-q+1+t'}}^{m_{t'}'}}{m_{t'}'!}\right) y^{\nu_k-1}e^{-\mu_k y} \tag{7.17}$$

where

$$\nu_k = \sum_{t=1}^{k} m_t + \sum_{t'=1}^{q-1} m_{t'}' + \alpha_{l_1} \tag{7.18}$$

$$\mu_k = \sum_{t=1}^{k} \zeta_{l_{n_t}} + \sum_{t'=L-q+2}^{L} \zeta_{l_{t'}} + \zeta_{l_1}\ . \tag{7.19}$$

[4]Note that the definitions of α_i and β_i are different for the Nakagami and Weibull models.

$$\zeta_{l_u} = \alpha_{l_u}/\beta_{l_u} \tag{7.20}$$

The derivation of (7.17) is given in Appendix E. With appropriate scaling factors, the pdf of Y is essentially a linear combination of gamma distributions. This characteristic can be very useful for performance analysis as the properties of the gamma distribution are well-known.

From (7.17), together with [22, page 310, 3.351.3], the MGF can be obtained as

$$\mathcal{M}_Y^{(q)}(s) = \int_0^\infty f_Y^{(q)}(y)e^{sy}dy \tag{7.21}$$

$$= \sum_{k=0}^{L-q}\sum_{l_1=1}^{L}\sum_{S_{L,q,l_1}}\left(\frac{\alpha_{l_1}}{\beta_{l_1}}\right)^{\alpha_{l_1}}\frac{(-1)^k}{\Gamma(\alpha_{l_1})}\sum_{2\le n_1<\ldots<n_k\le L-q+1}\sum_{m_1=0}^{\alpha_{l_{n_1}}-1}\cdots\sum_{m_k=0}^{\alpha_{l_{n_k}}-1}$$

$$\sum_{m'_1=0}^{\alpha_{l_{L-q+2}}-1}\cdots\sum_{m'_{q-1}=0}^{\alpha_{l_L}-1}\left(\prod_{t=1}^{k}\frac{\zeta_{l_{n_t}}^{m_t}}{m_t!}\right)\left(\prod_{t'=1}^{q-1}\frac{\zeta_{l_{L-q+1+t'}}^{m'_{t'}}}{m'_{t'}!}\right)(\mu_k-s)^{-\nu_k}(\nu_k-1)! \tag{7.22}$$

From (7.22), the n^{th} moment of Y can be obtained as

$$\mathbf{E}[Y^n] = \left.\frac{d^n\mathcal{M}_Y^{(q)}(s)}{ds^n}\right|_{s=0} \tag{7.23}$$

$$= \sum_{k=0}^{L-q}\sum_{l_1=1}^{L}\sum_{S_{L,q,l_1}}\left(\frac{\alpha_{l_1}}{\beta_{l_1}}\right)^{\alpha_{l_1}}\frac{(-1)^k}{\Gamma(\alpha_{l_1})}\sum_{2\le n_1<\ldots<n_k\le L-q+1}\sum_{m_1=0}^{\alpha_{l_{n_1}}-1}\cdots\sum_{m_k=0}^{\alpha_{l_{n_k}}-1}$$

$$\sum_{m'_1=0}^{\alpha_{l_{L-q+2}}-1}\cdots\sum_{m'_{q-1}=0}^{\alpha_{l_L}-1}\left(\prod_{t=1}^{k}\frac{\zeta_{l_{n_t}}^{m_t}}{m_t!}\right)\left(\prod_{t'=1}^{q-1}\frac{\zeta_{l_{L-q+1+t'}}^{m'_{t'}}}{m'_{t'}!}\right)\frac{(\nu_k+n-1)!}{(\nu_k-1)!}\mu_k^{-(\nu_k+n)}(\nu_k-1)! \tag{7.24}$$

7.3 Symbol Error Rate Analysis

The general formula for calculating the average SER is

$$\overline{P}_s = \int_0^\infty P_s(y)f_Y^{(q)}(y)dy, \tag{7.25}$$

where $P_s(y)$ is the SER for the given modulation scheme at an SNR value of y.

7.3.1 Weibull Fading Channel

The average SER can be obtained by substituting the appropriate expression for $P_s(y)$ together with (7.12) into (7.25). After simplification, we have

$$\overline{P}_s = \sum_{l_1=1}^{L} \alpha\beta_{l_1} \sum_{S_{L,q,l_1}} \sum_{k=0}^{L-q} (-1)^k \sum_{2\le n_1<n_2<\ldots<n_k\le L-q+1} \Phi_k \tag{7.26}$$

where

$$\Phi_k = \int_0^\infty y^{\alpha-1} e^{-\xi_k y^\alpha} P_s(y) dy. \tag{7.27}$$

Binary Phase Shift Keying (BPSK)

For BPSK, the BER expression is given by

$$P_s(y) = cQ\left(\sqrt{by}\right), \tag{7.28}$$

with $b = 2$ and $c = 1$. Substituting (7.28) into (7.27), and using [23, eq. (21)], together with the fact that [24, p. 645]

$$\operatorname{erfc}\left(\sqrt{x}\right) = \frac{1}{\sqrt{\pi}} G_{2,0}^{1,2}\left(x \left| \begin{matrix} 1 \\ 0, \frac{1}{2} \end{matrix} \right. \right) \tag{7.29}$$

we have $\Phi_k = A_k$, where

$$A_k = \frac{c}{2\sqrt{\pi}} \left(\frac{\kappa^{1/2} \lambda^{\alpha-1} \left(\frac{b}{2}\right)^{-\alpha}}{(2\pi)^{\frac{1}{2}(\lambda+\kappa)-1}} \right) G_{2\lambda,\kappa+\lambda}^{\kappa,2\lambda}\left(\theta_{\alpha,b,k} \left| \begin{matrix} \left\{\frac{i-\alpha}{\lambda}\right\}, i=1,2,\ldots,\lambda, \left\{\frac{j-\frac{1}{2}-\alpha}{\lambda}\right\}, j=1,2,\ldots,\lambda \\ \left\{\frac{i'}{\kappa}\right\}, i'=0,1,\ldots,\kappa-1, \left\{\frac{j'-\alpha}{\lambda}\right\}, j'=0,1,\ldots,\lambda-1 \end{matrix} \right. \right) \tag{7.30}$$

In (7.30), $\alpha = \lambda/\kappa$, and

$$\theta_{\alpha,b,k} = \frac{\xi_k^{\kappa}\kappa^{-\kappa}}{\left(\frac{b}{2}\right)^{\lambda}\lambda^{-\lambda}}. \tag{7.31}$$

For the special case of SC, i.e. $q = 1$, (7.26) reduces to [8, eq. (13)].

The SER for a variety of modulation schemes over a non-fading AWGN channel can be expressed as (7.28) with different values of b and c [1]. For example, the SER for M-ary Differential Phase Shift Keying (M-DPSK) is well approximated by (7.28), with [25]

$$c = 2.06\sqrt{\frac{1+\cos\frac{\pi}{M}}{2\cos\frac{\pi}{M}}} \tag{7.32}$$

$$b = 2\left(1-\cos\frac{\pi}{M}\right). \tag{7.33}$$

M-ary Quadrature Amplitude Modulation (M-QAM)

The SER for M-QAM, where $M = 2^K$ and K is an even integer, over a non-fading AWGN channel is given by [1]

$$P_s(y) = 4pQ\left(\sqrt{by}\right) - 4p^2Q^2\left(\sqrt{by}\right) \tag{7.34}$$

where

$$p = \frac{\sqrt{M}-1}{\sqrt{M}} \tag{7.35}$$

$$b = \frac{3}{M-1}. \tag{7.36}$$

Using [1]

$$Q^n\left(\sqrt{by}\right) < (2\pi by)^{-n/2}e^{-\frac{nb}{2}y}, \tag{7.37}$$

together with (7.27), (7.34) and [23, eq. (21)], the integral $B_k = \int_0^\infty y^{\alpha-1} e^{-\xi_k y^\alpha} Q^2(\sqrt{by}) dy$ can be upper bounded by

$$B_k^+ = (2\pi b)^{-1} \int_0^\infty y^{\alpha-2} e^{-\xi_k y^\alpha} e^{-by} dy \tag{7.38}$$

$$= (2\pi b)^{-1} \frac{(\frac{\kappa}{\lambda})^{1/2} \lambda^{\alpha-(3/2)} b^{-(\alpha-1)}}{(2\pi)^{\frac{\kappa+\lambda}{2}-1}} G_{\lambda,\kappa}^{\kappa,\lambda} \left[\xi_k^\kappa b^{-\lambda} \frac{\lambda^\lambda}{\kappa^\kappa} \middle| \begin{matrix} \{\frac{i-\alpha+1}{\lambda}\},\ i=1,2,\ldots,\lambda \\ \{\frac{i}{\kappa}\},\ i=0,1,\ldots,\kappa-1 \end{matrix} \right] \tag{7.39}$$

The term Φ_k in (7.27) is then lower and upper bounded respectively by

$$\Phi_k^- = 4pA_k - 4p^2 B_k^+ \tag{7.40}$$

and

$$\phi_k^+ = 4pA_k. \tag{7.41}$$

Since $A_k = \int_0^\infty y^{\alpha-1} e^{-\xi_k y^\alpha} Q\left(\sqrt{by}\right) dy$ and $B_k = \int_0^\infty y^{\alpha-1} e^{-\xi_k y^\alpha} Q^2\left(\sqrt{by}\right) dy$, it follows that $B_k << A_k$ for large values of y. For large values of y, the bound in (7.37) is very tight and hence $B_k^+ \approx B_k$. Then, the lower and upper bounds in (7.40) and (7.41) are very close. This will be the case as the average channel gains increase.

7.3.2 Nakagami Fading Channels

The average SER can be obtained by substituting the appropriate expression for $P_s(y)$ together with (7.17) into (7.25). After simplifying, we have

$$\overline{P}_s = \sum_{k=0}^{L-q} \sum_{l_1=1}^{L} \sum_{S_{L,q,l_1}} \left(\frac{\alpha_{l_1}}{\beta_{l_1}}\right)^{\alpha_{l_1}} \frac{(-1)^k}{\Gamma(\alpha_{l_1})} \times$$

$$\sum_{2\le n_1<\ldots<n_k\le L-q+1} \sum_{m_1=0}^{\alpha_{l_{n_1}}-1} \cdots \sum_{m_k=0}^{\alpha_{l_{n_k}}-1} \sum_{m_1'=0}^{\alpha_{l_{L-q+2}}-1} \cdots \sum_{m_{q-1}'=0}^{\alpha_{l_L}-1}$$

$$\left(\prod_{t=1}^{k}\frac{\zeta_{l_{n_t}}^{m_t}}{m_t!}\right)\left(\prod_{t'=1}^{q-1}\frac{\zeta_{l_{L-q+1+t'}}^{m'_{t'}}}{m'_{t'}!}\right)\Xi(\mu_k,\nu_k) \tag{7.42}$$

where

$$\Xi(\mu_k,\nu_k) \;=\; \int_0^\infty y^{\nu_k-1}\exp\left(-\mu_k y\right)P_s(y)dy\;. \tag{7.43}$$

The exact expression for $\Xi(\mu_k,\nu_k)$ depends on the type of modulation used.

BPSK

Substituting (7.28) into (7.43), and making use of [1, (5A.4a)], we have

$$\Xi(\mu_k,\nu_k)=\frac{\Gamma(\nu_k)}{2\mu_k^{\nu_k}}\left\{1-d_k\sum_{j=0}^{\nu_k-1}\binom{2j}{j}\left(\frac{1-d_k^2}{4}\right)^j\right\} \tag{7.44}$$

$$d_k \;=\; \sqrt{\frac{c_k}{1+c_k}} \tag{7.45}$$

$$c_k \;=\; \frac{b}{2\mu_k}. \tag{7.46}$$

For the sake of notational simplicity, the dependence of μ_k on d_k and c_k is not explicitly shown.

M-QAM

Substituting (7.34) into (7.43), and using [1, (5A.4a)] and [1, (5.30)], the average SER can be expressed as in (7.42); the term $\Xi(\mu_k,\nu_k)$ in (7.42) is now

$$\begin{aligned}\Xi(\mu_k,\nu_k) \;=\; &\left\{2p\left[1-d_k\sum_{j=0}^{\nu_k-1}\binom{2j}{j}\left(\frac{1-d_k^2}{4}\right)^j\right]\right.\\ -4p^2&\left\{\frac{1}{4}-\frac{1}{\pi}d_k\left[\left(\frac{\pi}{2}-\tan^{-1}d_k\right)\sum_{j=1}^{\nu_k-1}\binom{2j}{j}\frac{1}{(4(1+c_k))^j}\right.\right.\\ &\left.\left.-\sin\left(\tan^{-1}d_k\right)\sum_{j=1}^{\nu_k-1}\sum_{i=1}^{j}\frac{T_{i,j}}{(1+c_k)^j}\right.\right.\end{aligned}$$

$$\left(\cos\left(\tan^{-1} d_k\right)\right)^{2(j-i)+1}\Bigg]\Bigg\}\Bigg\}\frac{\Gamma(\nu_k)}{\mu_k^{\nu_k}} \tag{7.47}$$

where d_k and c_k are given by (7.45) and (7.46) respectively.

M-PSK

The SER for M-PSK over a non-fading AWGN channel is given by

$$P_s(y) = \frac{1}{\pi}\int_0^{\frac{(M-1)\pi}{M}} \exp\left(-\frac{g}{\sin^2\theta}y\right) d\theta \tag{7.48}$$

where

$$g = \sin^2\left(\frac{\pi}{M}\right). \tag{7.49}$$

The SER can be obtained by substituting (7.48) and (7.17) into (7.25). Since (7.17) is a linear combination of $h(\nu_k, \mu_k, y) = y^{\nu_k - 1}\exp(-\mu_k y)$, the evaluation of (7.25) involves the double integral

$$\Xi(\mu_k, \nu_k) = \frac{1}{\pi}\int_0^{\infty}\int_0^{\frac{(M-1)\pi}{M}} \exp\left(-\frac{g}{\sin^2\theta}y\right) \times h(\nu_k, \mu_k, y) d\theta dy. \tag{7.50}$$

Using the Laplace transform,

$$M_Y(\nu_k, \mu_k, s) = \int_0^{\infty} e^{sy} h(\nu_k, \mu_k, y) dy \tag{7.51}$$

$$= \frac{\Gamma(\nu_k)}{\mu_k^{\nu_k}}\left(1 - \frac{s}{\mu_k}\right)^{-\nu_k} \tag{7.52}$$

$\Xi(\mu_k, \nu_k)$ can be re-written as

$$\Xi(\mu_k, \nu_k) = \frac{1}{\pi}\int_0^{\frac{(M-1)\pi}{M}} M_Y\left(\nu_k, \mu_k, -\frac{g}{\sin^2\theta}\right) d\theta \tag{7.53}$$

$$= \frac{\Gamma(\nu_k)}{\mu_k^{\nu_k}} \frac{1}{\pi} \int_0^{\frac{(M-1)\pi}{M}} \left(1 + \frac{g}{\mu_k \sin^2\theta}\right)^{-\nu_k} d\theta \tag{7.54}$$

Using [1, (5.80)], $\Xi(\nu_k, \mu_k)$ can be written as

$$\begin{aligned} \Xi(\nu_k, \mu_k) &= \left\{ \frac{M-1}{M} - \frac{d_k}{\pi} \left[\left(\frac{\pi}{2} + \tan^{-1}\lambda_k \right) \right.\right. \\ &\sum_{j=1}^{\nu_k - 1} \binom{2j}{j} \frac{1}{(4(1+c_k))^j} + \sin\left(\tan^{-1}\lambda_k\right) \sum_{j=1}^{\nu_k-1} \sum_{i=1}^{j} \frac{T_{i,j}}{(1+c_k)^j} \\ &\left.\left. \times \left(\cos\left(\tan^{-1}\lambda_k\right)\right)^{2(j-i)+1} \right] \right\} \frac{\Gamma(\nu_k)}{\mu_k^{\nu_k}} . \end{aligned} \tag{7.55}$$

In (7.55),

$$\lambda_k = d_k \cot\left(\frac{\pi}{M}\right), \tag{7.56}$$

where d_k is given by (7.45), and $c_k = g/\mu_k$.

7.4 Numerical Results

Let $\alpha = [\alpha_1, \ldots, \alpha_L]$, where $\{\alpha_i,\ i = 1, \ldots, L\}$ are defined in sections 7.2.1 and 7.2.2 for the Weibull and Nakagami models repectively. Similarly, let $\mathbf{X} = [\overline{X}_1, \ldots, \overline{X}_L]$ and $\beta = [\beta_1, \ldots, \beta_L]$, where $\{\overline{X}_i,\ i = 1, \ldots, L\}$ and $\{\beta_i,\ i = 1, \ldots, L\}$ are defined in sections 7.2.1 and 7.2.2 respectively. Finally, let $X_{avg} = \sum_{i=1}^{L} \overline{X}_i/L$ and $\beta_{avg} = \sum_{i=1}^{L} \beta_i/L$ be the overall average SNR among all users for their respective channel models.

Figs. 7.1 and 7.2 show the average SER, $\overline{P}_s$, for BPSK and 4-QAM on Weibull fading channels as a function of X_{avg} for different values of q with $\boldsymbol{\alpha}$= [2 2 2 2] and $\mathbf{X}/\overline{X}_1$ = [1 1 1 1] (i.i.d. case) or $\mathbf{X}/\overline{X}_1$ = [1 3 5 7] (i.n.d. case). Generally, the average SER for i.i.d. channels is lower for large q values compared to i.n.d. channels. For small values of q and X_{avg}, the

average SER for i.n.d. channels is lower than for i.i.d. channels. From Fig. 7.2, it can be seen that the lower and upper bounds from (7.40) and (7.41) are very tight, especially as X_{avg} increases. This is to be expected, as discussed in section 7.3.

Figs. 7.3 and 7.4 show the average SER, $\overline{P}_s$, for 8-PSK and 4-QAM respectively on Nakagami fading channels as a function of β_{avg} for different values of q with $\boldsymbol{\alpha}$= [2 2 2 2] and $\boldsymbol{\beta}$= [1 1 1 1] (i.i.d. case) or $\boldsymbol{\alpha}$= [1 2 3 2] and $\boldsymbol{\beta}/\beta_1$ = [1 3 5 7] (i.n.d. case). The results are qualitatively similar to those for Weibull fading channels.

7.5 Conclusions

In this chapter, some new analytical results for general order selection over Weibull and Nakagami fading channels are presented. By transforming the pdf into an appropriate form, exact expressions for the MGF and general moment of the q-th order statistic for i.n.d. Weibull and Nakagami fading channels were derived. Expressions for the average SER for several common modulation schemes are also obtained. Numerical results show that for large values of q, the average SER is generally lower with i.i.d. fading channels. For smaller values of q, this is not always the case.

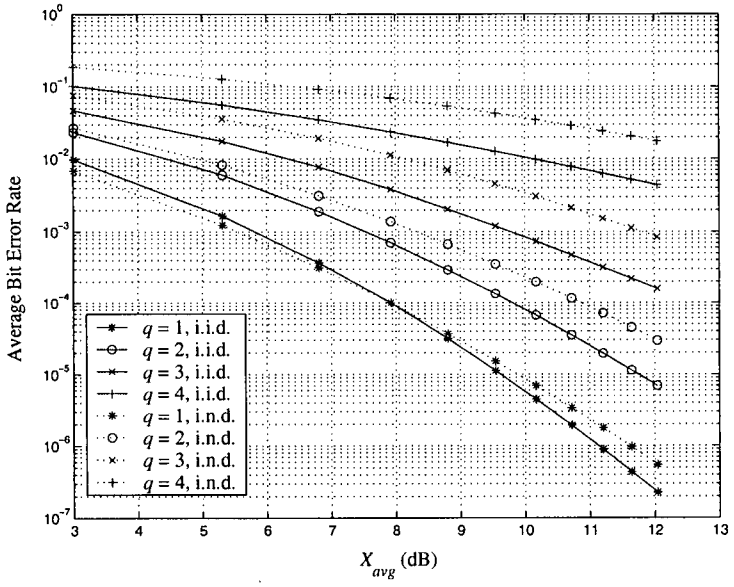

Figure 7.1: Average bit error rate, $\overline{P}_s$, for BPSK on Weibull fading channels, as a function of X_{avg} for different values of q, $\boldsymbol{\alpha}$= [2 2 2 2]: $\mathbf{X}/\overline{X}_1$ = [1 1 1 1] (i.i.d. case), and $\mathbf{X}/\overline{X}_1$ = [1 3 5 7] (i.n.d. case).

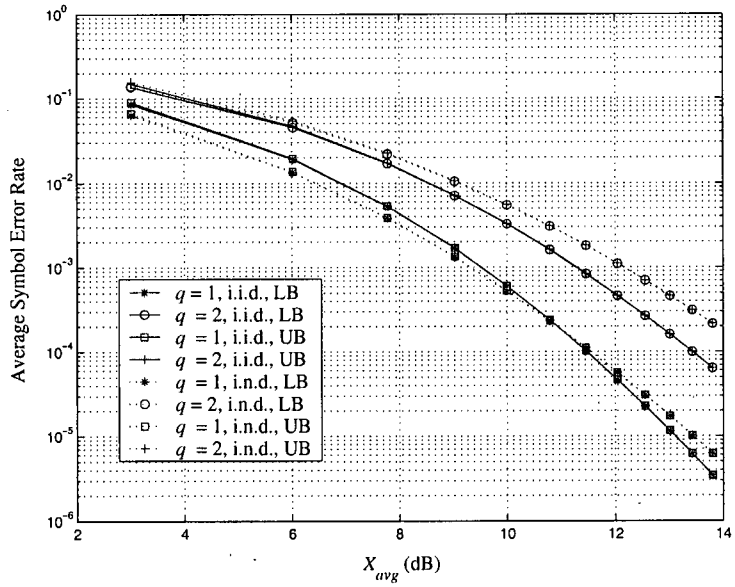

Figure 7.2: Average symbol error rate, $\overline{P}_s$, for 4-QAM on Weibull fading channels, as a function of X_{avg} for different values of q, $\boldsymbol{\alpha}$= [2 2 2 2]: $\mathbf{X}/\overline{X}_1$ = [1 1 1 1] (i.i.d. case), and $\mathbf{X}/\overline{X}_1$ = [1 3 5 7] (i.n.d. case).

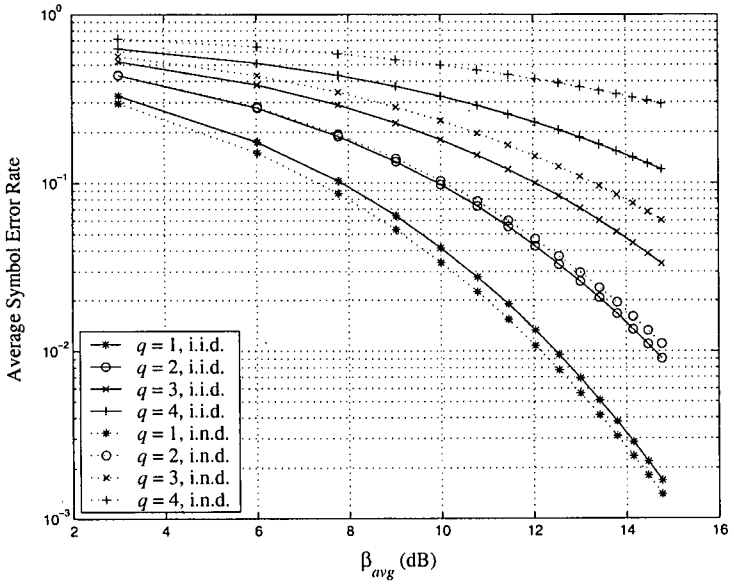

Figure 7.3: Average symbol error rate, $\overline{P}_s$, for 8-PSK on Nakagami fading channels, as a function of β_{avg} for different values of q with (a) $\boldsymbol{\alpha}$= [2 2 2 2], $\boldsymbol{\beta}/\beta_1$ = [1 1 1 1] (i.i.d. case) and (b) $\boldsymbol{\alpha}$= [1 2 3 2], $\boldsymbol{\beta}/\beta_1$ = [1 3 5 7] (i.n.d. case).

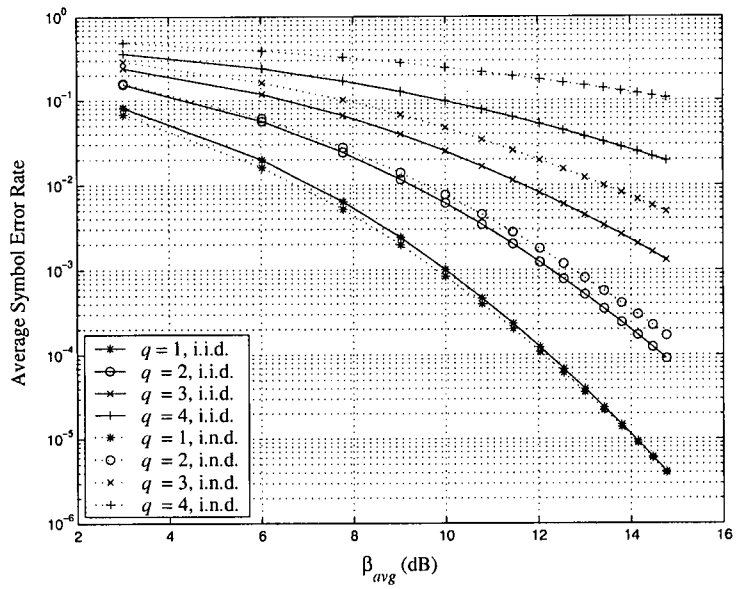

Figure 7.4: Average symbol error rate, $\overline{P}_s$, for 4-QAM on Nakagami fading channels, as a function of β_{avg} for different values of q with (a) $\boldsymbol{\alpha}$= [2 2 2 2], $\boldsymbol{\beta}/\beta_1$ = [1 1 1 1] (i.i.d. case) and (b) $\boldsymbol{\alpha}$= [1 2 3 2], $\boldsymbol{\beta}/\beta_1$ = [1 3 5 7] (i.n.d. case).

References

[1] M. K. Simon and M.-S. Alouini, *Digital Communication over Fading Channels*, 2nd ed. John Wiley & Sons, 2005.

[2] W. C. Jakes, *Microwave Mobile Comunications.* John Wiley & Sons, Inc., 1974.

[3] C.-D. Iskander and P. T. Mathiopoulos, "Finite-State Markov Modeling of Diversity Nakagami Channels," in *Proc. of the Seventh Canadian Workshop on Information Theory*, Vancouver, B.C., June 2001.

[4] J. G. Proakis, *Digital Communications*, 4th ed. McGraw-Hill, 2001.

[5] R. Annavajjala, A. Chockalingam, and L. B. Milstein, "Performance Analysis of Coded Communication Systems on Nakagami Fading Channels With Selection Combining Diversity," *IEEE Transactions on Communications*, vol. 52, no. 7, pp. 1214 – 1220, July 2004.

[6] D. A. Zogas, G. K. Karagiannidis, and S. A. Kotsopoulos, "On the Average Output SNR in Selection Combining With Three Correlated Branches Over Nakagami-m Fading Channels," *IEEE Transactions on Wireless Communications*, vol. 3, no. 1, January 2004.

[7] J. Cheng, C. Tellambura, and N. C. Beaulieu, "Performance of Digital Linear Modulations on Weibull Slow-Fading Channels," *IEEE Transactions on Communications*, vol. 52, no. 8, pp. 1265 – 1268, August 2004.

[8] N. C. Sagias, G. K. Karagiannidis, D. A. Zogas, and P. T. Mathiopoulos, "Selection Diversity for Wireless Communications with Non-Identical Weibull Statistics," in *Proc. of IEEE Global Telecommunication Conference GLOBECOM 2004*, December 2004, pp. 3690 – 3694.

[9] M.-S. Alouini and M. Simon, "Performance of Generalized Selection Combining over Weibull Fading Channels," in *Proc. of 54th IEEE Vehicular Technology Conference VTC, Fall*, vol. 3, Atlantic City, New Jersey, October 2001, pp. 1735–1739.

[10] A. Annamalai and C. Tellambura, "Performance evaluation of generalized selection diversity systems over Nakagami-m fading channels," *Wireless Communications and Mobile Computing*, vol. 3, no. 1, pp. 99 – 116, February 2001.

[11] Y. Ma and C. C. Chai, "Unified Error Probability Analysis for Generalized Selection Combining in Nakagami Fading Channels," *IEEE Journal on Selected Areas in Communications*, vol. 18, no. 11, pp. 2198 – 2210, November 2000.

[12] Y. Ma and S. Pasupathy, "Efficient Performance Evaluation for Generalized Selection Combining on Generalized Fading Channels," *IEEE Transactions on Wireless Communications*, vol. 3, no. 1, pp. 29 – 34, January 2004.

[13] R. K. Mallik, P. Gupta, and Q. T. Zhang, "Minimum Selection GSC in Independent Rayleigh Fading," *IEEE Transactions on Vehicular Technology*, vol. 54, no. 3, pp. 1013 – 1021, May 2005.

[14] Y. Ma, R. Schober, and S. Pasupathy, "Performance of M-PSK with GSC and EGC with Gaussian Weighting Errors," *IEEE Transactions on Vehicular Technology*, vol. 54, no. 1, pp. 149 – 162, January 2005.

[15] Y. Chen and C. Tellambura, "Performance Analysis of Three-Branch Selection Combining over Arbitrarily Correlated Rayleigh-Fading Channels," *IEEE Transactions on Wireless Communications*, vol. 4, no. 3, pp. 861 – 865, May 2005.

[16] F. Berggren and R. Jäntti, "Multiuser Scheduling over Rayleigh Fading Channels," in *Proc. of IEEE Global Telecommunication Conference GLOBECOM 2003*, vol. 1, December 2003, pp. 158 – 162.

[17] R. Kwan and C. Leung, "Downlink Scheduling Optimization in CDMA Networks," *IEEE Communications Letters*, vol. 8, no. 10, pp. 611 – 613, October 2004.

[18] ——, "Channel-Based Downlink Scheduling Schemes for CDMA Networks," in *Proc. of IEEE Vehicular Technology Conference (VTC)*, Los Angeles, California, September 2004.

[19] S. K. Kim and C. G. Kang, "Delay Analysis of Packet Scheduling with Multi-Users Diversity in Wireless CDMA Systems," *Wireless Networks*, vol. 11, pp. 235 – 241, 2005.

[20] R. J. Vaughan and W. N. Venables, "Permanent expressions for order statistics densities," *J. Roy. Statist. Soc. Ser. B*, vol. 34, pp. 308 – 310, 1972.

[21] A. C. Aitken, *Determinants and Matrices.* Edinburgh, Oliver & Boyd, 1956.

[22] I. S. Gradshteyn and I. M. Ryzhik, *Table of Integrals, Series, and Products.* Academic Press Inc., 1980.

[23] V. S. Adamchik and O. I. Marichev, "The Algorithm for Calculating Integrals of Hypergeometric Type Functions and its Realization in REDUCE System ," in *Proc. of International Conference on Symbolic and Algebraic Computation*, Tokyo, Japan, 1990, pp. 212 – 224.

[24] A. P. Prudnikov, Y. A. Brychkov, and O. I. Marichev, *Integrals and Series, More Special Functions.* N. Y.: Gordon and Breach Science Publication, 1986, vol. 3.

[25] R. F. Pawula, "Asymptotics and Error Rate Bounds for M-ary DPSK," *IEEE Transactions on Communications*, vol. 32, no. 1, pp. 93 – 94, January 1984.

Chapter 8

An Accurate Method for Approximating Probability Distributions in Wireless Communications

8.1 Introduction

Diversity combining is a commonly employed technique for reducing the effects of fading over wireless communication channels. The motivation behind diversity combining is to exploit the stochastic nature of the gains experienced on different links (branches). Common types of diversity combining include maximal-ratio combining (MRC), equal-gain combining (EGC), and selection combining (SC) [1]. More recently, a hybrid of MRC and SC, known as generalized selection combining (GSC), in which a certain number of the strongest branch signals are selected and combined, has received much attention [1]. Although diversity combining is a well-studied topic, the analysis techniques and results are in general rather complicated. For example, in many cases, exact closed-form expressions for the probability density function (pdf) or the cumulative distribution function (cdf) of the signal-to-noise ratio (SNR) at the combiner output are very complex, if not impossible, to derive [1].

An alternative approach is to explore methods for approximating the probability distributions using simpler expressions. In this chapter, we use the method of *Pearson systems* [2] to obtain approximate expressions for pdf's. A summary of *Pearson systems* is given in

[1]The material in this chapter is largely based on R. Kwan and C. Leung, "An Accurate Method for Approximating Probability Distributions in Wireless Communications." *Proc. of IEEE Wireless Communications and Networking Conference (WCNC'06)*, Las Vegas, April 2006.

section 8.2. In section 8.3, the method is applied in various diversity schemes for wireless communications. Numerical results are provided in section 8.4 to illustrate the accuracy of the approximations.

8.2 Systems of Distributions

Pearson systems arise as solutions to a simple differential equation [2]. Such solutions lead to seven different families of curves, characterized by their skewness and kurtosis [3]; these families are referred to as *systems of distributions*, *systems of frequency curves* or, simply, *Pearson systems* [3]. Pearson systems were originally intended to approximate a wide variety of distributions based on empirical observations. According to the procedure outlined in [3], a selection parameter κ can be computed based on the first four moments of the empirical data in order to determine the appropriate family of curves for the approximation. Depending on the value of κ, the exact form of the curve can be obtained. The selection parameter, κ, is given by

$$\kappa = \frac{\beta_1(\beta_2+3)^2}{4(4\beta_2-3\beta_1)(2\beta_2-3\beta_1-6)} \tag{8.1}$$

where β_1 and β_2 are the skewness and kurtosis respectively [4], and are defined as $\beta_1 = \mu_3^2/\mu_2^3$ and $\beta_2 = \mu_4/\mu_2^2$. The terms $\mu_i = E[(Z-\nu_1)^i]$ and $\nu_i = E[Z^i]$ are the i^{th} central and non-central moments respectively. It may be noted that "general" distributions such as Weibull, lognormal, gamma and Student's t are associated with lines on the β_1, β_2 plane, while more limited models such as normal, exponential and uniform are represented by points in the β_1, β_2 plane [5].

The most common (main) types of curves are the type I, type IV, and type VI curves, which correspond to the cases $\kappa < 0$, $0 < \kappa < 1$, and $\kappa > 1$ respectively. There are a number of less common "transition" types which correspond to different values of κ, β_1 and β_2. In

addition, there are a number of so-called "uncommon" types which are of little practical interest. More details on the different types of curves can be found in [3].

8.2.1 Pearson Type I ($-\infty < \kappa < 0$)

The expression for the type I curve is given by

$$f_Z^{(I)}(z) = \begin{cases} K_0(1+\frac{z}{b_1})^{\theta_1}(1-\frac{z}{b_2})^{\theta_2}, & -b_1 \le z \le b_2 \\ 0, \text{ otherwise} \end{cases} \tag{8.2}$$

where

$$K_0 = \frac{1}{b_1+b_2}\left(\frac{\theta_1^{\theta_1}\theta_2^{\theta_2}}{(\theta_1+\theta_2)^{\theta_1+\theta_2}}\right)\frac{1}{B(\theta_1+1,\theta_2+1)} \tag{8.3}$$

$$\theta_1 = \frac{1}{2}\left[t-2-s^*t(t+2)\sqrt{\frac{\beta_1}{K_1}}\right] \tag{8.4}$$

$$\theta_2 = \frac{1}{2}\left[t-2+s^*t(t+2)\sqrt{\frac{\beta_1}{K_1}}\right] \tag{8.5}$$

$$b_1 = \frac{\theta_1}{\theta_2}\frac{b_0}{(1+\frac{\theta_1}{\theta_2})} \tag{8.6}$$

$$b_2 = b_0 - b_1 \tag{8.7}$$

and

$$b_0 = \frac{1}{2}\sqrt{\mu_2\left\{\beta_1(t+2)^2+16(t+1)\right\}} \tag{8.8}$$

$$K_1 = \beta_1(t+2)^2+16(t+1) \tag{8.9}$$

$$t = \frac{6(\beta_2-\beta_1-1)}{6+3\beta_1-2\beta_2} \tag{8.10}$$

$$s^* = \text{sign}(\mu_3). \tag{8.11}$$

The peak (mode) of (8.2) occurs at $z = 0$. To approximate the pdf of Z, the mean of (8.2) is set equal to that of Z, i.e. ν_1. This results in

$$f_Z(z) = \begin{cases} K_0(1+\frac{z-\Delta}{b_1})^{\theta_1}(1-\frac{z-\Delta}{b_2})^{\theta_2}, \\ \qquad -b_1+\Delta \le z \le b_2+\Delta \\ 0, \text{ otherwise} \end{cases} \tag{8.12}$$

where the adjustment factor Δ is given by

$$\Delta = \nu_1 - \int_{-b_1}^{b_2} z f_Z^{(I)}(z)dz \tag{8.13}$$

$$= \nu_1 - \frac{b_0(\theta_1+1)}{\theta_1+\theta_2+2} + b_1. \tag{8.14}$$

A closed-form expression for the cdf of Z is not given in [3], but can be obtained as (see Appendix F)

$$F_Z(z) = \begin{cases} b_1 K_0 p^{\theta_2} l^{-(\theta_1+1)} B_{x(z)}(\theta_1+1, \theta_2+1), \\ \qquad\qquad z \ge -b_1+\Delta \\ 0, \text{ otherwise} \end{cases} \tag{8.15}$$

where $B_{x(z)}(.,.)$ is the incomplete beta function [6], with $l = p'/p$, $p = 1+(b_1/b_2)$, $p' = b_1/b_2$, and $x(z) = l\left(1+\frac{z-\Delta}{b_1}\right)$.

8.2.2 Pearson Type IV $(0 < \kappa < 1)$

The expression for the type IV curve is given by

$$f_Z^{(IV)}(z) = K_0\left(1+\frac{z^2}{a^2}\right)^{-\theta_1} \exp\left(-\theta_2 \tan^{-1}\frac{z}{a}\right), \qquad -\infty < z < \infty \tag{8.16}$$

where

$$\theta_1 = \frac{1}{2}(r+2) \tag{8.17}$$

$$\theta_2 = \frac{-r(r-2)\sqrt{\beta_1}}{\sqrt{16(r-1)-\beta_1(r-2)^2}} \tag{8.18}$$

$$a = \sqrt{\frac{\mu_2}{16}\left(16(r-1)-\beta_1(r-2)^2\right)} \tag{8.19}$$

$$K_0 = (aF(r,\theta_2))^{-1} \tag{8.20}$$

and

$$r = \frac{6(\beta_2-\beta_1-1)}{2\beta_2-3\beta_1-6} \tag{8.21}$$

$$F(r,\theta_2) = \int_{-\frac{\pi}{2}}^{\frac{\pi}{2}} \cos^r(u)\exp(-\theta_2 u)du. \tag{8.22}$$

To approximate the pdf of Z, the mean of (8.16) is set equal to that of Z, i.e. ν_1. This results in

$$f_Z(z) = f_Z^{(IV)}(z-\Delta), \quad -\infty < z < \infty \tag{8.23}$$

where $\Delta = \nu_1 + \theta_2 a/r$. In this case, a closed-form expression for the cdf of Z cannot easily be obtained but it can be computed via numerical integration.

8.2.3 Pearson Type VI ($1 < \kappa < \infty$)

The expression for the type VI curve is given by

$$f_Z^{(VI)}(z) = \begin{cases} K_0\,(z-a)^{\theta_2}\,z^{-\theta_1}, & a \le z < \infty \\ 0, \text{ otherwise} \end{cases} \tag{8.24}$$

where

$$a = \frac{1}{2}\sqrt{\mu_2 \lambda} \tag{8.25}$$

$$\theta_i = \frac{r(r+2)}{2}\sqrt{\frac{\beta_1}{\lambda}} + (-1)^i \left(\frac{r-2}{2}\right), \; i = 1, 2 \tag{8.26}$$

$$K_0 = \frac{a^{\theta_1 - \theta_2 - 1}\Gamma(\theta_1)}{\Gamma(\theta_1 - \theta_2 - 1)\Gamma(\theta_2 + 1)} \tag{8.27}$$

and

$$r = \frac{6(\beta_2 - \beta_1 - 1)}{6 + 3\beta_1 - 2\beta_2} \tag{8.28}$$

$$\lambda = \beta_1(r+2)^2 + 16(r+1). \tag{8.29}$$

In (8.27), $\Gamma(.)$ denotes the Gamma function [6]. After equating the mean of (8.24) to that of Z, i.e. ν_1, the resulting pdf is given by

$$f_Z(z) = f_Z^{(VI)}(z - \Delta) \tag{8.30}$$

where $\Delta = \nu_1 - a(\theta_1 - 1)/(\theta_1 - \theta_2 - 2)$. Although a closed-form expression for the cdf of Z is not given in [3], it can be obtained as (see Appendix F)

$$F_Z(z) = \begin{cases} 1 - K_0 a^{\theta_2 - \theta_1 + 1} B_{\frac{a}{z-\Delta}}(\theta_1 - \theta_2 - 1, \theta_2 + 1), \\ \qquad\qquad a + \Delta \leq z < \infty \\ 0, \text{ otherwise.} \end{cases} \tag{8.31}$$

8.2.4 Transition Types

For $\kappa = \pm\infty$, the pdf corresponds to the type III curve, and is given by

$$f_Z^{(III)}(z) = K_0 \left(1 + \frac{z}{a}\right)^{\gamma a} e^{-\gamma z} \tag{8.32}$$

where $K_0 = p^{p+1}/(e^p\Gamma(p+1))$ is a normalization constant with $p = \gamma a$, and the expressions for a and γ can be found in [3]. By letting $x = (1 + (z/a))/b$, $\lambda = \gamma ab$, and $m = \gamma a + 1$, (8.32) can be transformed into the well-known gamma pdf

$$f_X(x) = \frac{\lambda^m}{\Gamma(m)} x^{m-1} e^{-\lambda x}, \; x > 0. \tag{8.33}$$

The parameters m and λ can be obtained by matching the moments and are given by $m = \frac{\nu_2}{\nu_2 - \nu_1^2}$ and $\lambda = \frac{m}{\nu_1}$. For large values of $|\kappa|$, the gamma pdf can still provide a good approximation. The various transition types and their associated parameter values are summarized in Table 2.1.

8.3 Some Applications

8.3.1 MRC over Non-Identical Weibull Fading Channels

The performance of MRC diversity systems has been studied extensively for Rayleigh, Rician and Nakagami channel models [1],[7]-[11]. A lesser-known distribution for modelling fading channels is the Weibull distribution. Experimental data for the indoor wireless channel have been found to closely match the Weibull distribution [12, 13]. This distribution can also be a good model for the outdoor fading channel [14, 15, 16]. Recently, closed-form expressions for the moments and the moment generating function (MGF) of the SNR at the output of a maximal-ratio combiner, assuming the branch SNR's are non-identically Weibull distributed, have been derived in [17]. However, to the authors' best knowledge, exact closed-form expressions for the corresponding pdf and cdf of the SNR are not available.

Let $\{X_i, \; i = 1, \ldots, L\}$ be the SNR of the i^{th} input branch of a L-branch maximum ratio

combiner; X_i has a Weibull distribution,

$$f_{X_i}(x) = \begin{cases} \alpha_i \gamma_i x^{\alpha_i - 1} \exp\left(-\gamma_i x^{\alpha_i}\right), & x \geq 0 \\ 0, \text{ otherwise.} \end{cases} \tag{8.34}$$

where α_i is the fading figure and γ_i is the moment-related parameter[2]. The MRC output SNR is given by

$$Z = X_1 + X_2 + \ldots + X_L. \tag{8.35}$$

The m^{th} moment of Z can be obtained using the multinomial expansion, and is given by

$$\begin{aligned} E\left[Z^m\right] = & \sum_{m_1=0}^{m} \sum_{m_2=0}^{m_1} \cdots \sum_{m_{L-1}=0}^{m_{L-2}} \binom{m}{m_1} \binom{m_1}{m_2} \cdots \binom{m_{L-2}}{m_{L-1}} \\ & E\left[X_1^{m-m_1}\right] E\left[X_2^{m_1-m_2}\right] \times \ldots \times E\left[X_{L-1}^{m_{L-2}-m_{L-1}}\right] E\left[X_L^{m_{L-1}}\right] \end{aligned} \tag{8.36}$$

where

$$E[X_i^k] = \left(\frac{1}{\gamma_i}\right)^{k/\alpha_i} \Gamma\left(1 + \frac{k}{\alpha_i}\right) \tag{8.37}$$

Instead of trying to obtain exact expressions for the pdf and cdf of Z, they can be accurately approximated using the first four moments of Z and the Pearson method outlined in section 8.2.

[2]The term γ_i is conveniently denoted as the moment-related parameter for the distribution, which is different from the SIR defined earlier in this thesis.

8.3.2 General Order Selection Combining over Non-Identical Weibull Fading Channels

SC is a simple diversity technique in which the branch with the highest SNR is selected [1]. A closed-form expression is derived for the moments of the output SNR of an L-branch SC with non-identical Weibull fading branches in [18]. Average symbol error rate expressions for a number of modulation schemes are given in terms of the Meijer G function.

In some scenarios, such as multiuser scheduling, it is useful to examine the performance of not only the user with the highest SNR, but also other users who are in the queue during the same scheduling period [19]. The selection of the r^{th} highest order statistics is referred to as *general order selection combining* (GOSC). In [20], some results for GOSC over non-identical Nakagami fading channels are presented. However, similar results for Weibull channels are not available. In this chapter, it is shown that the pdf and cdf of the SNR for GOSC over non-identical Weibull fading channels can be accurately approximated using the Pearson method.

Let $\{X_i,\ i = 1,\ldots,L\}$ be a set of independent, non-identically distributed Weibull variates as in (8.34). The corresponding order statistics are obtained by arranging these L X_i's in a non-decreasing order and are denoted by $X_{(1)}, X_{(2)}, \ldots, X_{(L)}$. Thus, $X_{(L)}$ is the largest of the X_i's. In the case when $\alpha_1 = \alpha_2 = \ldots = \alpha_L = \alpha$[3], it is shown in [21] that the m^{th} moment of $X_{(1)}$ is given by

$$\mu_{1:L}^{(m)} = B(m,\alpha)\mathbf{I}_L \tag{8.38}$$

where

$$\mathbf{I}_j = \sum_{1\le i_1<i_2<\ldots<i_j\le L} \frac{1}{(\gamma_{i_1}+\gamma_{i_2}+\ldots+\gamma_{i_j})^{m/\alpha}}\,. \tag{8.39}$$

[3]The term α is conveniently denoted as the fading parameter of the distribution in the case when all α_i's are equal, which is different from the orthogonality factor defined earlier in this thesis.

The m^{th} moment of $X_{(r)}$ can be obtained recursively as

$$\mu_{r:L}^{(m)} = \mu_{r-1:L}^{(m)} + \sum_{j=1}^{r} A_j(m,\alpha)\mathbf{I}_{L-r+j},\ r = 2,\ldots,L \tag{8.40}$$

where

$$A_j(m,\alpha) \ = \ (-1)^{j-1}\binom{L-r+j}{j-1}B(m,\alpha)\ . \tag{8.41}$$

Once the first four moments are obtained from (8.40), the pdf and cdf can be accurately approximated using the Pearson method.

8.3.3 Generalized Selection Combining (GSC) over Non-Identical Weibull Fading Channels

The idea behind GSC is to combine the signals from the l strongest paths out of the L available paths, and represents a compromise between the SC and MRC techniques [1, 22, 23]. For GSC over non-identical Weibull channels, exact closed-form expressions for the pdf or cdf of the SNR at the combiner output are difficult to obtain.

Let

$$Z \ = \ X_{(L)} + X_{(L-1)} + \ldots + X_{(L-l+1)}. \tag{8.42}$$

The m^{th} moment of Z can be expressed as

$$E\left[Z^m\right] \ = \ \sum_{m_1=0}^{m}\sum_{m_2=0}^{m_1}\cdots\sum_{m_{l-1}=0}^{m_{l-2}}\binom{m}{m_1}\binom{m_1}{m_2}\cdots\binom{m_{l-2}}{m_{l-1}}$$
$$E\left[X_{(L-l+1)}^{m-m_1}\ X_{(L-l+2)}^{m_1-m_2}\cdots\ X_{(L-l)}^{m_{l-2}-m_{l-1}}X_{(L)}^{m_{l-1}}\right]. \tag{8.43}$$

Unfortunately, the random variables (r.v.'s) $\{X_{(i)},\ i = L-l+1,\ldots,L\}$ are no longer

independent, and their general product moments are very difficult to obtain analytically. However, the first four moments can be readily estimated using relatively short simulations. It is shown in section 8.4 that the cdf can hence be accurately approximated.

8.3.4 Equal-Gain Combining (EGC) over Correlated, Non-Identical Nakagami Fading Channels

Let $\{R_i,\ i = 1, \ldots, L\}$ be the gain of the i^{th} branch of a L-branch pre-detection EGC diversity receiver. Assuming that equally likely symbols of energy E_s are transmitted over a Nakagami fading channel and the received signal is corrupted by the additive white Gaussian noise (AWGN) with two-sided power spectral density $N_0/2$, the instantaneous SNR per symbol at the EGC output is given by [1]

$$Z = \frac{E_s}{LN_0}\left(R_1 + R_2 + \ldots + R_L\right)^2. \tag{8.44}$$

The instantaneous SNR, $X_i = E_s R_i^2/N_0$, for each branch follows the gamma distribution [1]

$$f_{X_i}(x_i) = \left(\frac{\alpha_i}{\bar{X}_i}\right)^{\alpha_i} \frac{x_i^{\alpha_i - 1}}{\Gamma(\alpha_i)} e^{-\alpha_i x_i/\bar{X}_i},\ x_i > 0, \tag{8.45}$$

where $\bar{X}_i$ is the average value of X_i, and $\alpha_i > 0$ is a shaping parameter.

The performance of EGC systems has been extensively studied [1], [24]-[28] In [26], an infinite series expression for the pdf of the sum of two correlated Nakagami-m r.v.'s is derived. Subsequently, the symbol error rates for different modulation schemes are obtained for dual-branch EGC over correlated Nakagami-m channels. In [27], the MGF of Z is approximated using the Padé approximation. For correlated branch SNR r.v.'s $\{X_i,\ i = 1, \ldots, L\}$, statistical parameters such as the k^{th} moment, the skewness and kurtosis of Z are derived in [28]. However, available results suggest that exact closed-form expressions for the pdf or cdf of Z would be very complicated, if at all possible [26].

Instead of exact expressions, simple accurate approximations for the pdf and cdf of Z can be obtained using the first four moments of Z [28, eqs. (4) and (14)] in conjunction with the method outlined in section 8.2.

8.4 Numerical Results

In this section, results are provided to illustrate the accuracy of the approximate cdf curves obtained using Pearson's method. These curves are compared with cdf curves obtained using Monte-Carlo simulation.

Figs. 8.1, 8.2 and 8.3 show the cdf and the complementary cdf of the SNR at the output of the MRC, GOSC and GSC receivers respectively for the Weibull channel with $L = 3$ and different values of α_i and γ_i as defined in (8.34). The $\underline{\alpha} = [\alpha_1\ \alpha_2\ \alpha_3]$ and $\underline{\gamma} = [\gamma_1\ \gamma_2\ \gamma_3]$ values used are listed in Table 8.2. It can be seen that the approximate and simulation curves agree closely in all three figures. Fig. 8.3 shows that the approximate cdf curve is quite insensitive to the number, $N_{samples}$, of samples used to estimate the moments. On the other hand, the simulation cdf curve is quite sensitive to $N_{samples}$.

For EGC, we consider $L = 2$. The $\underline{\alpha} = [\alpha_1\ \alpha_2]$ and $\underline{\bar{X}} = [\bar{X}_1\ \bar{X}_2]$ (as defined in (8.45)) values used are given in Table 8.2. Fig. 8.4 shows the cdf and the complementary cdf of the EGC output SNR for dual-branch Nakagami fading channels as described in section 8.3.4. The moments of the EGC output SNR are obtained using [28, eq. (14)]. In this example, significant discrepancies between the approximate and simulation results can be observed at the lower end of the cdf's. Fig. 8.5 shows the average Bit Error Rate (BER) for Binary Phase Shift Keying (BPSK) modulation as a function of the average EGC output SNR over the same fading model as for Fig. 8.4, with $\underline{\bar{X}}/\bar{X}_2 = [1.4\ 1.0]$. It can be seen that the approximate cdf from the Pearson method yields reasonably accurate BER results.

8.5 Conclusions

In this chapter, the Pearson system of distributions has been used to approximate the pdf's and cdf's of the combiner output SNR's for a number of well-known diversity techniques in Nakagami and Weibull fading channels. Although exact closed-form expressions for some of the distributions are difficult to obtain, relatively simple approximations are shown to be quite accurate.

Type	β_1	β_2	κ
III	$2\beta_2 - 3\beta_1 - 6 = 0$		$\pm\infty$
II	0	< 3	0
Gaussian	0	3	0
VII	0	> 3	0
V	–		1

Table 8.1: Transition types and associated parameter values.

Fig. 8.1		
Case 1	$\underline{\alpha}$ = [4.50 3.30 3.75]	$\underline{\gamma}$ = [1.00 2.50 3.85]
Case 2	$\underline{\alpha}$ = [3.00 2.20 2.50]	$\underline{\gamma}$ = [1.00 0.40 0.60]
Fig. 8.2		
	$\underline{\alpha}$ = [2.00 2.00 2.00]	$\underline{\gamma}$ = [0.10 0.24 0.08]
Case 1	$r = 2$	
Case 2	$r = 1$	
Fig. 8.3		
	$\underline{\alpha}$ = [4.00 4.00 4.00]	$\underline{\gamma}$ = [0.40 1.00 0.70]
Case 1	$N_{samples} = 4000000$	
Case 2	$N_{samples} = 8000$	
Fig. 8.4		
	$\underline{\alpha}$ = [2.00 2.00]	$\rho = 0.15$
Case 1	$\underline{\bar{X}}$ = [1.50 2.25]	
Case 2	$\underline{\bar{X}}$ = [0.70 0.50]	

Table 8.2: Parameter values used in Figs. 8.1-8.4.

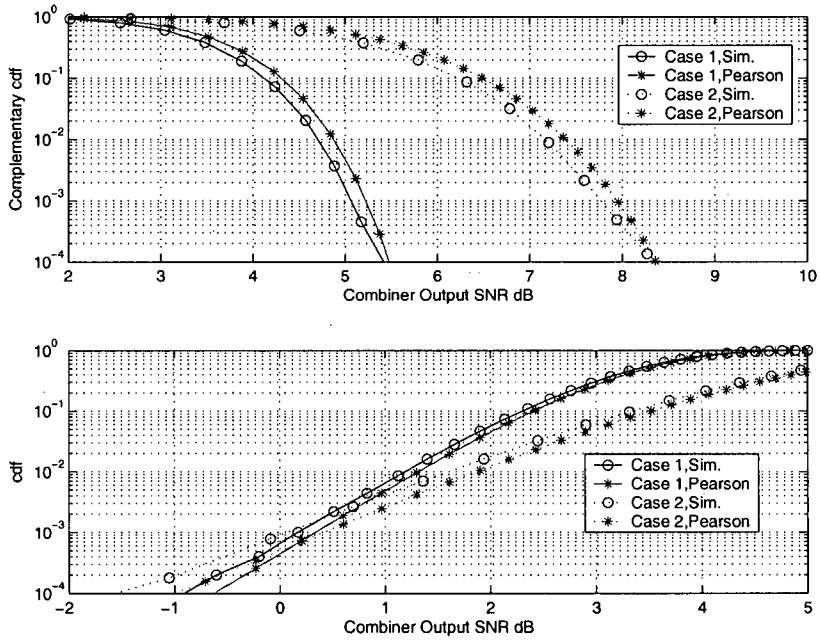

Figure 8.1: Complementary cdf and cdf of MRC output SNR for Weibull fading channels.

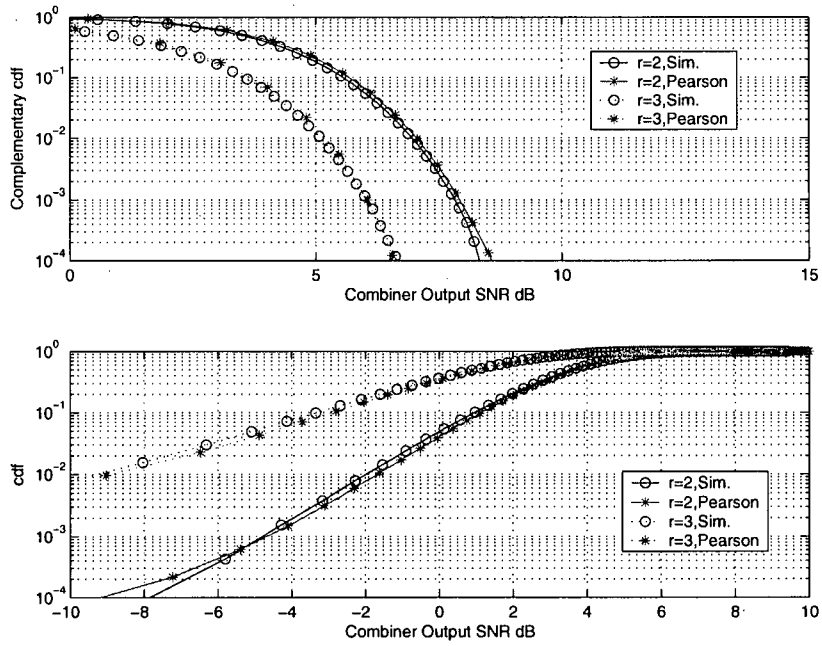

Figure 8.2: Complementary cdf and cdf of the second and third largest GOSC output SNR for Weibull fading channels.

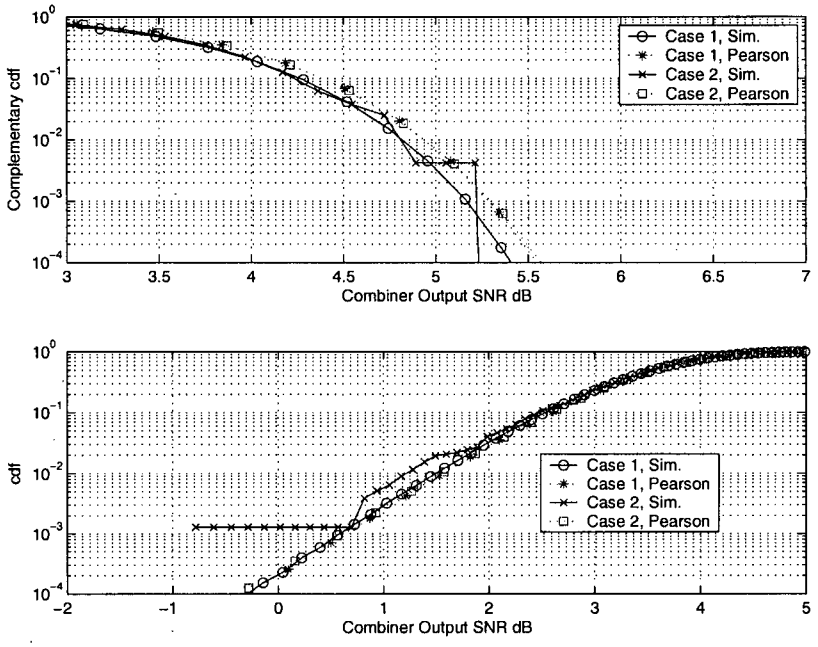

Figure 8.3: Complementary cdf and cdf of GSC output SNR for Weibull fading channels.

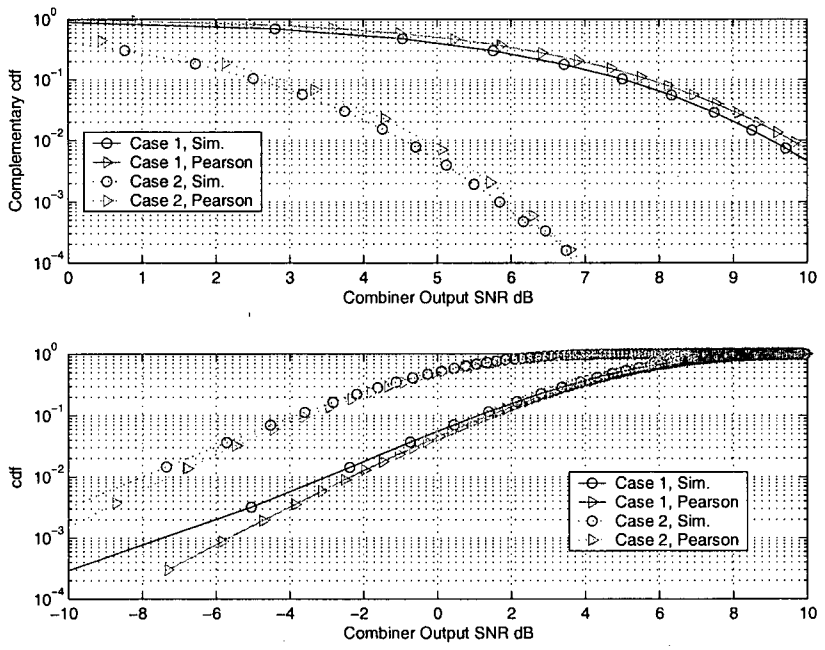

Figure 8.4: Complementary cdf and cdf of EGC output SNR for Nakagami fading channels with $\rho = 0.15$.

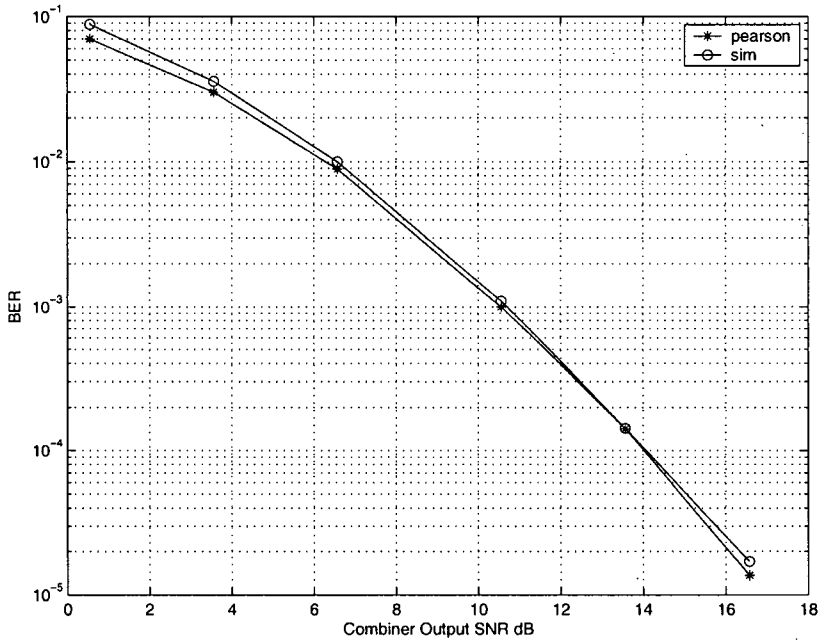

Figure 8.5: Average BER for BPSK with EGC over Nakagami fading channels with $\rho = 0.15$.

References

[1] M. K. Simon and M.-S. Alouini, *Digital Communication over Fading Channels*, 2nd ed. John Wiley & Sons, 2005.

[2] K. Pearson, "Contributions to the Mathematical Theory of Evolution. II. Skew Variations in Homogeneous Material ," *Philosophical transactions of the Royal Society of London, Series A*, vol. 186, pp. 343 – 414, 1895.

[3] W. P. Elderton and N. L. Johnson, *Systems of Frequency Curves.* Cambridge University Press, 1969.

[4] A. Stuart and J. K. Ord, *Distribution Theory*, 6th ed., ser. Kendall's Advanced Theory of Statistics. Edward Arnold, 1994, vol. 1.

[5] B. Schmeiser, "Methods for Modelling and Generating Probabilitic Components in Digital Computer Simulations when the Standard Distributions are not Adequate: A Survey," in *Winter Simulation Conference*, December 1977, pp. 50 – 57.

[6] I. S. Gradshteyn and I. M. Ryzhik, *Table of Integrals, Series, and Products.* Academic Press Inc., 1980.

[7] Q. T. Zhang, "Maximal-Ratio Combining over Nakagami Fading Channels with an Arbitrary Branch Covariance Matrix," *IEEE Transactions on Vehicular Technology*, vol. 48, no. 4, pp. 1141 – 1150, July 1999.

[8] V. A. Aalo, "Performance of Maximal-Ratio Diversity System in a Correlated Nakagami-Fading Environment," *IEEE Transactions on Communications*, vol. 43, no. 8, pp. 2360 – 2369, August 1995.

[9] M. Z. Win, G. Chrisikos, and J. H. Winters, "MRC Performance for M-ary Modulation in Arbitrarily Correlated Nakagami Fading Channels," *IEEE Communications Letters*, vol. 4, no. 10, pp. 301 – 303, October 2000.

[10] J. Luo, J. R. Zeidler, and S. McLaughlin, "Performance Analysis of Compact Antenna Arrays with MRC in Correlated Nakagami Fading Channels," *IEEE Transactions on Vehicular Technology*, vol. 50, no. 1, pp. 267 – 277, January 2001.

[11] Q. T. Zhang, "A Generic Correlated Nakagami Fading Model for Wireless Communications," *IEEE Transactions on Communications*, vol. 51, no. 11, pp. 1745 – 1748, November 2003.

[12] H. Hashemi, "The Indoor Radio Propagation Channel," in *Proc. of IEEE*, vol. 81, July 1993, pp. 943 – 968.

[13] F. Babich and G. Lombardi, "Statistical Analysis and Characterization of the Indoor Propagation Channel," *IEEE Transactions on Communications*, vol. 48, pp. 455 – 464, March 2000.

[14] N. S. Adawi et al, "Coverage Prediction for Mobile Radio Systems Operating in the 800/900 MHz Frequency Range," *IEEE Transactions on Vehicular Technology*, vol. 37, no. 1, pp. 3 – 72, February 1988.

[15] N. H. Shepherd, "Radio Wave Loss Deviation and Shadow Loss at 900 MHz," *IEEE Transactions on Vehicular Technology*, vol. 26, pp. 309 – 313, 1977.

[16] G. Tzeremes and C. G. Christodoulou, "Use of Weibull Distribution for Describing Outdoor Multipath Fading ," in *IEEE Antennas and Propagation Society International Symposium*, vol. 1, 2002, pp. 232 – 235.

[17] G. K. Karagiannidis et al, "Equal-Gain and Maximal-Ratio Combining Over Nonidentical Weibull Fading Channels," *IEEE Transactions on Wireless Communications*, vol. 4, no. 3, pp. 841 – 846, May 2005.

[18] N. C. Sagias, G. K. Karagiannidis, D. A. Zogas, and P. T. Mathiopoulos, "Selection Diversity for Wireless Communications with Non-Identical Weibull Statistics," in *Proc. of IEEE Global Telecommunication Conference GLOBECOM 2004*, December 2004, pp. 3690 – 3694.

[19] R. Kwan and C. Leung, "Downlink Scheduling Optimization in CDMA Networks," *IEEE Communications Letters*, vol. 8, no. 10, pp. 611 – 613, October 2004.

[20] ——, "Order Statistics for Non-Identically Distributed Nakagami Fading Channels with An Application," in *Proc. of IEEE Vehicular Technology Conference (VTC)*, September 2005.

[21] H. M. Barakat and Y. H. Abdelkader, "Computing the Moments of Order Statistics from Nonidentically distirbuted Weibull Variables," *Journal of Computational and Applied Mathematics*, vol. 117, pp. 85 – 90, 2000.

[22] Y. Ma, R. Schober, and S. Pasupathy, "Performance of M-PSK with GSC and EGC with Gaussian Weighting Errors," *IEEE Transactions on Vehicular Technology*, vol. 54, no. 1, pp. 149 – 162, January 2005.

[23] Y. Chen and C. Tellambura, "Performance Analysis of Three-Branch Selection Combining over Arbitrarily Correlated Rayleigh-Fading Channels," *IEEE Transactions on Wireless Communications*, vol. 4, no. 3, pp. 861 – 865, May 2005.

[24] A. Annamalai, C. Tellambura, and V. K. Bhargava, "Equal-Gain Diversity Receiver Performance in Wireless Channels," *IEEE Transactions on Communications*, vol. 48, pp. 1732 – 1745, October 2000.

[25] R. K. Mallik, M. Z. Win, and J. H. Winters, "Performance of M-QAM with Coherent Equal Gain Combining in Correlated Nakagami-m Fading," *IEEE Transactions on Communications*, vol. 50, pp. 1041 – 1044, July 2002.

[26] C.-D. Iskander and P. T. Mathiopoulos, "Performance of Dual-Branch Coherent Equal-Gain Combining in Correlated Nakagami-m Fading," *IEE Electronics Letters*, vol. 39, no. 15, pp. 1152 – 1154, July 2003.

[27] G. K. Karagiannidis, "Moments-Based Approach to the Performance Analysis of Equal Gain Diversity in Nakagami-m Fading," *IEEE Transactions on Communications*, vol. 52, no. 5, pp. 685 – 690, May 2004.

[28] G. K. Karagiannidis, D. A. Zogas, and S. A. Kotsopoulos, "Statistical Properties of the EGC Output SNR Over Correlated Nakagami-m Fading Channels ," *IEEE Transactions on Wireless Communications*, vol. 3, no. 5, pp. 1764 – 1769, September 2004.

Chapter 9

Conclusions and Future Work

9.1 Summary of Contributions

The main contributions of this thesis are summarized below:

- The problem of allocating radio resources in the downlink of a CDMA network is studied. The modulation and coding schemes, numbers of multicodes, and transmit powers used for all mobile stations (MS's) are jointly chosen so as to maximize the total transmission bit rate, subject to certain constraints. Based on the discrete and non-linear nature of the proposed model, a mixed-integer non-linear programming optimization problem is formulated. It is found that the optimal allocation generally involves simultaneous transmissions to several MS's. A scheduler which uses knowledge of MS traffic loads is also proposed and shown to yield a significant improvement in throughput.

- Analytical expressions are derived for optimal resource allocation in the case of a single MS. Based on the single-MS solution, a sub-optimal, sequential optimization procedure for multiple MS's is presented. Numerical results show that joint optimization performs noticibly better than the sequential procedure when radio resources are abundant. However, when the MS's are optimally ordered based on their channel conditions and/or traffic loads, the sequential solution is an attractive alternative to the more complex joint optimization.

- Since the selection of the modulation and coding scheme (MCS) and the number of

multicodes requires an estimation of the downlink channel quality, it is important to assess the performance degradation due to estimation errors. It is shown that the throughput is quite sensitive to channel quality estimation errors. The sensitivity can be reduced by using a more conservative estimate of the channel quality. The above analysis does not include any fading statistics. Subsequently, the estimation error analysis is extended to include the Nakagami fading channel model.

- By modelling the channel dynamics using a Hidden Markov Model (HMM), the impact of channel estimation errors in a system employing AMC and multicodes is studied. Unlike the previous studies, the channels are modelled as discrete states. An HMM filter is used and shown to yield an improved estimate of the channel state. Simulation results show that the HMM filter provides a significant throughput improvement over the unfiltered case, especially when the channel state information (CSI) is quite noisy or the normalized Doppler rate (defined as the product of the Doppler rate of the channel and the transmission period) is small.

- An expression for the probability density function (pdf) is derived for the ratio, Γ, of gamma variates of the form $\Gamma = X_1/(a_1X_1 + a_2X_2)$, where a_1 and a_2 are constants and X_1 and X_2 are independent gamma distributed random variables. This distribution arises naturally in performance analyses of the downlink on which simultaneously transmitted interfering and desired signals from the same base station normally undergo the same fade. The result is used to analyze the performance of a downlink CDMA system involving AMC and multicodes.

- Exact closed-form results for general order selection (GOS) over independent but not necessarily identically distributed (i.n.d.) Weibull and Nakagami fading channels are presented. The GOS model is important in performance analyses of multiuser scheduling, where the statistics of ranked channel conditions are desired. Exact closed-form expressions for the symbol error rate are obtained for a number of modulation schemes.

Numerical results show that for the same average channel gains, the performance on i.n.d. channels may be better or worse than on i.i.d. channels.

- The Pearson system of distributions is examined as a means to approximate statistical distributions which are often difficult to derive in closed-form. The usefulness of this approach is illustrated for a number of diversity techniques employed on Nakagami and Weibull fading channels. The resulting relatively simple approximations are shown to be quite accurate.

9.2 Future Work

In a WCDMA network, the High Speed Downlink Shared Channel (HS-DSCH) is designed to carry packet data from the radio access network to the user. Although most research efforts so far have been devoted to "best effort" packet services, the HS-DSCH is also intended to support other kinds of applications such as interactive and streaming traffic [1]. If a shared channel is used to carry real-time traffic, the delay and jitter requirements have to be much more stringent. As a result, the study of delay sensitivity issues on the shared channel is very important. A number of articles have addressed the problem of scheduling delay-sensitive traffic [2]-[13]. In [12], the issue of delay-sensitive scheduling in WCDMA networks is investigated. In this work, real-time data are sorted based on their deadlines, and those with the earliest deadline are given a higher priority for transmission. However, the authors do not take into account the buffer content sizes, and resources are not jointly optimized for multiple users. In [13], a general structure of opportunistic scheduling policies is presented, which exploit channel and/or buffer content variations for achieving the required QoS. Subsequently, the performance is compared for a number of special but well-known cases of the general policy.

According to the 3GPP specification [14, 15, 16], the shared channel such as the HS-DSCH in WCDMA does not operate in isolation. It is only designed to be an advanced

alternative to the more traditional dedicated channel in the downlink. The HS-DSCH does not employ fast power control to compensate for channel variations. Instead, to maximize the throughput in the downlink, the data rate is adjusted to match the instantaneous channel condition. In contrast to the HS-DSCH, the dedicated channels are designed to maintain a constant data rate by means of fast power control. Such an arrangement allows the dedicated channels to be natural candidates for voice services [16]. In addition, the dedicated channels have the diversity advantage of soft-handover, which is not present in the shared channels. Figure 9.1 shows the relationship between the dedicated and the shared channels. Since both the shared and dedicated channels require power and code resources, it is important to allocate these resources to both types of channels efficiently. It has been shown in [17] by simulations that HS-DSCH can increase the system throughput significantly due to the fact that less reservation of power control headroom is required for HSDPA. However, both power and code resources are assumed to be statically allocated. In [18], the dedicated channels, i.e. the voice traffic, are given a higher priority over the shared channel in terms of the power allocation. On the other hand, the maximum code resource for the shared channels is assumed to be fixed.

Since the dedicated and shared channels are competing for resources, any resources allocated to the shared channel has a direct impact upon the performance of the dedicated channels, and vice versa. If the maximum allowable power and code resources allocated to the dedicated and shared channels are dynamically changed based on the traffic load and the channel conditions, a significant performance gain might be achieved.

The following summarizes some of the possible topics for future study:

- The issue of resource-sharing between the shared and the dedicated channels can be investigated. To optimally allocate the maximum allowable power and code resources dynamically between the shared and the dedicated channels is important from the radio resource management point of view. By carefully selecting the maximum allowable resources, a relatively small sacrifice of the shared channel performance could result in

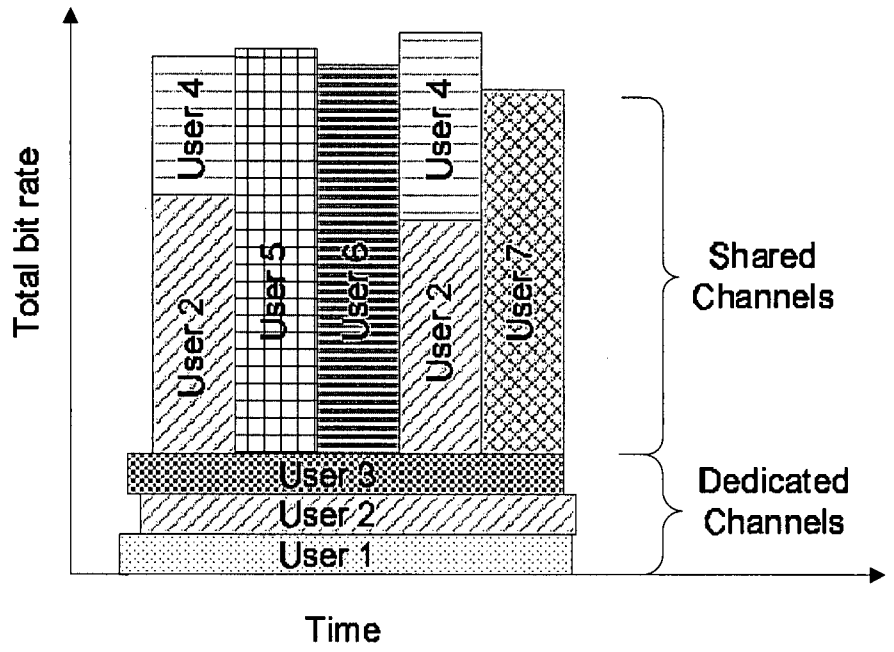

Figure 9.1: Cooperation between the dedicated and the shared channels.

a significant improvement in the performance of the dedicated channel and vice versa.

- A new optimization model may address the issues of jointly minimizing the amount of power and code resources in the context of shared and dedicated channels, when both real-time and non-real-time traffic are present.

- It would be useful to examine the possibility of incorporating the technique of OFDM into the current model involving AMC, downlink transmit power, and multicodes. This would add an extra degree of freedom in the optimization procedure.

- The effects of channel estimation errors on the ranked SNR statistics in the context of general order selection diversity should be examined.

- The analysis of general order selection diversity discussed in this thesis is based on user channel conditions. However, if the selection also includes the amount of user data in the buffer, or the packet delays, the statistics of the resulting selection criterion would

be more complicated. The derivation of the statistics for such a selection criterion is an interesting problem.

- By incorporating the statistical distribution of the downlink received SIR, stochastic optimization models can be developed in order to take into account the uncertainties of the system, which are often more realistic in practice.

References

[1] "Physical Layer Aspects of UTRA High Speed Downlink Packet Access," 3rd Generation Partnership Project, Technical Report 3G TR25.858, 2002.

[2] Z. Gao and S. Q. Li, "A Packet Scheduling Scheme in Wireless CDMA Data Network," in *Proc. of IEEE International Conference on Communications, Cicuits, and Systems, and West Sino Expositions*, vol. 1, June 29 - July 1 2002, pp. 211 – 215.

[3] M. Andrews, K. Kumaran, K. Ranaman, A. Stolyar, and P. Whiting, "Providing Quality of Service over a Shared Wireless Link," *IEEE Communications Magazine*, vol. 39, no. 2, pp. 150 – 154, February 2001.

[4] M. Kazmi, P. Godlewski, and C. Cordier, "Admission Control Strategy and Scheduling Algorithms for Downlink Packet Transmission in WCDMA," in *Proc. of 52nd IEEE Vehicular Technology Conference, VTC'00*, vol. 2, September 2000, pp. 674 – 680.

[5] N. Joshi, S. R. Kadaba, S. Patel, and G. S. Sundaram, "Downlink Scheduling in CDMA Data Network," in *Proceedings of the 6th annual international conference on Mobile computing and networking*, 2000, pp. 179 – 190.

[6] P. Liu, R. Berry, and M. L. Honig, "Delay-Sensitive Packet Scheduling in Wireless Networks," in *IEEE Proc. of Wireless Communications and Networks Conference WCNC*, vol. 3, 16-20 March 2003, pp. 1627 – 1632.

[7] K. Chang and Y. Han, "QoS-Based Adaptive Scheduling for a Mixed Service in HDR System," in *The 13th IEEE International Conference on Personal, Indoor and Mobile Radio Communications (PIMRC)*, vol. 4, 15-18 Sept. 2002, pp. 1914 – 1918.

[8] S. Shakkottai and A. L. Stolyar, "Scheduling Algorithm for a Mixture of Real-Time and Non-Real-Time Data in HDR," in *Proc. of MIT Information Technology Conference (ITC)*, November 2001.

[9] S. Shakkottai and R. Srikant, "Scheduling Real-Time Traffic With Deadlines over a Wireless Channel," *Wireless Networks, Kluwer Academic Publishers*, vol. 8, no. 1, pp. 13 – 26, August 2002.

[10] "Streaming support for HSDPA," Siemens, Sophia Antipolis, France, Technical Document R2-022882, 12-15 November 2002, 3GPP TSG-RAN2 meeting 33.

[11] P. Hosein, "Capacity of Voice Services over Time-Shared Wireless Packet Data Channels," in *Proc. of IEEE INFOCOM*, March 2005, pp. 2032 – 2043.

[12] E. H. Kuang and H. W. Chang, "A QoS-based Hybrid Multiple Access Transmission Strategy in WCDMA Downlink," in *Proc. of IEEE Wireless Communications and Networking Conference WCNC*, vol. 3, March 2003, pp. 1685 – 1690.

[13] A. Farrokh, F. Blomer, and V. Krishnamurthy, "A Comparision of Opportunistic Scheduling Algorithms for Streaming Media in High-Speed Downlink Packet Access (HSDPA)," in *Proc. of Interactive Multimedia and Next Generation Networks: Second International Workshop on Multimedia Interactive Protocols and Systems, MIPS*, ser. Lecture Notes in Computer Science, vol. 3311. Springer, November 2004, pp. 130 – 142.

[14] H. Holma and A. Toskala, Eds., *WCDMA for UMTS Radio Access for Third Generation Mobile Communications.* John Wiley & Sons, 2002.

[15] Http://www.3gpp.org.

[16] S. Parkvall, E. Englund, P. Malm, T. Hedberg, M. Persson, and J. Peisa, "WCDMA evolved – High-speed packet-data services ," *Ericsson Review*, no. 2, pp. 56 – 65, 2003.

[17] K. I. Pedersen, T. F. Lootsma, M. Støttrup, F. Frederiksen, T. E. Kolding, and P. E. Mogensen, "Network Performance of Mixed Traffic on High Speed Downlink Packet Access and Dedicated Channels in WCDMA," in *Proc. of IEEE Vehicular Technology Conference (VTC)*, vol. 6, September 2004, pp. 4496–4500.

[18] A. Furuskar, S. Parkvall, M. Persson, and M. Samuelsson, "Performance of WCDMA high speed packet data," in *The 55th IEEE Proc. of Vehicular Technology Conference (VTC)*, vol. 3, May 2002, pp. 1116 – 1120.

Appendix A

Linearization of the MINLP models

A.1 Assigned Bit Rate Based Model

In this appendix , it is shown that we can linearize the MINLP problems for both the basic and load-based models. Solving the linearized versions to obtain the results in section 2.3.3 in a 1.7 GHz personal computer with 384 MBytes of RAM was found to take much less time (typically a factor of 7) than the non-linearized version. Using the substitution,

$$m_{ij} = a_{ij} n_i \tag{A.1}$$

$$K_{ij} = \lambda_{i,j}(\alpha P_T + \sum_{k \in \mathcal{B}} I_k h_{ki}/h_i + I_N/h_i) \tag{A.2}$$

the MINLP problem in (2.5) can be transformed to an equivalent mixed-integer linear problem as

$$\max_{\mathbf{a},\mathbf{P},\mathbf{n}} \left\{ \sum_{i=1}^{L} \sum_{j=1}^{J} m_{ij} r_{ij} - \upsilon \right\}, \tag{A.3}$$

subject to linear constraints

$$a_{ij} \in \{0,1\}, \forall i = 1,...,L, \forall j = 1,...J \tag{A.4}$$

$$\sum_{j=1}^{J} a_{ij} = 1 \tag{A.5}$$

$$n_i \leq N_{i,max}, \quad \forall i = 1,...,L \tag{A.6}$$

$$\sum_{i=1}^{L} n_i \leq N_{max} \tag{A.7}$$

$$\sum_{i=1}^{L} P_i \leq P_{max} \tag{A.8}$$

$$\sum_{j=1}^{J} m_{ij} K_{ij} \leq P_i, \quad \forall i = 1, ..., L \tag{A.9}$$

$$m_{ij} \leq n_i, \quad \forall i = 1, ..., L,$$

$$\forall j = 1, ..., J \tag{A.10}$$

$$m_{ij} \leq N_{i,max} a_{ij},$$

$$\forall i = 1, ..., L, \quad \forall j = 1, ..., J \tag{A.11}$$

$$m_{ij} \geq n_i - (1 - a_{ij}) N_{i,max},$$

$$\forall i = 1, ..., L, \quad \forall j = 1, ..., J \tag{A.12}$$

$$m_{ij} \geq 0, \quad \forall i = 1, ..., L, \quad \forall j = 1, ..., J \tag{A.13}$$

A.2 Load-Based Model

Using the substitution

$$Y_i = \sum_{j=1}^{J} m_{ij} r_{ij} / W, \tag{A.14}$$

the MINLP problem in (2.15) can be transformed into an equivalent mixed-integer linear problem as

$$\max_{\mathbf{a},\mathbf{P},\mathbf{n}} \left\{ \sum_{i=1}^{L} t_i - \upsilon \right\}, \tag{A.15}$$

subject to the constraints (A.4) - (A.13), together with

$$t_i \leq D_i, \quad \forall i = 1, ..., L \tag{A.16}$$

$$t_i + M t_i' \geq D_i, \quad \forall i = 1, ..., L \tag{A.17}$$

$$t_i \leq Y_i, \quad \forall i = 1, ..., L \tag{A.18}$$

$$t_i + Mt_i'' \geq Y_i, \quad \forall i = 1, ..., L \tag{A.19}$$

$$t_i' + t_i'' = 1, \quad \forall i = 1, ..., L \tag{A.20}$$

$$t_i', t_i'' \in \{0, 1\}, \quad \forall i = 1, ..., L. \tag{A.21}$$

where $M \in \mathcal{R}^+$ and $M >> 0$.

Appendix B

Proof of Theorems and Clarifications in Chapter 3

B.1 Proof of theorem 3.1

Proof: The extrema of $\tilde{R}_{i,j}(\lambda_{i,j})$ can be obtained by setting $d\tilde{R}_{i,j}(\lambda_{i,j})/d\lambda_{i,j} = 0$. Thus,

$$\frac{d\tilde{R}_{i,j}(\lambda_{i,j})}{d\lambda_{i,j}} = r_{i,j}\gamma_i \frac{d}{d\lambda_{i,j}}\left(\frac{1-\epsilon_{i,j}(\lambda_{i,j})}{\lambda_{i,j}}\right) \tag{B.1}$$

$$= r_{i,j}\gamma_i \left\{\frac{\lambda_{i,j}(1-\epsilon_{i,j}(\lambda_{i,j}))' - (1-\epsilon_{i,j}(\lambda_{i,j}))}{\lambda_{i,j}^2}\right\} \tag{B.2}$$

$$= 0 \tag{B.3}$$

$$\Longrightarrow \epsilon_{i,j}(\lambda_{i,j}) - \lambda_{i,j}\epsilon'_{i,j}(\lambda_{i,j}) - 1 = 0 \tag{B.4}$$

To determine which solution in (B.4) is a maximum, we need the second derivative of $\tilde{R}_{i,j}(\lambda_{i,j})$, which is given by

$$\frac{d^2\tilde{R}_{i,j}(\lambda_{i,j})}{d\lambda_{i,j}^2} = r_{i,j}\gamma_i \frac{d^2}{d\lambda_{i,j}^2}\left(\frac{1-\epsilon_{i,j}(\lambda_{i,j})}{\lambda_{i,j}}\right) \tag{B.5}$$

$$= r_{i,j}\gamma_i \left\{\frac{-\lambda_{i,j}^3\epsilon''_{i,j}(\lambda_{i,j}) + 2\lambda_{i,j}^2\epsilon'_{i,j}(\lambda_{i,j}) + 2\lambda_{i,j}(1-\epsilon_{i,j}(\lambda_{i,j}))}{\lambda_{i,j}^4}\right\} \tag{B.6}$$

to be negative. Substituting (B.4) into (B.6), we require

$$\tilde{R}''_{i,j}(\lambda_{i,j}^{(opt)}) = -\frac{\epsilon''_{i,j}(\lambda_{i,j}^{(opt)})}{\lambda_{i,j}^{(opt)}} \tag{B.7}$$

to be negative, i.e.

$$\epsilon''_{i,j}(\lambda_{i,j}^{(opt)}) > 0. \tag{B.8}$$

■

B.2 Proof of Theorem 3.2

Proof: We assume that the link-level error rate curve $\epsilon_{i,j}(x)$ can be modelled by a sigmoid function, i.e.

$$\epsilon_{i,j}(x) = \frac{1}{1 + a_1 e^{a_2(x-a_3)}},\ x \geq 0 \tag{B.9}$$

where $\{a_1, a_2\} \in \mathcal{R}^+$ and $a_3 \in \mathcal{R}$ are constants. From Theorem 3.1, an optimal solution should satisfy $\epsilon_{i,j}(x) - x\epsilon'_{i,j}(x) - 1 = 0$, where

$$\epsilon'_{i,j}(x) = \frac{-a_1 a_2 e^{a_2(x-a_3)}}{(1 + a_1 e^{a_2(x-a_3)})^2} \tag{B.10}$$

Thus, we have

$$\frac{1}{1 + a_1 e^{a_2(x-a_3)}} - \frac{-x a_1 a_2 e^{a_2(x-a_3)}}{(1 + a_1 e^{a_2(x-a_3)})^2} - 1 = 0 \tag{B.11}$$

$$\frac{(1 + a_1 e^{a_2(x-a_3)}) + x a_1 a_2 e^{a_2(x-a_3)}}{-(1 + a_1 e^{a_2(x-a_3)})^2} = 0 \tag{B.12}$$

$$\frac{(1 + a_1 e^{a_2(x-a_3)}) + x a_1 a_2 e^{a_2(x-a_3)}}{-(1 + 2a_1 e^{a_2(x-a_3)} + a_1^2 e^{2a_2(x-a_3)})} = 0 \tag{B.13}$$

$$a_2 x - a_1 e^{a_2(x-a_3)} = 1. \tag{B.14}$$

To isolate x, further algebraic manipulations give

$$\begin{aligned} a_2x &= a_1e^{a_2x}e^{-a_2a_3}+1 && \text{(B.15)}\\ e^{-a_2x}(a_2x) &= a_1e^{-a_2a_3}+e^{-a_2x} && \text{(B.16)}\\ e^{-a_2x+1}(-a_2x+1) &= -a_1e^{-a_2a_3+1} && \text{(B.17)}\\ -a_2x+1 &= W\left(-a_1e^{-a_2a_3+1}\right) && \text{(B.18)}\\ x &= \frac{W\left(-a_1e^{-a_2a_3+1}\right)-1}{-a_2}, && \text{(B.19)} \end{aligned}$$

where the function $W(.)$ is called Lambert W function, and is defined to be the multivalued inverse function of $w \mapsto we^w$. According to [1], if u is real, then for $-1/e \leq u < 0$, there are two possible values of $W(u)$. As shown in Fig. B.1, the branch satisfying $-1 \leq W(u)$ is usually denoted as $W_0(u)$, while the branch corresponding to $W(u) \leq -1$ is usually given as $W_{-1}(u)$. On the other hand, if u is real, and $u \geq 0$, then $W(u)$ only has a single value. Now, since $-a_1e^{-a_2a_3+1} < 0$, if real solutions exist, they must take on values x_0 and x_{-1} corresponding to the branches 0 and -1 respectively. In order for real solutions to exist,

$$\begin{aligned} -e^{-1} &\leq -a_1e^{-a_2a_3+1} && \text{(B.20)}\\ a_1e^{-a_2a_3+1} &\leq e^{-1} && \text{(B.21)}\\ e^{1-a_2a_3+\ln(a_1)} &\leq e^{-1} && \text{(B.22)}\\ 1-a_2a_3+\ln(a_1) &\leq -1. && \text{(B.23)} \end{aligned}$$

Now, according to Theorem 3.1, in order to maximize $\tilde{R}_{i,j}$, the solution(s) given in (B.19) should lie in the region such that $\epsilon''_{i,j}(x) > 0$. In other words,

$$\begin{aligned} \epsilon''_{i,j}(x) &> 0 && \text{(B.24)}\\ \frac{2a_1^2a_2^2e^{2a_2(x-a_3)}}{(1+a_1e^{a_2(x-a_3)})^3} - \frac{a_1a_2^2e^{a_2(x-a_3)}}{(1+a_1e^{a_2(x-a_3)})^2} &> 0 && \text{(B.25)}\\ a_1e^{a_2(x-a_3)}-1 &> 0 && \text{(B.26)} \end{aligned}$$

$$a_2 x > \ln(1/a_1) + a_2 a_3 \tag{B.27}$$

$$1 + \ln(a_1) - a_2 a_3 > 1 - a_2 x. \tag{B.28}$$

Using (B.28), (B.23) and (B.18), we have

$$-1 > 1 - a_2 x \tag{B.29}$$

$$-1 > W\left(-a_1 e^{-a_2 a_3 + 1}\right). \tag{B.30}$$

Thus, (B.30) shows that in order to maximize $\tilde{R}_{i,j}$, the optimal solution should lie in branch -1, which is uniquely given by

$$x_{-1} = \frac{W_{-1}\left(-a_1 e^{-a_2 a_3 + 1}\right) - 1}{-a_2}. \tag{B.31}$$

■

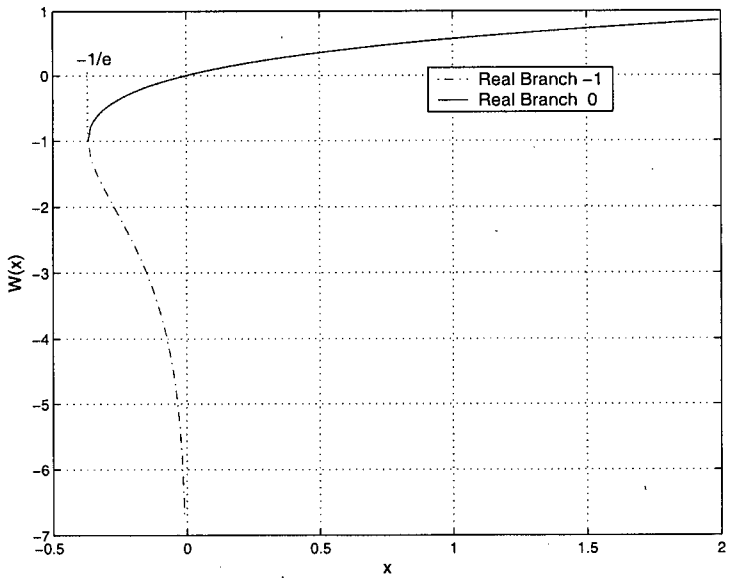

Figure B.1: Lambert W function. The dotted line corresponds to the real branch -1, while the solid line corresponds to the real branch 0.

B.3 Proof of theorem 3.3

Proof: From Theorem 3.2 it is known that $\lambda_{i,j}^{(opt)}$ is the unique value which corresponds to a maximum of $\tilde{R}_{i,j}(\lambda_{i,j})$. Thus if there exists a value of $\lambda_{i,j}$ such that $\lambda_{i,j} > \lambda_{i,j}^{(opt)}$ and $\tilde{R}'_{i,j}(\lambda_{i,j}) > 0$, $\lim_{\lambda_{i,j}\to\infty} \tilde{R}_{i,j}(\lambda_{i,j})$ will be unbounded. However, this contradicts the fact that $\lim_{\lambda_{i,j}\to\infty} \tilde{R}_{i,j}(\lambda_{i,j}) = 0$ as can be seen from the first part of (3.4). Hence, $\tilde{R}_{i,j}(\lambda_{i,j})$ decreases monotonically with $\lambda_{i,j}$ for $\lambda_{i,j} > \lambda_{i,j}^{(opt)}$. ■

B.4 Relationship between $\sigma_i^{(t)}$ and σ_i

The relationship between the standard deviation of the Gaussian distribution and that of the truncated version is now obtained. Let the pdf of the truncated Gaussian random variable be

$$f_{\mathcal{B}}(\beta_{\gamma_i}) = \begin{cases} \frac{1}{\sqrt{2\pi}\sigma_i} e^{-\beta_{\gamma_i}^2/2\sigma_i^2} & , \text{ if } \beta_{\gamma_i} > -1 \\ C_{\beta_{\gamma_i}} \delta(\beta_{\gamma_i} + 1) & , \text{ if } \beta_{\gamma_i} = -1 \end{cases}, \tag{B.32}$$

where the constant $C_{\beta_{\gamma_i}}$ is given by

$$C_{\beta_{\gamma_i}} = \int_{-\infty}^{-1} \frac{1}{\sqrt{2\pi}\sigma_i} e^{-\beta_{\gamma_i}^2/(2\sigma_i^2)} d\beta_{\gamma_i} \tag{B.33}$$

$$= \frac{1}{2}\text{erfc}\left(\frac{1}{\sqrt{2}\sigma_i}\right). \tag{B.34}$$

The standard deviation of the truncated Gaussian is given by

$$\sigma_i^{(t)} = \sqrt{E[\beta_{\gamma_i}^2] - (E[\beta_{\gamma_i}])^2}, \tag{B.35}$$

where

$$E[\beta_{\gamma_i}^2] = \int_{-1}^{\infty} \frac{\beta_{\gamma_i}^2}{\sqrt{2\pi}\sigma_i} e^{-\beta_{\gamma_i}^2/(2\sigma_i^2)} d\beta_{\gamma_i} + (-1)^2 C_{\beta_{\gamma_i}} \tag{B.36}$$

$$= \frac{1}{\sqrt{2\pi}\sigma_i}\Big(-\sigma_i^2\beta_{\gamma_i}e^{-\beta_{\gamma_i}^2/(2\sigma_i^2)} \frac{1}{2}\sigma_i^3\sqrt{2\pi}\ \mathrm{erf}(\frac{\beta_{\gamma_i}}{\sqrt{2}\sigma_i})\Big)\Big]_{-1}^{\infty} + C_{\beta_{\gamma_i}} \quad \text{(B.37)}$$

$$= \frac{1}{\sqrt{2\pi}\sigma_i}\left(\sigma_{\gamma_i}^3\sqrt{\frac{\pi}{2}}\ \mathrm{erfc}\left(\frac{-1}{\sqrt{2}\sigma_i}\right) - \sigma_i^2e^{-1/(2\sigma_i^2)}\right) + C_{\beta_{\gamma_i}} \quad \text{(B.38)}$$

and

$$E[\beta_{\gamma_i}] = \int_{-1}^{\infty}\frac{\beta_{\gamma_i}}{\sqrt{2\pi}\sigma_i}e^{-\beta_{\gamma_i}^2/(2\sigma_i^2)}d\beta_{\gamma_i} + (-1)C_{\beta_{\gamma_i}} \quad \text{(B.39)}$$

$$= \frac{-1}{\sqrt{2\pi}}\sigma_i e^{-\beta_{\gamma_i}^2/(2\sigma_i^2)}\Big]_{-1}^{\infty} + (-1)C_{\beta_{\gamma_i}} \quad \text{(B.40)}$$

$$= \frac{\sigma_i}{\sqrt{2\pi}}e^{-1/(2\sigma_i^2)} - C_{\beta_{\gamma_i}}. \quad \text{(B.41)}$$

Appendix C

Derivation of the integral in (4.28)

To simply notations, let $c_1 = c_1^{(j)}(\hat{\gamma})$, $k_1 = nc_1$, and $a = K_j + \epsilon$. The objective is to evaluate the integral

$$
\begin{aligned}
I &= \int_a^\infty e^{-k_1\gamma/\hat{\gamma}} p_{\gamma|\hat{\gamma}}(\gamma|\hat{\gamma}) d\gamma, && \text{(C.1)} \\
&= \int_a^\infty e^{-k_1\gamma/\hat{\gamma}} \frac{m}{(1-\rho)\bar{\Gamma}} \left(\frac{\gamma}{\rho\hat{\gamma}}\right)^{\frac{m-1}{2}} \times \\
&\quad I_{m-1}\left(\frac{2m\sqrt{\rho\gamma\hat{\gamma}}}{(1-\rho)\bar{\Gamma}}\right) \exp\left(-\frac{m(\rho\gamma+\hat{\gamma})}{(1-\rho)\hat{\gamma}}\right) d\gamma && \text{(C.2)} \\
&= \int_a^\infty \frac{m}{(1-\rho)\bar{\Gamma}} e^{-(\frac{k_1}{\hat{\gamma}} + \frac{m}{(1-\rho)\bar{\Gamma}})\gamma - \frac{m\rho\hat{\gamma}}{(1-\rho)\bar{\Gamma}}} \times \\
&\quad \left(\frac{\gamma}{\rho\hat{\gamma}}\right)^{\frac{m-1}{2}} I_{m-1}\left(\frac{2m\sqrt{\rho\gamma\hat{\gamma}}}{(1-\rho)\bar{\Gamma}}\right) d\gamma && \text{(C.3)} \\
&= \int_a^\infty A_1 \left(\frac{\gamma}{\rho\hat{\gamma}}\right)^{\frac{m-1}{2}} e^{-A_2\gamma} I_{m-1}\left(\frac{2m\sqrt{\rho\gamma\hat{\gamma}}}{(1-\rho)\bar{\Gamma}}\right) d\gamma && \text{(C.4)}
\end{aligned}
$$

where A_1 and A_2 are given by

$$
\begin{aligned}
A_1 &= \frac{m}{(1-\rho)\bar{\Gamma}} e^{-\frac{m\rho\hat{\gamma}}{(1-\rho)\bar{\Gamma}}} && \text{(C.5)} \\
A_2 &= \frac{k_1}{\hat{\gamma}} + \frac{m}{(1-\rho)\bar{\Gamma}} && \text{(C.6)}
\end{aligned}
$$

Letting $z = A_2\gamma$, and, subsequently, $z = q^2/2$, (C.4) becomes

$$
I = \int_{A_2 a}^\infty A_1 \left(\frac{A_2^{-1} z}{\rho\hat{\gamma}}\right)^{\frac{m-1}{2}} e^{-z} \times
$$

$$I_{m-1}\left(\frac{2m\sqrt{\rho A_2^{-1} z\hat{\gamma}}}{(1-\rho)\bar{\Gamma}}\right) A_2^{-1} dz \tag{C.7}$$

$$= \int_{\sqrt{2A_2 a}}^{\infty} A_1 A_2^{-1} \left(\frac{A_2^{-1}}{2\rho\hat{\gamma}}\right)^{\frac{m-1}{2}} q^m \times$$
$$e^{-\frac{q^2}{2}} I_{m-1}(A_3 q) dq \tag{C.8}$$

$$= A_1 A_2^{-1} \left(\frac{A_2^{-1}}{2\rho\hat{\gamma}}\right)^{\frac{m-1}{2}} e^{A_3^2/2} A_3^{m-1} \times$$
$$\frac{1}{A_3^{m-1}} \int_{\sqrt{2A_2 a}}^{\infty} q^m e^{-\frac{q^2+A_3^2}{2}} I_{m-1}(A_3 q) dq \tag{C.9}$$

$$= \frac{m}{(1-\rho)\bar{\Gamma}} \left(\frac{1}{2\rho\hat{\gamma}}\right)^{\frac{(m-1)}{2}} A_2^{-\frac{(m+1)}{2}} \times$$
$$e^{-A_4} A_3^{m-1} Q_m(A_3, \sqrt{2A_2 a}) \tag{C.10}$$

where A_3 and b are given by

$$A_3 = \frac{2m\sqrt{\rho A_2^{-1}\hat{\gamma}/2}}{(1-\rho)\bar{\Gamma}} \tag{C.11}$$

$$= \sqrt{\frac{2m^2\rho\hat{\gamma}^2}{(1-\rho)\bar{\Gamma}(k_1(1-\rho)\bar{\Gamma} + m\hat{\gamma})}} \tag{C.12}$$

$$A_4 = \frac{m\rho\hat{\gamma}k_1}{k_1(1-\rho)\bar{\Gamma} + m\hat{\gamma}} \tag{C.13}$$

and $Q_m(.)$ is the generalized Marcum Q-function defined in (4.29). Substituting (C.6), (C.11), and (C.13) into (C.10), and after some algebraic manipulations, (C.10) becomes

$$I = \left(\frac{m\hat{\gamma}}{k_1(1-\rho)\bar{\Gamma} + m\hat{\gamma}}\right)^m \exp\left(-\frac{\rho k_1 m\hat{\gamma}}{k_1(1-\rho)\bar{\Gamma} + m\hat{\gamma}}\right) \times$$
$$Q_m\left(\sqrt{\frac{2\rho m^2\hat{\gamma}^2}{\bar{\Gamma}(1-\rho)(k_1(1-\rho)\bar{\Gamma} + m\hat{\gamma})}}, \sqrt{2A_2 a}\right) \tag{C.14}$$

which is identical to the integral in (4.30).

Appendix D

Optimality with an integer number of multicodes

The problem of choosing the optimal MCS and number of multicodes for a given SIR amounts to a discrete optimization problem. This problem is usually difficult and not amenable to an analytical solution [2]. In [3], it was possible to derive an analytical solution for the optimal bit rate for a single user by assuming that the number of multicodes is a real value. The solution may not be optimal if the number of multicodes is an integer.

Fig. D.1 shows the bit rate as a function of SIR for MCS i and MCS j assuming integer and continuous multicodes. In this figure, MCS j is assumed to provide the highest bit rate among all MCS's when the multicodes are assumed to be take on continuous values. When the discrete multicode model is obtained by applying the floor function as in (6.55), a series of staircases is generated. Since the staircases can potentially overlap each other, especially in the low SIR region, the bit rate for MCS j may no longer be optimal over the entire SIR region.

Let $[(k+1)\lambda_j - \Delta l_{k+1,j}, (k+1)\lambda_j]$, $k = 1, \ldots, N_{max}$ be the intervals within which the bit rate corresponding to MCS i with a continuous number of multicodes exceeds that corresponding to MCS j with an integer number of multicodes. Fig. D.1 shows that this occurs when

$$(k+1)\lambda_j - \Delta l_{k+1,j} < k'\lambda_i < (k+1)\lambda_j,$$
$$k = 1, \ldots, N_{max}, k' = 1, \ldots, N_{max}, \ \forall i \neq j. \tag{D.1}$$

The bit rate results presented in this paper do not satisfy (D.1), and are, therefore, optimal.

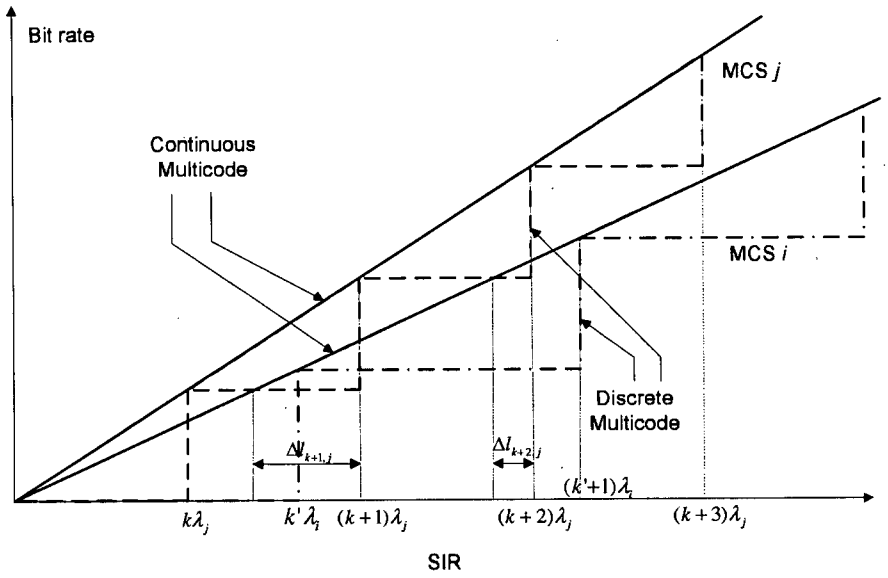

Figure D.1: The bit rate as a function of SIR for MCS i and MCS j assuming an integer and a continuous number of multicodes.

Appendix E

Derivation of (7.17)

Using [4, page 940, 8.352.1], the term $1 - F_{l_u}(y)$ in (7.8) can be expanded as

$$1 - F_{l_u}(y) = \left(1 - \frac{1}{\Gamma(\alpha_{l_u})}\gamma\left(\alpha_{l_u}, \frac{\alpha_{l_u}}{\beta_{l_u}}y\right)\right) \tag{E.1}$$

$$= \exp\left(-\frac{\alpha_{l_u}}{\beta_{l_u}}y\right)\sum_{m=0}^{\alpha_{l_u}-1}\left(\frac{\alpha_{l_u}y}{\beta_{l_u}}\right)^m\frac{1}{m!}. \tag{E.2}$$

In (7.9), the term $Q_{L-q+2}^{L}(y) = \prod_{u=L-q+2}^{L}(1 - F_{l_u}(y))$ can be re-written as

$$Q_{L-q+2}^{L}(y) = \exp\left(-\sum_{u=L-q+2}^{L}\xi_{l_u}y\right)\prod_{u=L-q+2}^{L}\sum_{m=0}^{\alpha_{l_u}-1}\frac{(\xi_{l_u}y)^m}{m!} \tag{E.3}$$

$$= \sum_{m_1'=0}^{\alpha_{l_{L-q+2}}-1}\cdots\sum_{m_{q-1}'=0}^{\alpha_{l_L}-1}\left(\prod_{t'=1}^{q-1}\frac{\xi_{l_{L-q+1+t'}}^{m_{t'}'}}{m_{t'}'!}\right)\times$$

$$y^{\sum_{t'=1}^{q-1}m_{t'}'}\exp\left(-\sum_{t'=L-q+2}^{L}\xi_{l_{t'}}y\right), \tag{E.4}$$

where $\xi_{l_u} = \alpha_{l_u}/\beta_{l_u}$ and α_{l_u} is assumed to take on integer values. Using the result for the first order statistics [5], together with some algebraic manipulations, the term $P_2^{L-q+1}(y) = \prod_{j=2}^{L-q+1}F_{l_j}(y)$ can be expressed as

$$P_2^{L-q+1}(y) = \sum_{k=0}^{L-q}(-1)^k\sum_{2\le n_1<\ldots<n_k\le L-q+1}\sum_{m_1=0}^{\alpha_{l_{n_1}}-1}\cdots\sum_{m_k=0}^{\alpha_{l_{n_k}}-1}$$

$$\left(\prod_{t=1}^{k}\frac{\xi_{l_{n_t}}^{m_t}}{m_t!}\right)y^{\sum_{t=1}^{k}m_t}\exp\left(-\sum_{t=1}^{k}\xi_{l_{n_t}}y\right). \tag{E.5}$$

Substituting (E.4) and (E.5) into (7.9), the desired result follows.

Appendix F

Derivation of (8.15) and (8.31)

F.1 Derivation of (8.15)

Let $z' = z - \Delta$. The pdf in (8.12) can be expressed as

$$f_{Z'}(z') = K_0(1 + \frac{z'}{b_1})^{\theta_1}(1 - \frac{z'}{b_2})^{\theta_2}, \quad -b_1 \leq z' \leq b_2 \tag{F.1}$$

Furthermore, let $w = 1+(z'/b_1)$, $p = 1+(b_1/b_2)$, and $p' = b_1/b_2$, $F_{Z'}(z') = \int_0^{u'} f_{Z'}(z')dz'$ becomes

$$\begin{aligned} F_{Z'}(u') &= \int_0^{1+(u'/b_1)} K_0 b_1 w^{\theta_1}(p - p'w)^{\theta_2} dw, \\ & \qquad -b_1 \leq u' \leq b_2 \end{aligned} \tag{F.2}$$

Letting $l = p'/p$, $w' = lw$, and $x(u') = l(1 + (u'/b_1))$, $F_{Z'}(u')$ becomes

$$\begin{aligned} F_{Z'}(u') &= \int_0^{x(u')} b_1 K_0 p^{\theta_2} l^{-(\theta_1+1)} \times \\ & \qquad w'^{\theta_1}(1 - w')^{\theta_2} dw', \quad -b_1 \leq u' \leq b_2 \qquad \text{(F.3)} \\ &= b_1 K_0 p^{\theta_2} l^{-(\theta_1+1)} B_{x(u')}(\theta_1 + 1, \theta_2 + 1) \qquad \text{(F.4)} \end{aligned}$$

Finally, letting $u' = u - \Delta$, the result follows.

F.2 Derivation of (8.31)

Let $z' = z - \Delta$ and $t' = t - \Delta$, the cdf of (8.24) can be written as

$$F_Z(t') = \int_a^{t'} K_0 (z' - a)^{\theta_2} (z')^{-\theta_1} dz' \tag{F.5}$$

$$= \int_a^{t'} K_0 a^{\theta_2 - \theta_1} \left(\frac{z'}{a} - 1 \right)^{\theta_2} \left(\frac{z'}{a} \right)^{-\theta_1} dz' \tag{F.6}$$

Furthermore, let $u = a/z'$, we have

$$F_Z(t') = \int_1^{\frac{a}{t'}} K_0 a^{\theta_2 - \theta_1} \left(\frac{1}{u} - 1 \right)^{\theta_2} \left(\frac{1}{u} \right)^{-\theta_1} (-au^{-2}) du \tag{F.7}$$

$$= \int_{\frac{a}{t'}}^1 K_0 a^{\theta_2 - \theta_1 + 1} (1 - u)^{\theta_2} u^{\theta_1 - \theta_2 - 2} du \tag{F.8}$$

$$= 1 - \int_0^{\frac{a}{t'}} K_0 a^{\theta_2 - \theta_1 + 1} (1 - u)^{\theta_2} u^{\theta_1 - \theta_2 - 2} du \tag{F.9}$$

Using the definition of the incomplete beta function [4], the desired result follows.

References

[1] R. M. Corless, G. H. Gonnet, D. E. G. Hare, D. J. Jeffrey, and D. E. Knuth, "On the Lambert W Function," *Adv. Comput. Math.*, vol. 5, pp. 329 – 359, 1996.

[2] R. Kwan and C. Leung, "Optimal Downlink Scheduling Schemes for CDMA Networks," in *Proc. of IEEE Wireless Communication and Networking Conference (WCNC)*, Atlanta, Georgia, March 2004.

[3] ——, "Channel-Based Downlink Scheduling Schemes for CDMA Networks," in *Proc. of IEEE Vehicular Technology Conference (VTC)*, Los Angeles, California, September 2004.

[4] I. S. Gradshteyn and I. M. Ryzhik, *Table of Integrals, Series, and Products.* Academic Press Inc., 1980.

[5] R. Kwan and C. Leung, "Selection Diversity in Non-Identically Distributed Nakagami Fading Channels," in *Proc. of IEEE Sarnoff Symposium*, Princeton, New Jersey, April 2005.